Implement Flexible mmWave Automotive Radar Testing **p58**

Noise Can Be a Good Thing When Characterizing Materials **p72**

The Internet of Things: Billions Upon Billions and Growing **p118**

Microwaves & RF®

YOUR TRUSTED ENGINEERING RESOURCE FOR OVER 50 YEARS

MAY 2018 mwrf.com

IMS 2018 PHILADELPHIA

Showcasing the best of the best from all corners of the industry **p27**

- Amplifiers – Solid State
- Attenuators – Variable/ Programmable
- Couplers (Quadrature, 180° & Directional)
- Detectors – RF/Microwave
- DLVAs, ERDLVAs & SDLVAs
- DTOs, VCOs, PLO, DROs, & Frequency Synthesizers
- Filters & Switched Filter Banks
- Form, Fit, Functional Products & Services
- Frequency Discriminators & IFMs
- Integrated MIC/MMIC Assemblies (IMAs)
- IQ Vector Modulators
- Limiters – RF/Microwave
- Log Amplifiers
- Millimeter Wave Components (Up to 50 GHz)
- Miscellaneous Products
- Monopulse Comparators
- Multifunction Integrated Assemblies (MIAs)
- Phase Shifters & Bi-Phase Modulators
- Power Dividers/Combiners (Passive & Active)
- Pulse Modulators (SPST)
- Rack & Chassis Mount Products
- Receiver Front Ends & Transceivers
- SDLVAs, ERDLVAs & DLVAs
- Single Side Band Modulators
- SMT & QFN Products
- Switch Matrices
- Switched Filter Banks
- Switches – Solid State
- Systems - Radar Sense & Avoid
- Systems – Fly Eye Radars
- Threshold Detectors
- USB Products

Planar Monolithics Industries, Inc.

Industry Leader in Theshold Detectors for Radar & Surveillance Sensors

PMI offers a full line of RF and Microwave Threshold Detectors that range from 2 MHz to 40 GHz. Threshold levels of detection can be fixed or adjustable based on the radar and surveillance sensor application needs. PMI's Threshold Detectors offer Ultra-High Speed along with High Dynamic Range and Broad Operating Frequency. More available at: http://www.pmi-rf.com/Products/detectors/threshold_detectors.htm


CDT-2M18-30-BB-DE-D


TD-50M4G-CD-SFF


TD-1G12G-RL-CD-SFF-NH


TD-30T-0418-MH
TD-30T-0518-MH-SMA
TD-30T-218-FC-HS


TD-16G40G-20-292F

THRESHOLD DETECTORS - ADJUSTABLE

PMI Model No.	FREQ Range (GHz)	Input Power Range (dBm)	Detected Output Type	Response Time	Connector Type	Size (Inches)
CDT-2M18-30-BB-DE-D http://www.pmi-rf.com/Products/detectors/ CDT-2M18-30-BB-DE-D-1.htm	0.002 - 18	-30 to 0	TTL	5 µs	SMA	2.5 x 2.9 x 0.5
TD-50M4G-CD-SFF http://www.pmi-rf.com/Products/detectors/ TD-50M4G-CD-SFF.htm	0.05 - 4	-20 to 0	TTL	20 ns	SMA	0.85 x 0.625 x 0.2
TD-1G12G-RL-CD-SFF-NH http://www.pmi-rf.com/products/detectors/ TD-1G12G-RL-CD-SFF-NH.htm	1.0 - 12	-30 to +10	TTL	10 ns	SMA	1.1 x 0.6 x 0.19
TD-30T-0418-MH http://www.pmi-rf.com/Products/detectors/ TD-30T-0418-MH-1.htm	0.4 - 18	-18 to +5	TTL	100 ns	GPO	0.8 x 0.62 x 0.4
TD-30T-0518-MH-SMA http://www.pmi-rf.com/Products/detectors/ TD-30T-0518-MH-1.htm	0.5 - 18	-18 to +5	TTL	100 ns	SMA	0.8 x 0.62 x 0.4
TD-30T-SHS-218-0218 http://www.pmi-rf.com/Products/detectors/ TD-30T-SHS-218-0218-1.htm	0.2 - 18	-20 to +10	TTL	15 ns	SMA	2.2 x 1.5 x 0.4
TD-30T-218-FC-HS http://www.pmi-rf.com/Products/detectors/ TD-30T-218-FC-HS1.htm	2 - 18	-20 to +5	TTL	100 ns	SMA	0.8 x 0.62 x 0.4
TD-16G40G-20-292F http://www.pmi-rf.com/Products/detectors/ TD-20-16G40G-20-292FF.htm	16 - 40	-20 to 0	TTL	100 ns	2.92mm	1.0 x 0.62 x 0.22


GMTA-1002


GMTA-1005


TD-30T-SHS-218-12G18G-PECL

THRESHOLD DETECTORS - FIXED

PMI Model No.	FREQ Range (GHz)	Fixed Threshold Level (dBm)	Detected Output Type	Response Time	Connector Type	Size (Inches)
GMTA-1002 http://www.pmi-rf.com/Products/detectors/ GMTA-1002.htm	2 - 18	-23	TTL	100 µs	SMA	1.0 x 0.65 x 0.3
GMTA-1005 http://www.pmi-rf.com/Products/detectors/ GMTA-1005.htm	8 - 18	-42	TTL	100 µs	SMA	1.15 x 1.1 x 0.37
TD-30T-SHS-218-12G18G-PECL http://www.pmi-rf.com/products/detectors/ TD-30T-SHS-218-12G18G-PECL.htm	12 - 18	+10	LVPECL	15 ns	SMA	2.2 x 1.5 x 0.4

West Coast Operation:
4921 Robert J. Mathews Pkwy, Suite 1
El Dorado Hills, CA 95762 USA
Tel: 916-542-1401, Fax: 916-265-2597

East Coast Operation:
7311-F Grove Road
Frederick, MD 21704 USA
Tel: 301-662-5019, Fax: 301-662-1731

sales@pmi-rf.com • www.pmi-rf.com
ISO9001 REGISTERED

SKYWORKS®

Broad Portfolio of Connectivity Solutions

Visit Us at IMS2018 • Booth 509 • Philadelphia, PA • June 10–15

Aerospace and Defense

For high-reliability, space, instrumentation, avionics, land mobile radio and overall military communication applications.

Part Number	Description	Freq. Range (GHz)
APD1520-240	Silicon PIN Diode, Packaged and Bondable Chip	0.100 to 30.000
CLA460x Series	Limiter Diodes for LNA and Receiver Protection	Up to 30.000
ISO13316	Hermetic, GaAs SPST Non-Reflective Switch	DC to 6.000
SKY67159-396LF	Broadband Low-Noise Amplifier	0.200 to 3.800
SKY16602-632LF	Low-Threshold PIN Diode Limiter	0.200 to 4.000

Small Cell Infrastructure

For applications including CBRS, FDD and TDD 2G/3G/4G LTE systems, small cell, micro and macro base stations, active antenna arrays and massive MIMO.

Part Number	Description	Freq. Range (GHz)
SKY6629x Series	High Efficiency Power Amplifiers	0.700 to 6.000
SKYFR-xxx	Circulators and Isolators	–

Internet of Things (IoT)

For applications spanning fitness/smart watches, trackers, wireless headphones, in-home appliances, smart thermostats, alarms, lighting, sensors, access points, routers, automotive infotainment, telematics, and more.

Part Number	Description	Freq. Range (GHz)
SKYA21003	SPDT Switch (AEC-Q100 Level 2 Qualified)	0.100 to 6.000
SKYA21041	802.11ac Switch/Low Noise Amplifier Front-end Module (AEC-Q100 Qualified)	4.900 to 5.900
SKY66111-11	Front-end Module with Low Power, Bluetooth® Low Energy Range Extension	2.400 to 2.485
SKY66114-11	Front-end Module with Bluetooth® Low Energy / 802.15.4 / ZigBee® Support	2.400 to 2.483
SKY68001-31	LTE Universal Multiband Front-end Module for IoT	0.699 to 0.915 1.710 to 1.910
SKY85310-21	256 QAM WLAN/Bluetooth® Front-end Module	2.400
SKY85712-21	WLAN Front-end Module	5.000

For more information about all of our solutions, please visit us at www.skyworksinc.com.

sales@skyworksinc.com | USA: 781-376-3000 | Asia: 886-2-2735 0399 | Europe: 33 (0)1 43548540 | NASDAQ: SWKS |

Another Industry First!

20 MHz-6000 MHz Broadband Amplifier

70 Watts Output Power Highest Power Density Across Frequency Band

by Aethercomm

Aethercomm has developed another industry first!

- Gallium Nitride Technology
- Broadest Bandwidth
- Operation from 20 MHz to 6000 MHz
- 40 to 100 Watts PSat typical
- Small Form Factor - 5.0” (width) by 6.5” (length) by 2.0” (height)
- Composite Power Added Efficiency of 36%

19 YEARS IN BUSINESS 19 1999-2018

QUALITY SYSTEM CERTIFICATION DNV·GL AS/EN/JISQ 9100

IMS Connecting Minds. Exchanging Ideas. Booth 1012

Aethercomm®

We make hardware that saves lives.™

Tel 760.208.6002
sales@aethercomm.com
www.aethercomm.com


5G
CAUTION
STATIC SENSITIVE
MICRO LAMBDA
WIRELESS, INC.

IN THIS ISSUE

FEATURES

118

PRODUCTS & TECHNOLOGY

NEWS & COLUMNS

defense electronics

Starts on page **91**

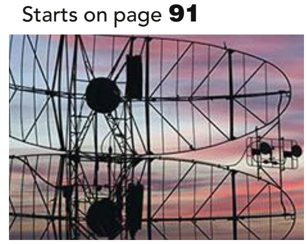

ON MICROWAVES&RF.COM

Mysterious Wireless Band Fits IoT Apps

Some useful frequencies are elusive or simply unknown to many engineers, so it wouldn't hurt to take some time and dig through the FCC "bible" of federal regulations. Especially when it comes to the burgeoning Internet of Things.

http://www.mwrf.com/systems/mysterious-wireless-band-fits-iot-apps

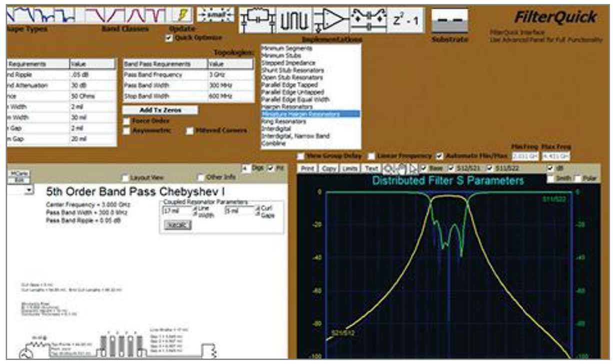

How Port Tuning Makes Filter Design More Efficient

With the help of the latest software tools, port tuning can accelerate the design of planar filters. This article demonstrates that with the design of a miniature hairpin resonator filter.

http://www.mwrf.com/software/how-port-tuning-makes-filter-design-more-efficient

Millimeter Waves: Time for a Checkup?

Microwave cable assemblies are often taken for granted. But as millimeter-wave frequencies become more prevalent, it's essential that the smaller cables used at these higher frequencies be properly handled due to their fragility.

http://www.mwrf.com/components/millimeter-wave-cables-time-checkup

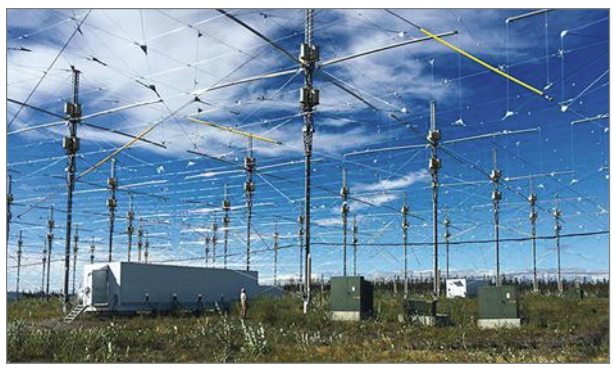

Modeling Mutual Coupling in Large Antenna Arrays

In his latest "Algorithms to Antenna" blog post, MathWorks' Rick Gentile takes a close look at the effectiveness of two different techniques that can be applied to model the effects of mutual coupling.

http://www.mwrf.com/components/algorithms-antenna-modeling-mutual-coupling-large-antenna-arrays

twitter.com/MicrowavesRF facebook.com/microwavesrf

ANALOG DEVICES
AHEAD OF WHAT'S POSSIBLE™

MEASURE RMS POWER TO 40GHz

LTC5596

IMPROVE MEASUREMENT ACCURACY & DETECTION SENSITIVITY

- RF Input 50Ω-Matched from 100MHz to 40GHz
- 35dB Log-Linear Dynamic Range to ±1dB Accuracy
- –32.6dBm Minimum Detectable Signal Sensitivity

OUTPUT AT DIFFERENT RF INPUTS

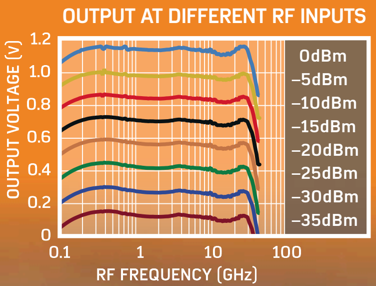

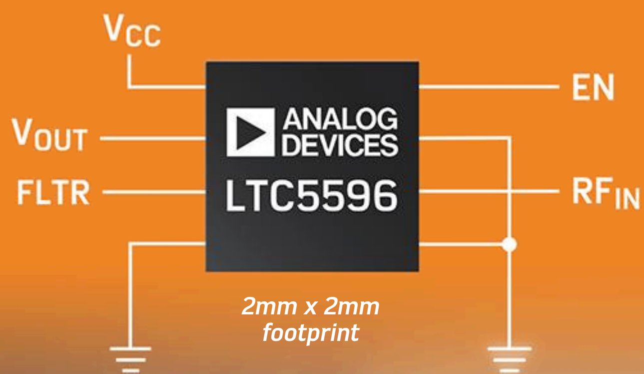

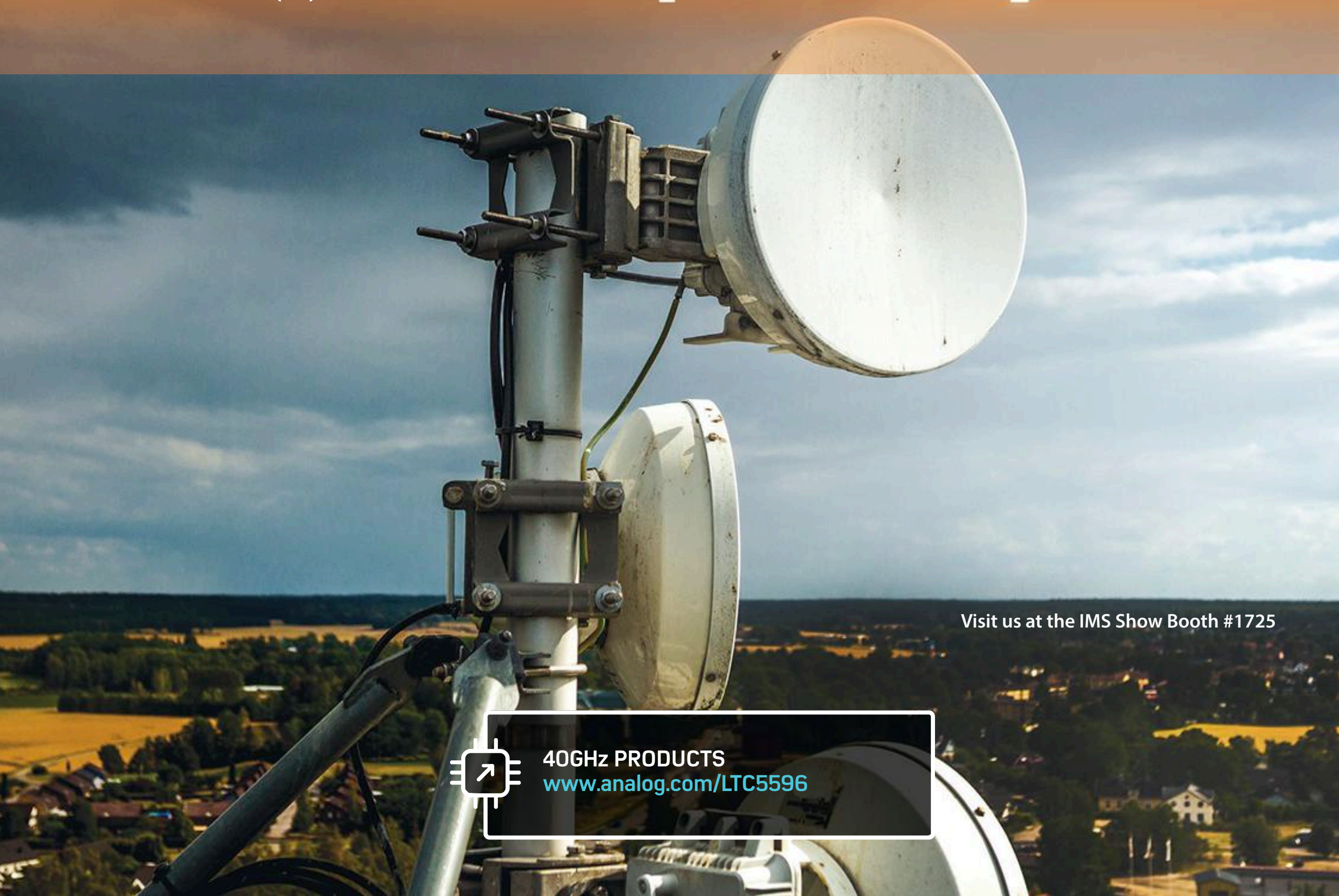

Visit us at the IMS Show Booth #1725

40GHz PRODUCTS
www.analog.com/LTC5596

JACK BROWNE | Technical Contributor
jack.browne@informa.com

More than Anything, IMS is About People

It's the single most anticipated technical event in the RF/microwave industry. The location changes from year to year, and may not always be convenient enough for many visitors. But the organizers of the 2018 IEEE MTT-S International Microwave Symposium (IMS) chose wisely in planning the event for Philadephia, Pa., and the Pennsylvania Convention Center in "The City of Brotherly Love."

The technical conference runs from June 10 through 15, while the exhibition floor is open from June 12 through 14. Both areas are expected to be packed for most of the week as this industry prepares for dramatic changes in how high-frequency devices and circuits are used around the world, including the billions of Internet of Things (IoT) devices (*see p. 118*) and potentially as many 5G smartphones and the infrastructures to support them.

Those two technologies—5G and IoT—are expected to transform many RF/microwave technologies into commodity items, simply because of the high-volume nature of each market. Many exhibitors at IMS will be ready with their explanations on how they plan to handle the expected growth from those two markets, including the increased use of millimeter-wave frequencies for increased bandwidth in 5G systems as well as the use of millimeter-wave circuits and devices in "self-driving" autonomous vehicles of the future.

A general feeling of excitement can be felt throughout the industry for these large-scale opportunities in high-frequency technology. It's also a different way of thinking for many designers. Many IoT products, for example, use wireless links at Wi-Fi or Bluetooth frequencies to make their connections to the internet. At one time, the hardware for those links sold as a device that was added to a computer to gain access to a wireless network. Now, with an IoT product, the wireless capability, including the antenna, is almost a "throw-away" part of the product, such as an IoT-controlled home thermostat.

RF/microwave designers are being asked to develop wireless/microwave antennas for IoT that add little to the product's total cost. Such cost controls involve efficient use of circuit materials as well as economic use of test equipment for design and, eventually, production testing. All this from an industry that once specialized in designing components that might have been required for only 10 radar or EW systems—and were priced more like custom designs than commodities.

The RF/microwave industry is perhaps witnessing more changes during this 2018 IMS than during any IMS of the past 30 years. It can be evidenced on the exhibition floor, where some of the top minds of the industry are ready to offer advice and guidance. For visitors to the 2018 IMS, this is a once-in-a-lifetime chance to meet designers and innovators and to perhaps start a relationship that will last a lifetime. Seeing new test equipment, software, and components is fun, but the real knowledge comes from the people at each booth and on the show floor, and the chances to see old friends and make some new ones. Have a safe show, everyone! mw

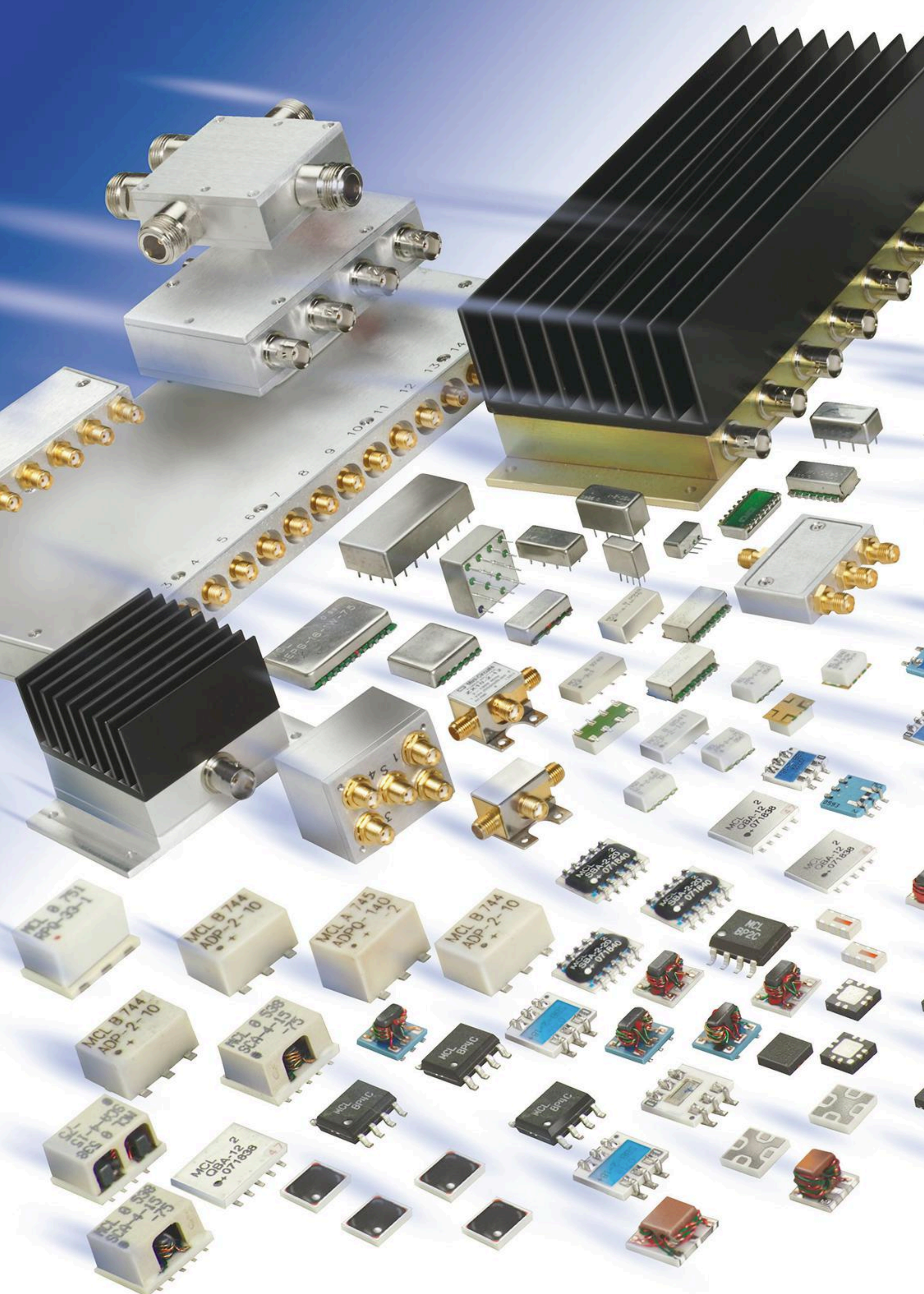

MCL B 744
ADP-2-10
MCL A 745
ADPQ-140
-2
MCL
QBA-12
071838
MCL
SBA-2-20
071840
MCL
BP2C
MCL
BP4C

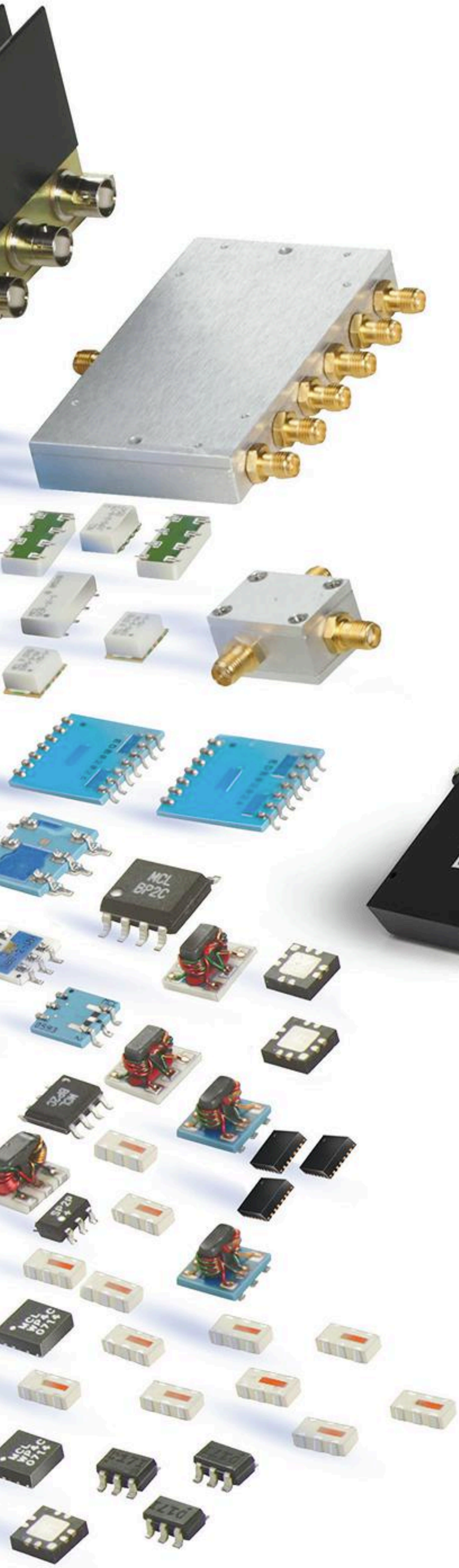

POWER SPLITTERS/ COMBINERS

from **2 kHz to 40 GHz** as low as 89¢ ea. (qty. 1000)

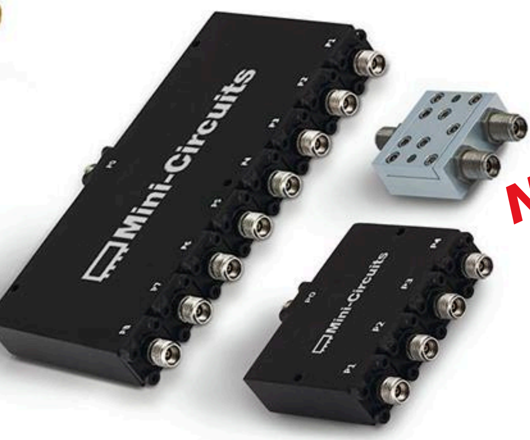

NEW!

COVERING 10 to 40 GHz IN A SINGLE MODEL

2-WAY ZN2PD-K44+
4-WAY ZN4PD-K44+
8-WAY ZN8PD-K44+

The industry's largest selection includes THOUSANDS of models from 2 kHz to 40 GHz, with up to 300 W power handling, in coaxial, flat-pack, surface mount and rack mount housings for 50 and 75Ω systems.

From 2-way through 48-way designs, with 0°, 90°, or 180° phase configurations, Mini-Circuits' power splitter/combiners offer a vast selection of features and capabilities to meet your needs from high power and low insertion loss to ultra-tiny LTCC units and much more.

Need to find the right models fast? Visit minicircuits.com and use Yoni2®! It's our patented search engine that searches actual test data for the models that meet your specific requirements! You'll find test data, S-parameters, PCB layouts, pricing, real-time availability, and everything you need to make a smart decision fast!

All Mini-Circuits' catalog models are available off the shelf for immediate shipment, so check out our website today for delivery as soon as tomorrow!

RoHS Compliant
Product availability is listed on our website.

Mini-Circuits®

www.minicircuits.com P.O. Box 350166, Brooklyn, NY 11235-0003 (718) 934-4500 sales@minicircuits.com 448 Rev U

Visit us at the IMS Show Booth #203

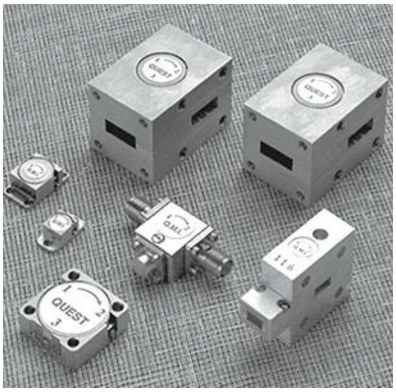

Microwaves&RF **MAY 2018**

EDITORIAL

EXECUTIVE DIRECTOR, CONTENT: **KAREN FIELD** karen.field@informa.com
TECHNICAL CONTRIBUTOR: **JACK BROWNE** jack.browne@informa.com
TECHNICAL ENGINEERING EDITOR: **CHRIS DeMARTINO** chris.demartino@informa.com
ASSOCIATE EDITOR/COMMUNITY MANAGER: **ROGER ENGELKE** roger.engelke@informa.com
ASSOCIATE EDITOR/COMMUNITY MANAGER: **JEREMY COHEN** jeremy.cohen@informa.com
ASSOCIATE CONTENT PRODUCER: **JAMES MORRA** james.morra@informa.com

ART DEPARTMENT

GROUP DESIGN DIRECTOR: **ANTHONY VITOLO** tony.vitolo@informa.com
CONTENT DESIGN SPECIALIST: **JOCELYN HARTZOG** jocelyn.hartzog@informa.com
CONTENT & DESIGN PRODUCTION MANAGER: **JULIE JANTZER-WARD** julie.jantzer-ward@informa.com

PRODUCTION

GROUP PRODUCTION MANAGER: **GREG ARAUJO** greg.araujo@informa.com
PRODUCTION MANAGER: **VICKI McCARTY** vicki.mccarty@informa.com

AUDIENCE MARKETING

USER MARKETING MANAGER: **DEBBIE BRADY** debbie.brady@informa.com

FREE SUBSCRIPTION / STATUS OF SUBSCRIPTION / ADDRESS CHANGE/ MISSING BACK ISSUES:
OMEDA **T** | 847.513.6022 **TOLL FREE** | 866.505.7173

SALES & MARKETING

MANAGING DIRECTOR: **TRACY SMITH** **T** | 913.967.1324 **F** | 913.514.6881 tracy.smith@informa.com

REGIONAL SALES REPRESENTATIVES:

AZ, NM, TX: **GREGORY MONTGOMERY** **T** | 480.254.5540 gregory.montgomery@informa.com

AK, NORTHERN CA, OR, WA, WESTERN CANADA: **STUART BOWEN** **T** | 425.681.4395 stuart.bowen@informa.com

AL, AR, SOUTHERN CA, CO, FL, GA, HI, IA, ID, IL, IN, KS, KY, LA, MI, MN, MO, MS, MT, NC, ND, NE, NV, OH, OK, SC, SD, TN, UT, VA, WI, WV, WY, CENTRAL CANADA: **JAMIE ALLEN** **T** | 415.608.1959 **F** | 913.514.3667 jamie.allen@informa.com

CT, DE, MA, MD, ME, NH, NJ, NY, PA, RI, VT, EASTERN CANADA:
SHANNON ALO-MENDOSA **T** | 978.501.9116 shannon.alo-mendosa@informa.com

INTERNATIONAL SALES:

GERMANY, AUSTRIA, SWITZERLAND: **CHRISTIAN HOELSCHER** **T** | 011.49.89.95002778
christian.hoelscher@husonmedia.com

BELGIUM, NETHERLANDS, LUXEMBURG, UNITED KINGDOM, SCANDINAVIA, FRANCE, SPAIN, PORTUGAL:
JAMES RHOADES-BROWN **T** | +011 44 1932 564999 **M** | +011 44 1932 564998 james.rhoadesbrown@husonmedia.com

ITALY: **DIEGO CASIRAGHI** diego@casiraghi-adv.com

PAN-ASIA: **HELEN LAI** **T** | 886 2-2727 7799 helen@twoway-com.com

PAN-ASIA: **CHARLES LIU** **T** | 886 2-2727 7799 liu@twoway-com.com

PLEASE SEND INSERTION ORDERS TO: orders@informa.com
INFORMA REPRINTS: **WRIGHT'S MEDIA** **T** | 877.652.5295
LIST RENTALS/ SMARTREACH CLIENT SERVICES MANAGER: **MARY RALICKI** **T** | 212.204.4284
mary.ralicki@informa.com

DIGITAL

GROUP DIGITAL DIRECTOR: **RYAN MALEC** ryan.malec@informa.com
CLIENT SUPPORT MANAGER: **KIM BLASKI** kim.blaski@informa.com

DESIGN ENGINEERING & SOURCING GROUP

EXECUTIVE DIRECTOR, CONTENT: **KAREN FIELD** karen.field@informa.com
VP OF MARKETING: **JACQUIE NIEMIEC** jacquie.niemiec@informa.com

INFORMA MEDIA INC.

605 THIRD AVENUE
NEW YORK, NY 10158 USA **T** | 212.204.4200

informa

Electronic Design | Machine Design | Microwaves & RF | Source ESB | Hydraulics & Pneumatics | Global Purchasing | Distribution Resource | Power Electronics | Defense Electronics

RF Amplifiers and Sub-Assemblies for Every Application

Delivery from Stock to 2 Weeks ARO from the catalog or built to your specifications!

- Competitive Pricing & Fast Delivery
- Military Reliability & Qualification
- Various Options: Temperature Compensation, Input Limiter Protection, Detectors/TTL & More
- Unconditionally Stable (100% tested)

ISO 9001:2000 and AS9100B CERTIFIED

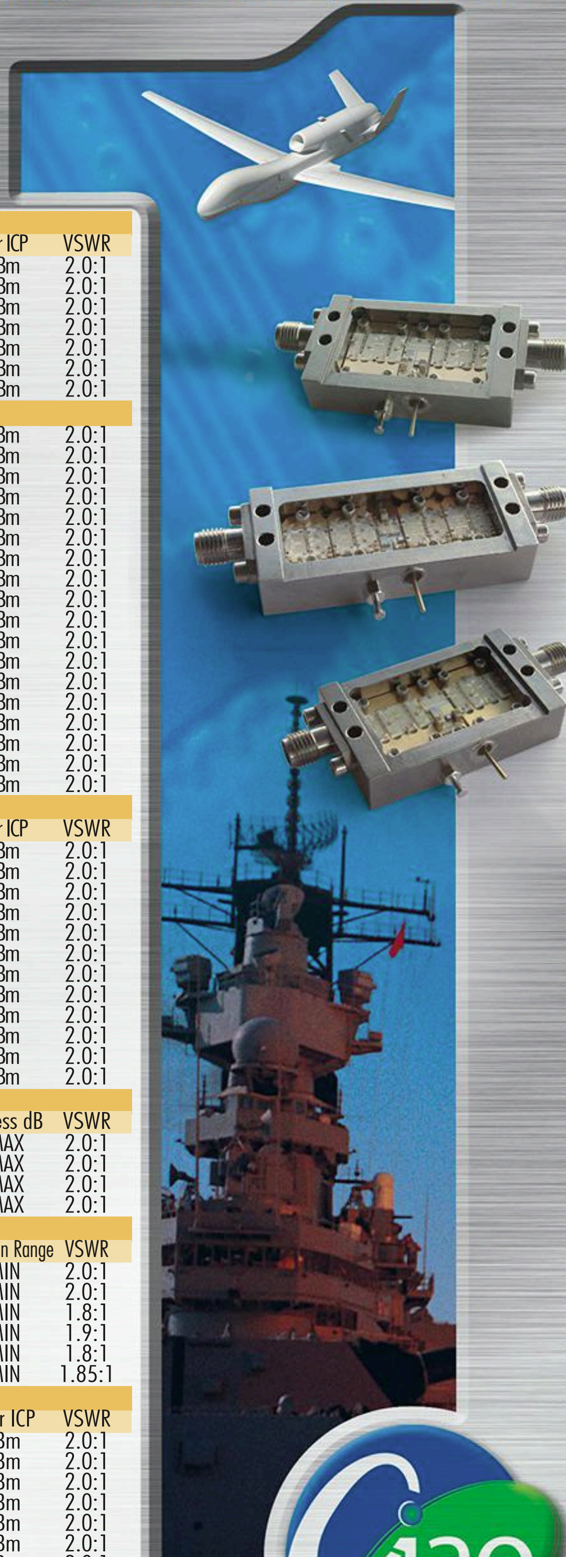

OCTAVE BAND LOW NOISE AMPLIFIERS

Model No.	Freq (GHz)	Gain (dB) MIN	Noise Figure (dB)	Power-out @ P1-dB	3rd Order ICP	VSWR
CA01-2110	0.5-1.0	28	1.0 MAX, 0.7 TYP	+10 MIN	+20 dBm	2.0:1
CA12-2110	1.0-2.0	30	1.0 MAX, 0.7 TYP	+10 MIN	+20 dBm	2.0:1
CA24-2111	2.0-4.0	29	1.1 MAX, 0.95 TYP	+10 MIN	+20 dBm	2.0:1
CA48-2111	4.0-8.0	29	1.3 MAX, 1.0 TYP	+10 MIN	+20 dBm	2.0:1
CA812-3111	8.0-12.0	27	1.6 MAX, 1.4 TYP	+10 MIN	+20 dBm	2.0:1
CA1218-4111	12.0-18.0	25	1.9 MAX, 1.7 TYP	+10 MIN	+20 dBm	2.0:1
CA1826-2110	18.0-26.5	32	3.0 MAX, 2.5 TYP	+10 MIN	+20 dBm	2.0:1

NARROW BAND LOW NOISE AND MEDIUM POWER AMPLIFIERS

Model No.	Freq (GHz)	Gain (dB) MIN	Noise Figure (dB)	Power-out @ P1-dB	3rd Order ICP	VSWR
CA01-2111	0.4 - 0.5	28	0.6 MAX, 0.4 TYP	+10 MIN	+20 dBm	2.0:1
CA01-2113	0.8 - 1.0	28	0.6 MAX, 0.4 TYP	+10 MIN	+20 dBm	2.0:1
CA12-3117	1.2 - 1.6	25	0.6 MAX, 0.4 TYP	+10 MIN	+20 dBm	2.0:1
CA23-3111	2.2 - 2.4	30	0.6 MAX, 0.45 TYP	+10 MIN	+20 dBm	2.0:1
CA23-3116	2.7 - 2.9	29	0.7 MAX, 0.5 TYP	+10 MIN	+20 dBm	2.0:1
CA34-2110	3.7 - 4.2	28	1.0 MAX, 0.5 TYP	+10 MIN	+20 dBm	2.0:1
CA56-3110	5.4 - 5.9	40	1.0 MAX, 0.5 TYP	+10 MIN	+20 dBm	2.0:1
CA78-4110	7.25 - 7.75	32	1.2 MAX, 1.0 TYP	+10 MIN	+20 dBm	2.0:1
CA910-3110	9.0 - 10.6	25	1.4 MAX, 1.2 TYP	+10 MIN	+20 dBm	2.0:1
CA1315-3110	13.75 - 15.4	25	1.6 MAX, 1.4 TYP	+10 MIN	+20 dBm	2.0:1
CA12-3114	1.35 - 1.85	30	4.0 MAX, 3.0 TYP	+33 MIN	+41 dBm	2.0:1
CA34-6116	3.1 - 3.5	40	4.5 MAX, 3.5 TYP	+35 MIN	+43 dBm	2.0:1
CA56-5114	5.9 - 6.4	30	5.0 MAX, 4.0 TYP	+30 MIN	+40 dBm	2.0:1
CA812-6115	8.0 - 12.0	30	4.5 MAX, 3.5 TYP	+30 MIN	+40 dBm	2.0:1
CA812-6116	8.0 - 12.0	30	5.0 MAX, 4.0 TYP	+33 MIN	+41 dBm	2.0:1
CA1213-7110	12.2 - 13.25	28	6.0 MAX, 5.5 TYP	+33 MIN	+42 dBm	2.0:1
CA1415-7110	14.0 - 15.0	30	5.0 MAX, 4.0 TYP	+30 MIN	+40 dBm	2.0:1
CA1722-4110	17.0 - 22.0	25	3.5 MAX, 2.8 TYP	+21 MIN	+31 dBm	2.0:1

ULTRA-BROADBAND & MULTI-OCTAVE BAND AMPLIFIERS

Model No.	Freq (GHz)	Gain (dB) MIN	Noise Figure (dB)	Power-out @ P1-dB	3rd Order ICP	VSWR
CA0102-3111	0.1-2.0	28	1.6 Max, 1.2 TYP	+10 MIN	+20 dBm	2.0:1
CA0106-3111	0.1-6.0	28	1.9 Max, 1.5 TYP	+10 MIN	+20 dBm	2.0:1
CA0108-3110	0.1-8.0	26	2.2 Max, 1.8 TYP	+10 MIN	+20 dBm	2.0:1
CA0108-4112	0.1-8.0	32	3.0 MAX, 1.8 TYP	+22 MIN	+32 dBm	2.0:1
CA02-3112	0.5-2.0	36	4.5 MAX, 2.5 TYP	+30 MIN	+40 dBm	2.0:1
CA26-3110	2.0-6.0	26	2.0 MAX, 1.5 TYP	+10 MIN	+20 dBm	2.0:1
CA26-4114	2.0-6.0	22	5.0 MAX, 3.5 TYP	+30 MIN	+40 dBm	2.0:1
CA618-4112	6.0-18.0	25	5.0 MAX, 3.5 TYP	+23 MIN	+33 dBm	2.0:1
CA618-6114	6.0-18.0	35	5.0 MAX, 3.5 TYP	+30 MIN	+40 dBm	2.0:1
CA218-4116	2.0-18.0	30	3.5 MAX, 2.8 TYP	+10 MIN	+20 dBm	2.0:1
CA218-4110	2.0-18.0	30	5.0 MAX, 3.5 TYP	+20 MIN	+30 dBm	2.0:1
CA218-4112	2.0-18.0	29	5.0 MAX, 3.5 TYP	+24 MIN	+34 dBm	2.0:1

LIMITING AMPLIFIERS

Model No.	Freq (GHz)	Input Dynamic Range	Output Power Range Psat	Power Flatness dB	VSWR
CLA24-4001	2.0 - 4.0	-28 to +10 dBm	+7 to +11 dBm	+/- 1.5 MAX	2.0:1
CLA26-8001	2.0 - 6.0	-50 to +20 dBm	+14 to +18 dBm	+/- 1.5 MAX	2.0:1
CLA712-5001	7.0 - 12.4	-21 to +10 dBm	+14 to +19 dBm	+/- 1.5 MAX	2.0:1
CLA618-1201	6.0 - 18.0	-50 to +20 dBm	+14 to +19 dBm	+/- 1.5 MAX	2.0:1

AMPLIFIERS WITH INTEGRATED GAIN ATTENUATION

Model No.	Freq (GHz)	Gain (dB) MIN	Noise Figure (dB)	Power-out @ P1-dB	Gain Attenuation Range	VSWR
CA001-2511A	0.025-0.150	21	5.0 MAX, 3.5 TYP	+12 MIN	30 dB MIN	2.0:1
CA05-3110A	0.5-5.5	23	2.5 MAX, 1.5 TYP	+18 MIN	20 dB MIN	2.0:1
CA56-3110A	5.85-6.425	28	2.5 MAX, 1.5 TYP	+16 MIN	22 dB MIN	1.8:1
CA612-4110A	6.0-12.0	24	2.5 MAX, 1.5 TYP	+12 MIN	15 dB MIN	1.9:1
CA1315-4110A	13.75-15.4	25	2.2 MAX, 1.6 TYP	+16 MIN	20 dB MIN	1.8:1
CA1518-4110A	15.0-18.0	30	3.0 MAX, 2.0 TYP	+18 MIN	20 dB MIN	1.85:1

LOW FREQUENCY AMPLIFIERS

Model No.	Freq (GHz)	Gain (dB) MIN	Noise Figure dB	Power-out @ P1-dB	3rd Order ICP	VSWR
CA001-2110	0.01-0.10	18	4.0 MAX, 2.2 TYP	+10 MIN	+20 dBm	2.0:1
CA001-2211	0.04-0.15	24	3.5 MAX, 2.2 TYP	+13 MIN	+23 dBm	2.0:1
CA001-2215	0.04-0.15	23	4.0 MAX, 2.2 TYP	+23 MIN	+33 dBm	2.0:1
CA001-3113	0.01-1.0	28	4.0 MAX, 2.8 TYP	+17 MIN	+27 dBm	2.0:1
CA002-3114	0.01-2.0	27	4.0 MAX, 2.8 TYP	+20 MIN	+30 dBm	2.0:1
CA003-3116	0.01-3.0	18	4.0 MAX, 2.8 TYP	+25 MIN	+35 dBm	2.0:1
CA004-3112	0.01-4.0	32	4.0 MAX, 2.8 TYP	+15 MIN	+25 dBm	2.0:1

CIAO Wireless can easily modify any of its standard models to meet your "exact" requirements at the Catalog Pricing.

Visit our web site at www.ciaowireless.com for our complete product offering.

Visit us at the IMS Show Booth #902

Ciao Wireless, Inc. 4000 Via Pescador, Camarillo, CA 93012

Tel (805) 389-3224 Fax (805) 389-3629 sales@ciaowireless.com

Ciao wireless

News

Wireless Amplifier Startup

Raises $3.8 Million in Funding

Guerrilla RF, a startup that supplies low-noise amplifiers for cellular base stations and small cells, said on Wednesday that it had raised $3.8 million in financing. The financial refuel comes with more than 50 products based its massive microwave integrated circuits shipping in production volumes.

"This year is off to a very fast start for us," said Ryan Pratt, co-founder and chief executive of Guerrilla RF, in a statement. "With multiple customer production ramps underway, it was clear we needed additional working capital." He added: "Based on the revenue growth we see, we believe we're in striking distance of profitability for the first time."

The Greensboro, N.C.-based company, which was founded after Pratt stepped down as an engineering director for Skyworks Solutions, has raised $11.6 million over the last five years. The company's investors include Bill Pratt, one of the founders of RF Micro Devices, which merged with Triquint Semiconductor to form Qorvo. ■

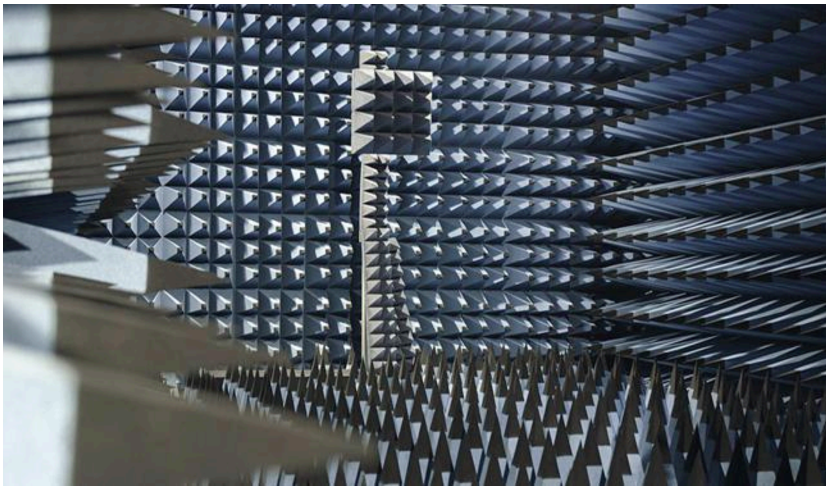

(Image courtesy of Fraunhofer Institute for Integrated Circuits)

ATM SYSTEMS AID Polish Air Stations

PARK AIR SYSTEMS an air-traffic-management (ATM) subsidiary of Northrop Grumman Corp., recently delivered its Sapphire ATM communications system equipment to four remote air stations in Poland, all serving the Warsaw Airport. The stations are located in Brzesk, Gabin, Radom, and Sieradz. The systems were delivered to the Polish Air Navigation Services Agency (PANSA) in December and were installed in first quarter 2018.

"PANSA was looking for an outstanding air-ground communications capability that is safe, reliable and easy to maintain," said Roman Drozdz, service director for Mawilux, Northrop Grumman's project integrator in Poland. "They found it in the market leading T6 radio, the smallest, lightest, and most environmentally friendly radio available."

The ATM systems rely on Northrop Grumman's Sapphire equipment, including its T6 tactical radios which use wideband AM waveforms at a standard VHF range of 118 to 137 MHz and a UHF range of 225 to 400 MHz. Installation of the equipment within these remote air stations will improve the coverage available to PANSA air traffic controllers based in Warsaw for communicating with military and civil aircraft.

"The feedback we received from PANSA following the training was very positive," said Danny Milligan, managing director, Park Air Systems, Northrop Grumman. "The dedicated training academy we have here at our UK facility and the tailored courses we can provide allowed us to exceed our customer's expectations."

The Sapphire radios are supplied with analog and IP interfaces for audio and data connections. These capabilities allow the radio systems to operate on the legacy networks, while also enabling transitions to the IP technology for future use. In its 50-year history, Northrop Grumman Park Air Systems has installed 60,000 radios in 180 countries around the world. ■

SUPERCONDUCTORS TEAM with Room-Temperature Circuits

IN PARTNERSHIP WITH the University of Massachusetts Amherst, superconductor specialist HYPRES Inc. *(www.hypres.com)* fabricated an energy-efficient digital data link between superconducting integrated circuits (ICs) and room-temperature electronic circuits. The team project was part of a Small Business Technology Transfer (STTR) project sponsored by the U.S. Office of Naval Research (ONR).

The project made it possible to achieve extremely high data rates at low signal levels by connecting low-power, cryogenically cooled superconducting ICs with room-temperature circuits and devices. The technique provides a way to reach signal sensitivity well beyond the range of room-temperature electronic circuits and devices.

The HYPRES superconducting ICs are based on single-flux-quantum (SFQ) logic and operate at a cryogenic temperature of 4K and at signal levels that would otherwise be buried by noise in room-temperature circuits and devices. (Note that absolute zero or zero degrees Kelvin, 0K, is equal to −273ºC.) The technology is attractive for electronic applications that can tolerate cryogenic operation or that require energy-efficient, high-speed data operation.

The research team developed a hybrid-temperature, heterogeneous-technology (HTHT) data link that distributes signal amplification among electronic stages at different operating temperatures, so that the overall data link can be optimized in terms of size, weight, and power (SWaP) consumption.

"Our approach was to start with the fastest superconductor output driver and connect it to a chain of cryogenic superconductor amplifiers at different temperatures between 4K and 300K," said Dr. Deepnarayan Gupta, president of HYPRES' Digital-RF Circuits and Systems business division and the principal investigator of the project. "We have already reached 20 Gb/s data rates per link using this approach, which is better than 14 Gb/s data links achieved without any cryogenic semiconductor amplification.

"We are now working towards enhancing the data link rate, as well as expanding the number of simultaneous channels with both electrical and optical approaches," Gupta added. "Better data links are vitally important to the next generation of our Advanced Digital-RF Receiver (ADR) product line *(see figure)* as well as for future applications, such as for streaming high-speed data processing, for which superconductor electronics offer compelling solutions."

Professor Joseph Bardin's group at the UMass Amherst deserves credit for the development of the key technology in the HTHT data link. "We pursued two alternative designs, both using silicon-germanium (SiGe) bipolar transistors," Bardin explained. "At cryogenic temperatures, these transistors produce higher gain and higher speeds. Through a careful design process, we have optimized the tradeoff between speed and power consumption for our cryogenic integrated circuits. Both designs have met our target performance metrics and now offer different alternatives to HYPRES' system engineers."

This combination of higher data communications speeds at lower power levels was well recognized by ONR program officer Dr. Deborah Van Vechten: "ONR encourages partnerships between university research groups and small businesses to harness innovative ideas into practical products. This team has moved through the different phases successfully and has attracted external funding to augment the STTR investment. The HTHT data link is now ready for transition." ■

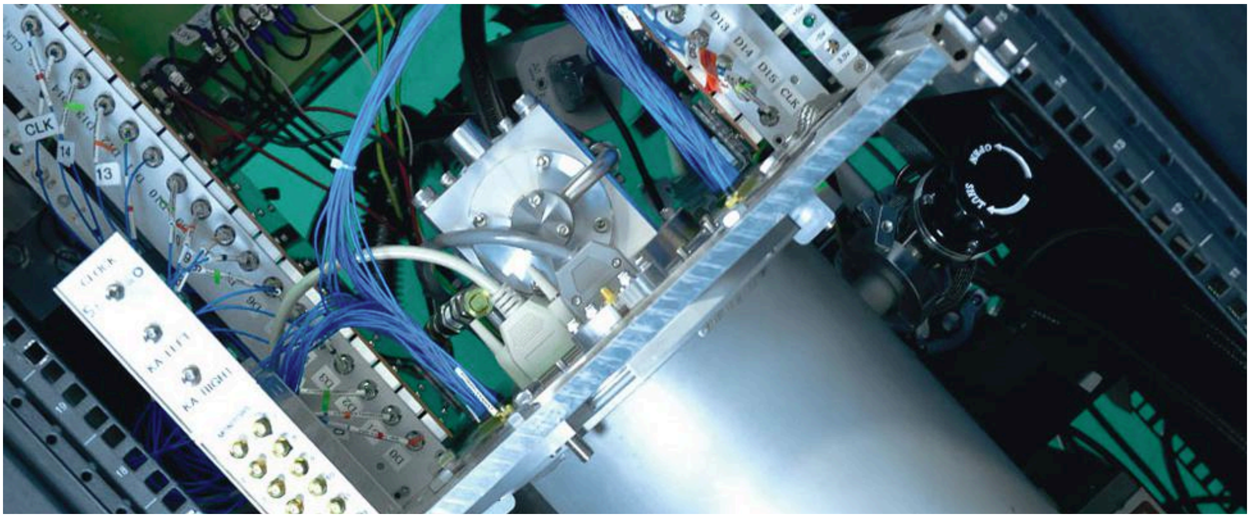

The HYPRES ADR product line will benefit from technology developed to enhance high-speed data links for the U.S. Navy. *(Graphic courtesy of HYPRES Corp.)*

MERCURY TEAMS WITH GREEN HILLS for Army Aviation Mission Displays

This is the type of BuiltSAFE ROCK-2 series of rugged computer systems that will benefit from the advances in graphics capabilities made possible for multiple-core-processor systems by Mercury Systems and Green Hills Software. *(Courtesy of Mercury Systems)*

AT THE RECENT Army Aviation Mission Solutions Summit in Nashville, Mercury Systems and Green Hills Software announced a joint collaboration leading to advances in next-generation flight display systems using multicore processor architectures. The graphics solution teams Mercury's BuiltSAFE hardware and software with a real-time operating system (RTOS) from Green Hills Software to achieve efficiencies in size, weight, and power (SWaP). There's a particular focus on avionics computers and display systems using enhanced vision systems (EVSs) and synthetic vision systems (SVSs) for degraded vision environments (DVEs).

Mercury's BuiltSAFE ROCK-2 subsystem features its OpenGL graphics suite. The subsystem is operated with Green Hills Software's INTEGRITY-178 time-variant unified multiprocessing RTOS with the FliteScene Digital Moving Map Software from Harris Corp. The INTEGRITY-178 scheduling mechanism results in a unified RTOS that provides time-variant scheduling of both asymmetric multiprocessing (AMP) and symmetric multiprocessing (SMP) applications simultaneously.

It also enables the creation of core affinity groups that define how processor cores will be used by graphics and other applications within the system. The combination of hardware and software conforms to the Future Airborne Capability Environment (FACE) V2.1 Technical Standard and enables multiple independent safety and/or security-critical applications to run within the ROCK-2's multicore operating environment in a predictable manner.

"The combination of Green Hills' operating system innovation with Mercury's hardware innovation delivers affordable and unparalleled technology leadership to the Army aviation community," said Ike Song, VP and general manager of Mercury Mission Systems. "Out-of-the-box support for Harris' FACE V2.1-conformant FliteScene software on the ROCK-2 delivers on the interoperability and portability objectives of the FACE technical standard, while eliminating the cost and design risk associated with deploying advanced digital map capabilities." ■

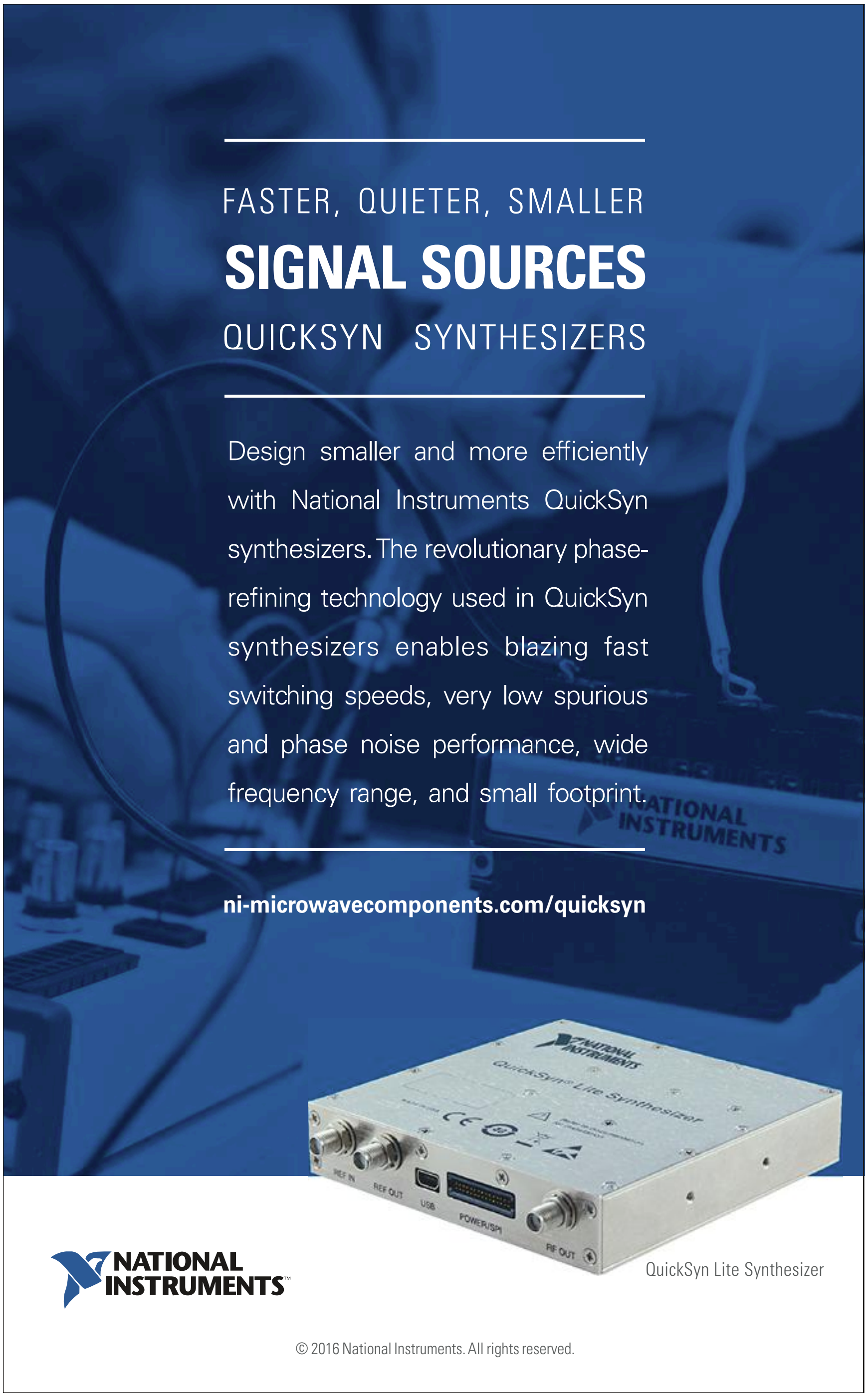

AIR FORCE, RAYTHEON Seek to Speed Software Development for GPS OCX

This is an artist's conception of how the OCX system will control legacy and newer GPS satellites for civilian and military applications. *(Courtesy of the USAF)*

MILITARY DEVELOPMENT AND PROCUREMENT of software has been typically over budget and behind schedule, although the Pentagon and industry leaders such as Raytheon Co. hope to change these trends. One of the key development programs is the operational control system for the GPS, known as OCX.

The OCX development program was initially managed by the U.S. Air Force, but transferred to the Department of Defense (DoD) because of the USAF's slow pace. The next-generation OCX program is obviously critical to all allied defense forces. And as Ellen Lord, undersecretary of defense for acquisition and sustainment for the DoD notes, "It's a program that I have spent quite a bit of time on." In working closely with industry partner and OCX prime contractor Raytheon, Lord was recently part of an OCX program review that included USAF Assistant Secretary for Acquisition Will Roper and Tom Kennedy, CEO of Raytheon.

Military programs have had a long history of problems with timely software development, with the OCX program one of the best-known programs suffering delays due to lack of software modernization and for using software development methods that were abandoned by the commercial industry many years earlier. By using "agile development" methods, the industry creates new versions of software quickly, even when understanding that additional versions will be needed based on user feedback concerning required improvements.

By not trying to get everything right the first time, this agile development approach helps speed software releases at a much faster pace than in military programs where the effort is made to get everything correct the first (and only) time. However, according to Lord, OCX software development was moving to an agile approach to speed the program: "I believe we are at an inflection point in terms of doing things differently. We are pivoting from the traditional waterfall software development methodology to agile development. So we are coding every day, testing every night."

The OCX program is designed to develop a system that will command all newer and legacy GPS satellites, manage all civilian and military GPS signals, and provide improved cyber security (see the conceptual image of the OCX system). The DoD has hired Jeff Boleng, former chief technology officer of Carnegie Mellon University Software Engineering Institute, to help repair the OCX and other military software problems, including software for the F-35 Joint Strike Fighter (JSF). Boleng is joining Lord's staff as special assistant for software acquisition. ■

MODELING EFFECTS OF Human Bodies on Indoor Wireless Systems

As applications for wireless signals continue to grow, signal propagation is taking place both indoors and outdoors, with indoor wireless systems having to operate among numerous interfering objects, including human bodies. Indoor applications are seeing a steady stream of new devices, including safety sensors and other Internet of Things (IoT) wireless monitors that can be tracked via wireless local area networks (WLANs). However, humans sometimes get in the way—literally. Human bodies can serve as interference for indoor wireless channels, resulting in absorption of limited signal power and changes in signal time and phase.

Fortunately, researchers at the Norwegian University of Science and Technology, Trondheim, developed a dynamic channel model for indoor wireless communications systems. It's based not on statistical evidence, but rather on measured results, showing the different conditions where someone passing through a line-of-sight (LOS) indoor wireless signal could cause significant signal fading.

Drawing from previous studies on the behavior of conducting cylinders at microwave frequencies, in particular a single-cylinder interference model of the human body,

The researchers were able to approximate the effects of a human body on RF/microwave fading in an indoor environment. But the previous model, with only one cylinder, was considered an oversimplification of the signal absorption and reflection brought about by a human body with its many moving parts, and when a human body is moving through an indoor electromagnetic (EM) operating environment.

The research team assumed a human-body model with 12 moving parts and represented it with 12 dielectric cylinders of different radii. The one body part considered an exception was the head, which was represented by a sphere. A human walking model was also developed to describe the movements of the different body parts and how those movements could affect the radio waves in that environment.

Applying data from biomechanical and robotic studies on human movements as part of walking gaits, the researchers built a database of interacting moving body parts and their effects on time-varying wireless channels. Moving parts were synchronized starting with left-leg motion and using relative time to record the phase changes of the different body parts during one full cycle of body motion.

The research team also considered the contributions of signal fading due to the absorption and reflection of signals by the indoor environment, with its walls, floor, and ceiling. They used measured relative permittivity values of different dielectric materials at a number of different frequencies (even through millimeter-wave frequencies) to gauge the impact of the human-body model on wireless channel characteristics in different types of indoor environments.

The extensive measurements made by the team, particularly at 2.45 GHz, support the accuracy of their indoor human-body model. By using the received signal strength of an LOS signal as a reference, they compared their human body model to collected data and a single-cylinder simulation, with their model showing close agreement with different references. Measurements were taken at different heights within the indoor environment to better understand the effects of both lower and upper human body parts on the wireless radio environment.

See "A Dynamic Channel Model for Indoor Wireless Signals," *IEEE Antennas & Propagation Magazine*, Vol. 60, No. 2, April 2018, p. 82.

BOOSTING THE BANDWIDTH of Triangular Microstrip Antennas

AS MORE DEVICES and services compete for wireless bandwidth in emerging applications such as Internet of Things (IoT) sensors in factories, warehouses, even in "smart homes," broadband antennas become a key high-frequency component of interest. Numerous antenna technologies are available, but microstrip antennas (MSAs) provide miniature, low-profile solutions for many short-range communications links.

In exploring the different possibilities of MSAs, researchers from the Dwarkadas Jivanlal Sanghvi College of Engineering at the University of Mumbai, India, experimented with the concept of increasing the isosceles angle in isosceles triangular microstrip antennas (ITMSAs) to increase antenna bandwidth. They discovered it is a viable and repeatable approach to boost triangular microstrip antenna bandwidth.

The research team learned that increasing the isosceles angle in a triangular MSA tunes the spacing between the microstrip patch and its resonant modes as part of the path to achieving wider microstrip patch antenna responses. Using extensive computer simulations, inevitably backed by measurements of actual microstrip antenna hardware, the team studied the magnetic- and electric-field patterns of the different microstrip triangle and slot patterns to determine what delivered not only the widest bandwidths, but the most repeatable EM responses.

By tuning the second-order transverse magnetic TM11 mode frequency and third-order TM20 model frequency with respect to the fundamental TM10 mode frequency, they were able to optimize the bandwidth for a particular triangular microstrip antenna pattern. Using slots cut into the microstrip patterns to work with the three resonant modes, they achieved maximum bandwidths of more than 1 GHz (or a 65% bandwidth). Some of the slot-cut patterns also provided broadside radiation patterns with as much as 8-dBi gain.

See "Broadband Variations of Isosceles Triangular Microstrip Antennas," *IEEE Antennas & Propagation Magazine,* Vol. 60, No. 2, April 2018, p. 34.

Show Preview

JACK BROWNE | Technical Contributor

Philadelphia Opens Its Doors to 2018 IMS

As the applications extrapolate for wireless devices and interest grows in millimeter-wave frequencies, the RF/microwave industry gathers together with great optimism for the future.

1. The IEEE International Microwave Symposium comes to Philadelphia, the "City of Brotherly Love," in 2018, in the Pennsylvania Convention Center. *(Courtesy of Thinkstock)*

Heightening interest for high-frequency applications, even through millimeter-wave (mmWave) frequencies, has the RF/microwave industry buzzing more than ever. Now the time has arrived for all involved to gather and share their thoughts and goals at a most appropriate site: Philadelphia, the City of Brotherly Love. In a town best known for its competitive spirit and "never-give-up" attitude *(Fig. 1)*, the RF/microwave industry will celebrate a world thirsting for high-frequency electronics.

From RF through mmWave frequencies and beyond, in everything from automotive radars and wireless Internet of Things (IoT) devices in "smart homes" to military electronic-warfare (EW) systems and fifth-generation (5G) wireless communications networks—all will be on display at the industry's leading event: The IEEE International Microwave Symposium (IMS), running from June 10-15 at the Pennsylvania Convention Center.

It's an event that combines a high-quality technical conference and a show floor with more than 500 exhibiting companies. For many, it's once-a-year chance to catch up with friends and competitors and to learn something new from the workshops, conferences, and technical sessions. Long-running "events-within-the-event," such as

IMS is an event that combines a high-quality technical conference and a show floor with more than 500 exhibiting companies. For many, it's once-a-year chance to catch up with friends and competitors and to learn something new from the workshops, conferences, and technical sessions.

the Automatic RF Techniques Group (*ARFTG, see p. 50*) and the Radio Frequency Integrated Circuit (RFIC) conference *(see p. 38)*, provide focused opportunities to learn about the latest developments in test and measurement as well as integrated circuits (ICs) and semiconductors, respectively.

The technical conference begins on Sunday, June 10, with workshops and short courses, followed by a pair of plenary talks and invited technical presentations throughout the week. The exhibition hall opens each morning at 9:30 AM starting Tuesday, June 12, wrapping up at 5 PM on Tuesday and Wednesday and with a shorter day on Thursday, June 14 (closing at 3 PM).

The exhibition hall is as much a social gathering as a business event, with a fairly large portion of visitors knowing some of the booth personnel before entering the exhibition hall. Each exhibition booth is designed to show the strengths of each company, often with active displays of products that visitors can start and stop to learn more about each product in a short time. For systems-level specifiers, the annual IEEE IMS is the opportunity to fill a list of RF/microwave components for radar, EW, communications, or even automotive safety systems, whether the requirements are for a commercial, industrial, or military design.

For system-level specifiers in commercial, industrial, and military markets, IMS is something like a "supermarket," with an opportunity to stroll from booth to booth to examine samples of each company's products. In recent years, specifiers working in additional market areas, such as medical electronics, have shown an interest in RF/microwave components and have scheduled time at the annual show.

Walking the IMS exhibition floor can easily take more than the scheduled three days, especially when the first stop is a test-and-measurement company with a variety of new "toys" on display. Experienced IMS visitors have learned to budget their time on the show floor, especially when one of their goals is to use the IMS exhibition to fill a need for a particular product. No matter the type of RF/microwave product, more than a few of each can be found on the 2018 IMS exhibition floor, with personnel at each company's exhibition booth more than willing to discuss a product's design approach and optimum application.

The annual IMS has traditionally been the best time and place to compare some of the top products for any type of component, software, or test equipment. Just to see all of the amplifiers on display could take more than a full day on the exhibition floor before taking time to visit company booths with additional active components, passive components, materials, software, and test equipment on display. While this preview of the 2018 IEEE IMS Exhibition can barely hint at the number of high-quality items populating the show floor in Philadelphia, the hope is that readers planning to attend will at least find something of interest here and its accompanying booth for which to start each day.

AMPLIFIERS ANYONE?

The 2018 IEEE IMS represents one of the largest collections of RF/microwave amplifiers under one roof, with amplifiers on display for hundreds of different applications in every imaginable package style. In terms of bandwidth, the BZ-00105000-700521-325525 from B & Z Technologies **(Booth 1202)** may cover as much frequency range as any one unit (and with one of the largest model numbers to match), with at least 21 dB gain and more typically 25-dB gain from 100 MHz to 50 GHz. It's what is now known as a "standard" amplifier package, with 2.4-mm female coaxial connectors, measuring 29.9 × 18.7 × 7.6 mm. The compact amplifier remains stable with temperatures from −55 to +85°C, with noise figure of 7 dB or better and typically 5 dB. The 50-Ω amplifier draws 195 mA from +12 to +15 V dc.

Another company known for its broadband amplifiers, as well as for being formerly MITEQ and Narda (and both being high-frequency innovators based on Long Island, N.Y.), is L3 Narda-MITEQ **(Booth 535)**. Each original firm has almost 50 years of service to the RF/microwave industry. Among the combined company's many components and subassemblies for commercial and military customers, the model TTA1840-35-HG is an in-stock tabletop amplifier (with external power supply) with wide bandwidth of 18 to 40 GHz. It delivers at least 45-dB gain with no higher than 3.5-dB noise figure over that frequency range, making it a strong candidate for boosting testing signals well into the mmWave frequency range.

Broadband RF/microwave amplifiers will also be on display at Ciao Wireless **(Booth 902)**, with some models reaching 40 GHz. A recently developed line of low-noise amplifiers (LNAs) in coaxial packages have integrated output power

When Everything is Important...
the NEW *Clarity™ Series* is the *Clear Choice*

Applications:

Research & Development Labs
VNA Test Port Extension Cables
High Volume Production Test
Bench or Portable Test equipment
RF Module Testing

Industry leading performance, unparalleled value, and stock to 4-week lead times.

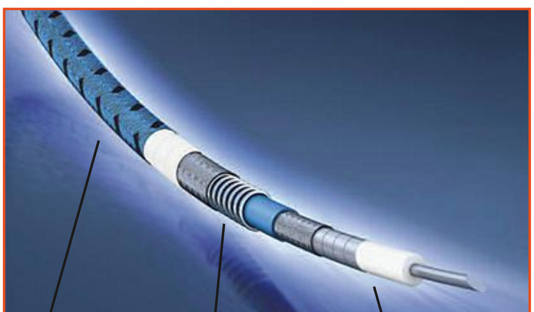

Phase stability <3.5°
Guaranteed up to 50,000 flexes
Super-sharp Sure-Grip™ knurl
Ergonomically designed Sure-Grip™ molding

TIMES MICROWAVE SYSTEMS
An Amphenol Company

World Headquarters: 358 Hall Avenue, Wallingford, CT 06492 • Tel: 203-949-8400, 1-800-867-2629 Fax: 203-949-8423
International Sales: 1+ 203 949 8503 • 1+ 800 867 2629
China Sales: TMC Building 4, No. 318 Yuanshan Road, Xinzhuang Industrial Park, Shanghai, China 201108 Tel: 86-21-5176-1209 Fax: 86-21-64424098

www.timesmicrowave.com

Visit us at the IMS Show Booth #1248

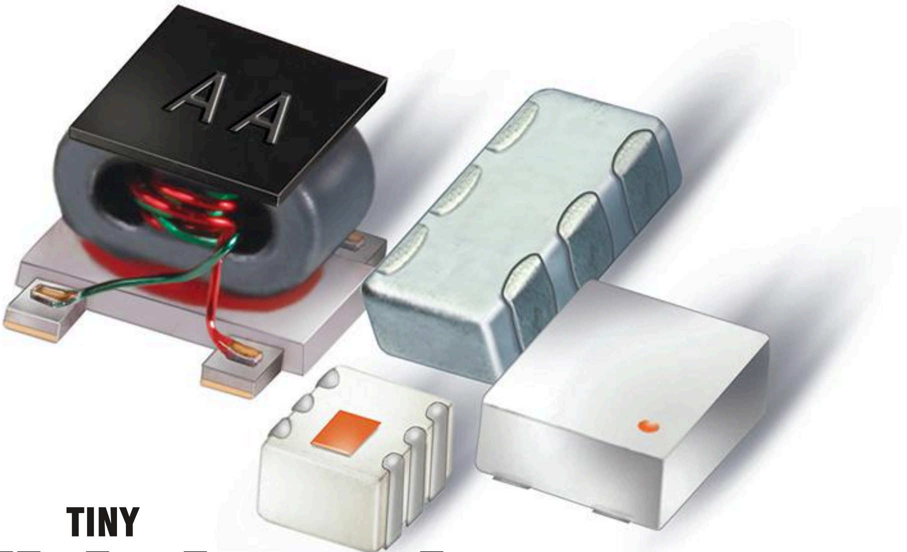

TINY

Wideband Transformers & Baluns!

NOW!

4 kHz - 18 GHz *From* 99¢ *ea.(qty.20)*

To support an even wider range of applications, Mini-Circuits tiny surface-mount transformers and baluns now cover frequencies from 4 kHz up to 18 GHz! Our latest designs achieve consistent performance across very wide frequency bands, and our baluns have demonstrated great utility for use with chipsets. With over 250 trusted models in stock representing a wide selection of circuit topologies and impedance ratios, chances are, we have a solution for your needs!

Our Low Temperature Co-Fired Ceramic (LTCC) models provide reliable performance in tough operating conditions, tiny size – as small as 0603 – and very low cost. All core-and-wire models are available with our exclusive Top Hat® feature, improving pick-and-place accuracy and throughput. We even manufacture our own transmission wire under rigorous control and use all-welded connections to ensure reliability and repeatability you can count on.

Visit minicircuits.com and use **Yoni2**®, our patented search engine to search our entire model database by performance criteria and find the models that meet your requirements. Order today and have them in hand as soon as tomorrow! Cost-effective custom designs and simulations with fast turnarounds are just a phone call away!

TC *0.15" x 0.15"*

NC *0.08 x 0.05"* *Ceramic*

NCR2 *0.08 x 0.10"* *Ceramic*

TCW *0.06 x 0.03"* *Ceramic*

RoHS compliant.

Mini-Circuits®

www.minicircuits.com P.O. Box 350166, Brooklyn, NY 11235-0003 (718) 934-4500 sales@minicircuits.com

Visit us at the IMS Show Booth #203

528 rev B

detectors with bandwidth as wide as 10 MHz to 40 GHz, so that users can adjust the operating voltage as a function of output power. The amplifiers are available with choices of gain, such as 20, 25, 30, and 35 dB, and provide enough bandwidth to cover multiple communications frequency bands with a single amplifier. Amplifier output power is typically +15 dBm with spurious levels of typically –60 dBc.

Although not a company name that might immediately come to mind when thinking of RF/microwave amplifiers, Maury Microwave **(Booth 1525)** has developed its MPA Series of broadband amplifiers to work with test equipment, such as signal generators, which might need a boost in level to enable a measurement. The MPA Series of instrumentation amplifiers covers frequency bands from 0.7 to 26.5 GHz with generous gain levels and as much as 50 W saturated output power. These GaN-based amplifiers include models covering 0.7 to 6 GHz, 2 to 6 GHz, 2 to 18 GHz, 6 to 18 GHz, 8 to 12 GHz, and 18 to 26.5 GHz. *(For more on the MPA Series amplifiers, see p. 124).*

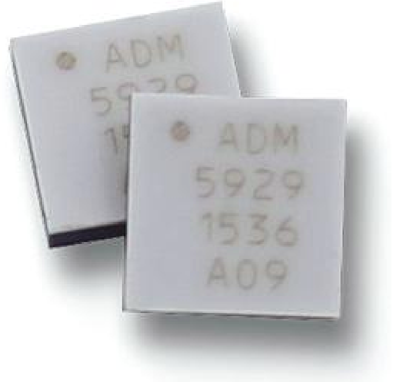

2. These miniature amplifiers have been developed to drive LO signals used with microwave mixers. *(Courtesy of Marki Microwave)*

3. The surface-mount LO-driver amplifiers of Fig. 3 are also available in coaxial form. *(Courtesy of Marki Microwave)*

Another firm that may not be on the top of the list for amplifier suppliers, Marki Microwave **(Booth 2031),** is well known for the quality of its frequency mixers and recently unveiled line of GaAs pHEMT MMIC amplifiers designed to complement those mixers as local-oscillator (LO) drivers. The RoHS-compliant, broadband amplifiers are available as bare die, in SMT housings *(Fig. 2)* such as 3- × 3-mm or

4- × 4-mm QFN packages, and as packaged amplifier modules with coaxial connectors *(Fig. 3)*. The amplifiers are designed to work with a wide range of LO sources, and feature rise times in excess of 10 ps.

As an example of the ADM line of broadband amplifiers, model ADM-0026-5929SM is a GaAs pHEMT distributed amplifier with typical small-signal gain of 13 dB from dc to 26.5 GHz. It has a typical noise figure of 5.5 dB across that wide frequency range with +15 dBm typical output power at 1-dB compression. The 50-Ω amplifier is unconditionally stable and typically draws about 165 mA from a +5-V dc supply. In addition to driving LO signals for mixers, it's well-suited for use in test-and-measurement and EW applications.

One of the more diversified collections of components for anyone stopping at a 2018 IMS booth will be that of Mini-Circuits **(Booth 203)**, with active and passive components for commercial and military applications as well as a growing lineup of equipment for making measurements on such component types. The company offers a tremendous assortment of products just in terms of RF/microwave amplifiers, including LNAs and power amplifiers.

For example, model ZVA-213UWX+ *(Fig. 4)* is a coaxially packaged amplifier that achieves low noise figure even across such a wide bandwidth of 0.1 to 20.0 GHz. The noise figure is typically 3.5 dB to 6 GHz, 2.5 dB from 6 to 12 GHz, 2.7 dB from 12 to 18 GHz, and 3.4 dB from 18 to 20 GHz. It provides at least 13-dB gain across the full frequency range, with +13 dBm or higher output power from 0.1 to 20.0 GHz. The LNA measures 130 × 0.98 × 0.56 in. with 2.92-mm coaxial connectors.

4. This broadband amplifier (model ZVA-213UWX+) maintains low noise figure (3.4 dB or less) from 0.1 through 20.0 GHz. *(Courtesy of Mini-Circuits)*

Mini-Circuits also provides much more output power (from a much larger unit) when needed, with its model 100W-63+ Class AB power amplifier *(Fig. 5)*. This robust unit delivers 100 W saturated output power from 2.5 to 6.0 GHz while drawing 8 A from a +30-V dc supply. Suitable for radar and communications systems, it's somewhat larger than the LNA, measuring 6.0 × 9.1 × 1.2 in. with SMA connectors. It's capable of 58-dB gain across the frequency range while maintaining ±2-dB typical gain flatness. It can be supplied with an optional fan attachment to keep things cool.

5. This Class AB power amplifier delivers 100 W saturated output power from 2.5 to 6.0 GHz. *(Courtesy of Mini-Circuits)*

With a long history of unveiling new microwave amplifiers at the annual IEEE IMS exhibition, CTT **(Booth 1213)** will keep its streak alive with two new GaN-based amplifiers in compact coaxial packages. Model AGN/145-5064 *(Fig. 6)* only measures 3.76 × 4.55 × 0.77 in., but delivers 100 W CW output power from 13.75 to 14.50 GHz. The robust little amplifier is a good fit for satellite-communications (satcom) uplinks and data links. For more bandwidth but less power, model AGX/180-4656 *(Fig. 7)* covers 3.0 to 18.0 GHz with 40 W CW output power in a package size of 5.16 × 4.90 × 0.28 in. With its wide bandwidth and power, it's a match for multiband satcom systems as well as for military electronic-warfare (EW) jammers.

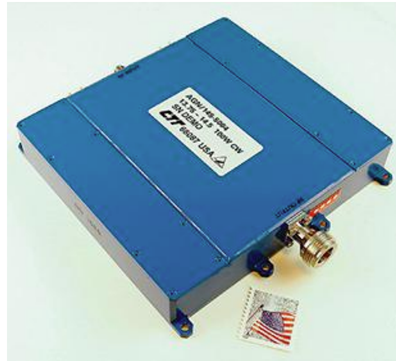

6. This miniature amplifier relies on GaN semiconductors to achieve 100 W CW output power from 13.75 to 14.50 GHz.

7. The AGX/180-4656 broadband amplifier covers 3 to 18 GHz with 40 W CW output power.

Elite RF LLC **(Booth 307)** will also show its diversity of high-frequency amplifiers at the 2018 IMS, with compact LNAs through 18 GHz and power amplifiers as well as multiple-function instrumentation amplifiers for test purposes. The amplifiers are based on optimized use of available high-frequency semiconductor technologies, such as silicon LDMOS and GaN active devices.

8. This LNA maintains a noise figure of 1.5 dB from 0.5 to 8.0 GHz. *(Courtesy of Elite RF LLC)*

9. Compact amplifiers such as this, with proper thermal design, can reach 100 W pulsed output power from 2.7 to 3.1 GHz. *(Courtesy of Elite RF LLC)*

As an LNA example, model M.50008G2144VV is designed for pulsed, modulated, and CW signals from 0.5 to 8.0 GHz *(Fig. 8)*. The Class A linear amplifier provides 38-dB gain with ±1-dB gain flatness and typical noise figure of 1.5 dB across the frequency range. It also generates +21 dBm output power at 1-dB compression. It's available for a number of different voltage supplies, with versions for +9 to +15 V dc, +18 to +50 V dc, and +5 V dc. The amplifier measures 3.5 × 3.0 × 1.0 in. with SMA connectors.

For more power and less bandwidth, the firm also offers the M2.73.1G503948 with 100 W of pulsed output power (at 20% duty cycle) from 2.7 to 3.1 GHz *(Fig. 9)*. The Class AB amplifier has 39-dB gain and operates on a +48-V dc supply. It comes equipped with a number of protective circuits, including protection from thermal overload, overvoltage, and overcurrent conditions. The amplifier measures 9.0 × 4.0 × 1.5 in. with SMA connectors. As with other Elite RF amplifiers, it has a five-year warranty.

Long-time RF/microwave supplier and regular IMS exhibitor, MACOM **(Booth 1125)**, will show a sampling of its large variety of high-frequency components and subsystems for commercial, industrial, and military applications, such as a new line of low-phase-noise amplifiers. The product family includes the model MAAL-011151-DIE distributed amplifier die with 17-dB linear gain from 2 to 18 GHz. Perhaps most impressive across that wide frequency range is its phase noise of a mere –154 dBc/Hz offset 1 kHz from the carrier. The amplifier chip also features a low 4-dB noise figure measured at 8 GHz and +16 dBm output power at 1-dB gain compression. The input and output ports are matched to 50 Ω and dc-blocked for ease of use, with typical return loss of better than 15 dB.

MACOM will also exhibit its model MADT-011000 single-ended, internally matched power detector for use from 5 to 44 GHz. Capable of detecting signal levels over a dynamic range of 30 dB, the detector is well-suited for applications in test equipment, radar, and microwave radios. It consumes only 70 μA current from a +4.5-V dc supply. It comes in a 3- × 3-mm, 16-lead QFN package or in bare die format, with electrostatic-discharge (ESD) protection.

Another manufacturer of amplifiers, the Beverly Microwave Div. of Communications & Power Industries (CPI) **(Booth 1149)**, will display, among many others, newer pulsed power amplifiers based on solid-state GaN transistors. The GaN power amplifiers are available for applications at L-, S-, C-, and X-band frequencies and include built-in-test (BIT) and programmable control. Typical operating parameters at S-band frequencies, for example, include 1.3 kW peak power at 10% duty cycle from 2.7 to 2.9 GHz. For those preferring electron tubes, the firm still designs and builds power amplifiers on traveling-wave tubes (TWTs) and other vacuum devices.

NuWaves Engineering **(Booth 2541)** will feature its RF/microwave amplifiers for military and aerospace applications at the show. As an example, the NuPower 11B02A *(Fig. 10)* delivers 10 W typical output power (7 W minimum) from 200 to 2600 MHz in a

10. Efficient lightweight amplifiers like the NuPower 11B02A provide 10 W output power from 200 to 2600 MHz for UAV applications. *(Courtesy of NuWaves Engineering)*

small, lightweight package well-suited for use in unmanned aerial vehicles (UAVs) in defense systems. It can provide its rated output power with only +3 dBm output power due to 38.5-dB gain. It offers three different operating settings to conserve power as needed. The amplifier measures 2.34 × 1.96 × 0.62 in. and weighs just 2 oz. In spite of the compact size, the amplifier can be equipped with an optional fan-cooled heat sink for enhanced reliability under harsh conditions.

Qorvo **(Booth 725)** will be active with its many IC-based products for advanced driver-assistance systems (ADAS) and 5G applications. Its patented Spatium RF/microwave PAs employ GaN device technology with novel power-combining techniques to support a wide range of applications in EW, radar, and military and commercial communications systems. For example, the KA120W-2731 delivers 100-W saturated output power from 27.5 to 31.5 GHz with 21-dB small-signal gain and 19% power-added efficiency. It's designed as a superior SWaP alternative to traveling-wave-tube amplifiers (TWTAs) for many of these applications.

REACHING FOR HIGHER MILLIMETER WAVES

THE 2018 IEEE Radio Frequency Integrated Circuit Symposium will be held at the Pennsylvania Convention Center in conjunction with the 2018 IEEE IMS. It begins on Sunday, June 12, with opening plenary sessions, and continues through June 11 and 12 with a variety of workshops and technical sessions.

Technical activities on Monday, June 11 include, for example, panel sessions on building blocks for 5G transceivers, advances in packaging and modeling, and techniques for synthesizing high-frequency signals. Presentations feature coverage of 28-GHz phased-array technology, the use of high-speed analog-to-digital converters (ADCs) in mixed-signal system designs, mmWave CMOS ICs for phased-array systems, and low-power radios for security applications.

The following day (June 12) provides coverage of mmWave power amplifiers, mmWave radar systems and beamforming techniques for those systems, and mmWave low-noise amplifiers (LNAs) along with receiver front ends. The emphasis is clearly on higher-frequency signals and how to generate and process them, for use in such emerging applications as ADAS vehicular electronics and 5G wireless networks.

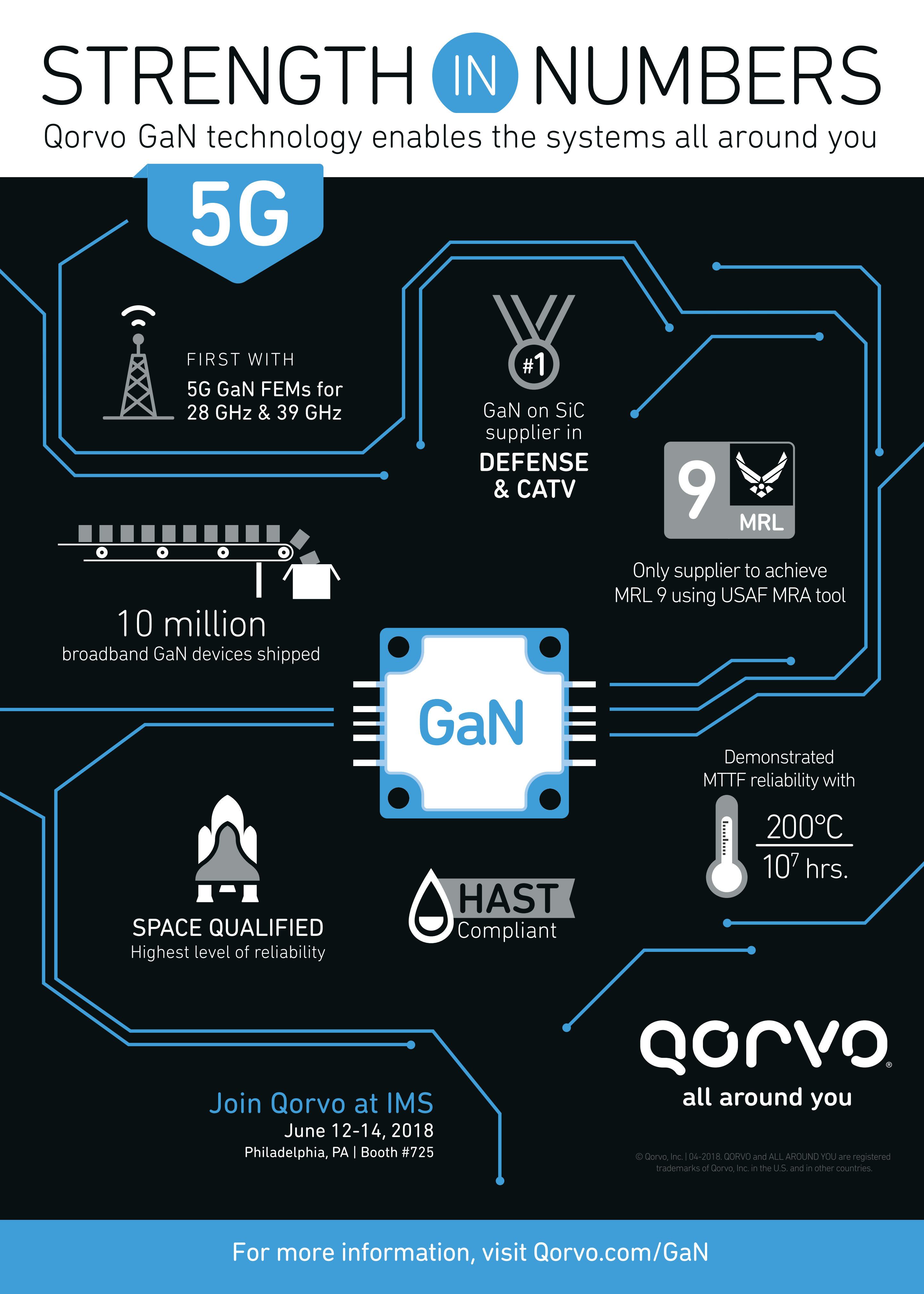
STRENGTH IN NUMBERS
Qorvo GaN technology enables the systems all around you
5G
FIRST WITH
5G GaN FEMs for 28 GHz & 39 GHz
#1
GaN on SiC supplier in
DEFENSE & CATV
9
MRL
Only supplier to achieve MRL 9 using USAF MRA tool
10 million
broadband GaN devices shipped
GaN
Demonstrated MTTF reliability with
200°C
10^7 hrs.
SPACE QUALIFIED
Highest level of reliability
HAST
Compliant
qorvo
all around you
Join Qorvo at IMS
June 12-14, 2018
Philadelphia, PA | Booth #725
© Qorvo, Inc. | 04-2018. QORVO and ALL AROUND YOU are registered trademarks of Qorvo, Inc. in the U.S. and in other countries.
For more information, visit Qorvo.com/GaN

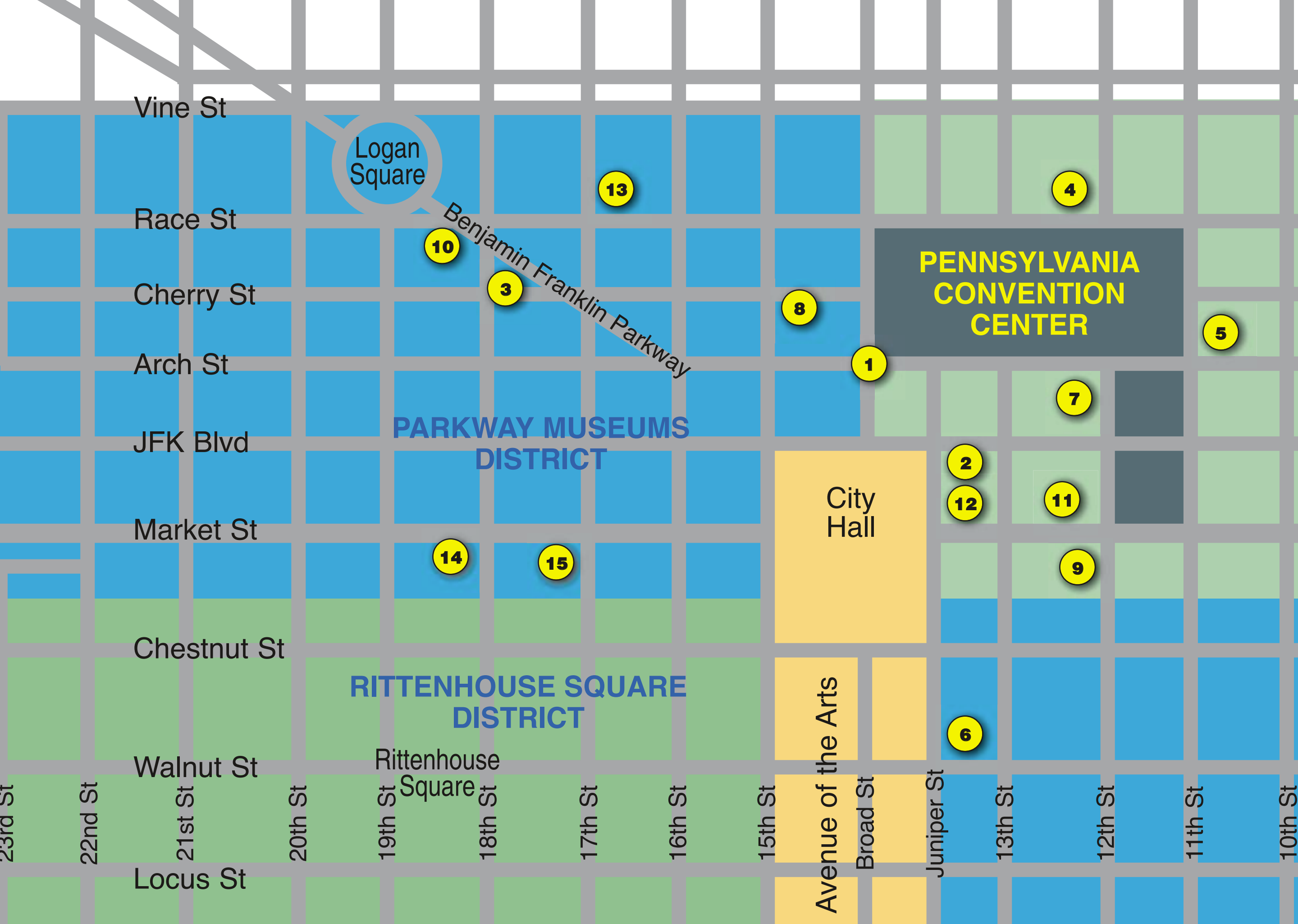

Map of Philadelphia area provided courtesy of CTT, Inc.

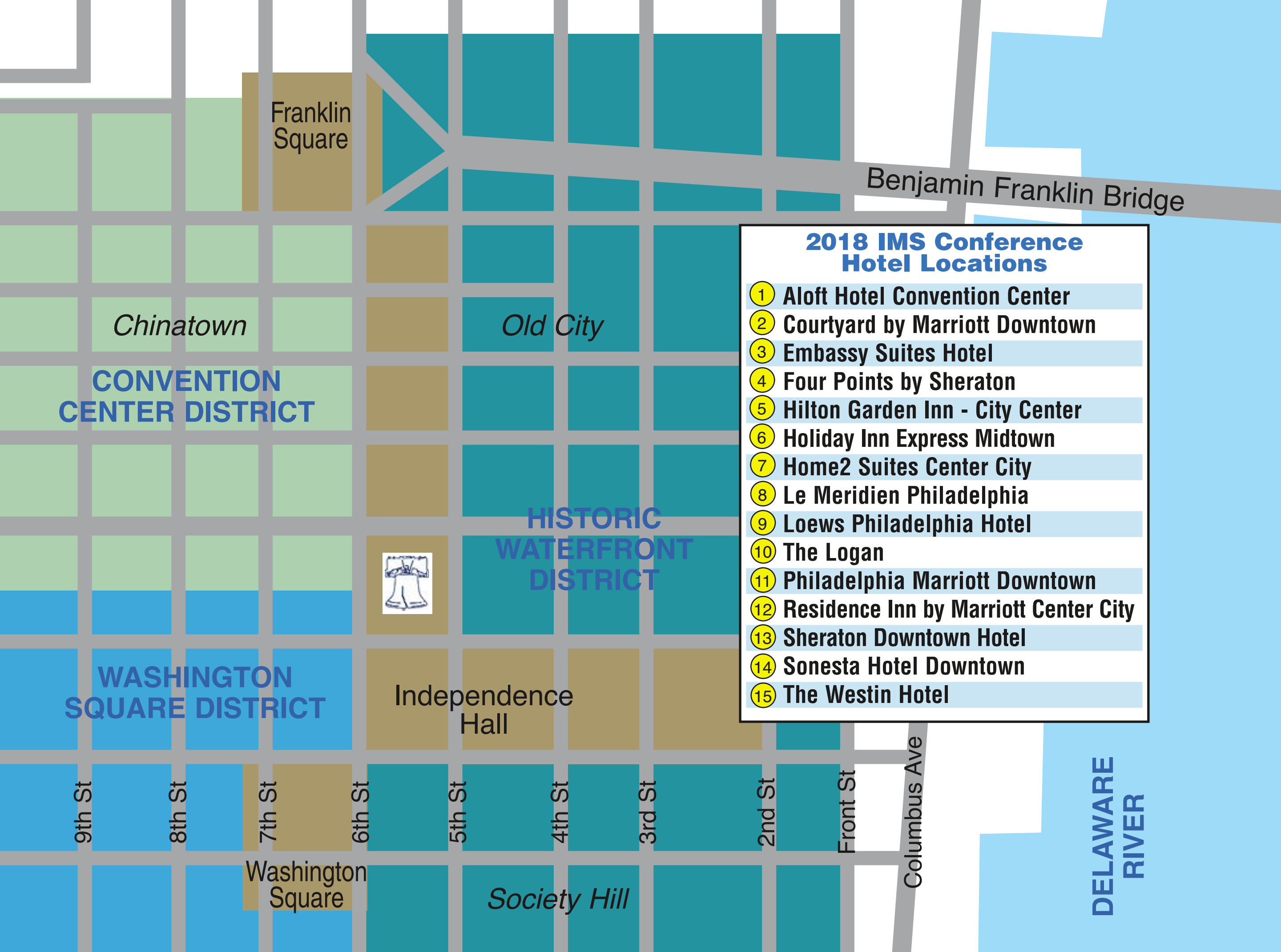

Whether your application is narrowband, wideband or ultra-wideband, operating in pulsed or CW mode, CTT's power amplifiers are an especially attractive choice for new multi-function frequency-agile systems that effectively conserve weight, space and power consumption.

The characteristics of the portion of the electromagnetic spectrum selected for any of these particular system designs are undoubtably the most important to the end user, as it has the greatest impact on the type of information required and received.

Engineered specifically to meet the stringent requirements imposed by many modern system designs, CTT's family of GaN and GaAs-based solid-state power amplifiers excel in a wide range of applications.

CTT has delivered production quantities of amplifiers with power levels from 10 through 200 Watts – and higher – for a variety of multi-function, radar and EW applications.

- AMDR • Shipboard Radar • AESA Radar
- VLO/FLO Threats • New Land Radar • EW • UAVs

More than thirty-seven years ago CTT, Inc. made a strong commitment to serve the defense electronics market with a simple goal: **quality**, **performance**, **reliability**, **service** and **on-time delivery** of our products.

Give us a call to find out how our commitment can support your success.

It's that simple.

Microwave Technology Leadership

- ❖ **Power Amplifiers**
  - **NEW GaN and GaAs Models**
  - Radar Bands up to 400W
  - EW Bands up to 200W
  - Pulse and CW
  - Solid-State Microwave Power Modules
  - Rack-Mount Configurations
- ❖ **Low-Noise Amplifiers**
- ❖ **Up and Downconverters**
- ❖ **Subsystems**
- ❖ **SWaP Optimization**
- ❖ **Custom Engineered Options**

nsai IS9100C ISO 9001:2008

CTT INC.

5870 Hellyer Avenue, Suite 70
San Jose • California 95138
Phone: 408-541-0596 • Fax: 408-541-0794
email: sales@cttinc.com
www.cttinc.com

Of course, this is just a small sampling of one product area, and of the many different amplifiers that may be found on the 2018 IEEE IMS show floor, let alone in the industry at large. But the immense number of RF/microwave and soon mmWave amplifiers available in the industry is an indication of the ever-growing need for boosting high-frequency signals in many different types of systems. It also highlights how new amplifiers with high performance, wide bandwidth, and high efficiency, such as the latest distributed amplifiers from Custom MMIC **(Booth 851)**, can grab the attention of circuit and system designers for a number of different projects *(see p. 122)*.

Some may prefer to design their own amplifiers and start with the transistors or ICs that can help them reach their set of design goals. The 2018 IEEE IMS also features some of the industry's leading device suppliers, with Ampleon **(Booth 1449)** showing its silicon LDMOS high-power transistors for industrial heating and medical use, as well as for radar and communications applications though C-band frequencies.

One of Ampleon's latest power-amplifier modules is the model BPC-10M6X2S200 for medical and industrial applications. It provides 200 W output power from 423 to 443 MHz on a lightweight pallet measuring just 125 × 33 mm and weighing only 85 g, and can be used with pulsed and CW signals. The module, which is matched to 50 Ω at input and output, boasts typical efficiency as high as 74% and gain as high as 38 dB. It can withstand VSWRs as severe as 10:1 for short durations without damage.

Another high-power transistor supplier, Integra Technologies **(Booth 815)**, will launch several new power-transistor products at IMS, including modules operating to 2 kW output power, X-band transistors, and devices with advanced thermal control. The firm will also show some devices with which the public may also be familiar, such as the model IGN-P0912L1KW—it leverages GaN-on-SiC technology to provide 1000 W peak pulsed power output from 960 to 1215 MHz. The device is designed for 2.5-ms pulse-width signals at 20% duty cycle.

For those with higher-frequency requirements, the firm is also announcing its model IGT5259L50 GaN-on-SiC transistor matched to 50 Ω to produce 50 W pulsed output power from 5 to 6 GHz (C-band frequencies), as well as its model IGN1214L500B high-power GaN-on-SiC high-electron-mobility transistor (HEMT) with 15.5-dB gain and 500 W output power at L-band frequencies (1200 to 1400 MHz). "We're thrilled to mark IMS 2018 as Integra's breakout moment in providing the industry's most advanced standard and semi-custom RF power devices," says Integra's CEO Suja Ramnath.

GENERATING SIGNALS

Those responsible for generating RF/microwave signals will argue that oscillators and frequency synthesizers are just important as amplifiers in high-frequency systems, especially as applications continue to move into the millimeter-wave range of frequencies. The 2018 IEEE IMS Exhibition will feature more than a few sources for RF/microwave signals, with spectral quality as needed for a wide range of applications.

Synergy Microwave Corp. **(Booth 409)** made noise late last year with the introduction of its model KSFLO27T50-12-100 phase-locked oscillator for use in frequency converters for 5G mmWave systems and in Ka-band radar systems. Different formulas for 5G wireless communications networks have captivated high-frequency source designers with their plans for performing high-speed backhaul data links using various bands at mmWave frequencies. The company is among the signal-source suppliers that met the challenge of generating such high-frequency signals with high stability. This compact phase-locked oscillator *(Fig. 11)* is just one example of its different miniature signal sources for outputs through 30 GHz.

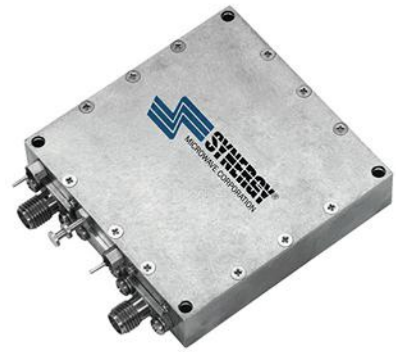

11. This phase-locked oscillator is one example of the move to higher frequencies, with its output frequency of 27. GHz. *(Courtesy of Synergy Microwave Corp.)*

The KSFLO27T50-12-100 produces +15.5 dBm or more output power at 27.5 GHz, using a reference frequency at 100 MHz to generate the stable mmWave output signals. The harmonics from the 27.5-GHz signals are typically −30 dBc, while spurious levels are controlled to −60 dBc or less. As might be expected for signal sources from Synergy Microwave Corp., the single-sideband (SSB) phase noise levels are low, even for this high output frequency, with typical phase noise of −72 dBc offset 100 Hz from the carrier, −80 dBc offset 1 kHz from the carrier, −82 dBc offset 10 kHz from the carrier, and −94 dBc offset 1 MHz from the carrier. The phase-locked oscillator measures only 2.250 × 2.250 × 0.375 in. with female SMA connectors and is designed for operating temperatures from −20 to +50°C.

SiTime **(Booth 1433)** will offer visitors details on it miniature oscillators based on microelectromechanical-systems (MEMS) technology *(Fig. 12)*. Two of its temperature-compensated crystal oscillators (TCXOs), models SiT5356 and SiT5357, serve as stable timing sources for a wide range of wireless systems requiring miniature timing sources. The SiT5356 can be programmed in 1-Hz steps from 1 to 60 MHz, while the SiT5357 can be factory

Start designing in days, not weeks, with Custom MMIC and X-Microwave

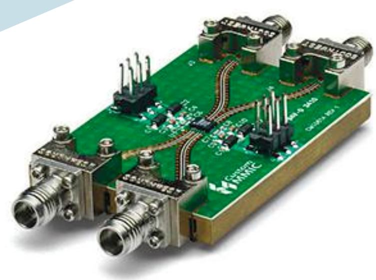

X microwave

Move quickly and efficiently through design, prototyping, and production with Custom MMIC X-MWblocks™ and the X-MWSystem™.

xmicrowave.com/CMD

Evaluating our MMICs is now twice as easy, and fast as ever. Not only do we stock pre-tested, low-cost boards for all our packaged devices, over 30 of our most popular models are now available in the X-MWSystem™ library. Get started today by downloading S-parameters from our website, and ordering the boards from the website that suits you best.

Where can we take you next?

Custom MMIC

CustomMMIC.com

Visit us at the IMS Show Booth #851

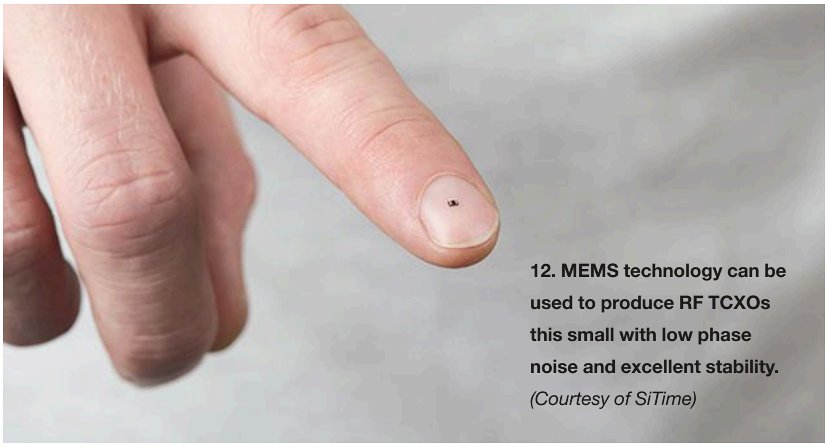

12. MEMS technology can be used to produce RF TCXOs this small with low phase noise and excellent stability. *(Courtesy of SiTime)*

set in 1-Hz steps from 60 to 220 MHz. Both MEMS TCXOs offer stability of ±0.1 to ±0.25 ppm. Both are compliant to GR-1244 Stratum 3 oscillator specifications.

For those in search of more conventional crystal-oscillator technology, Bliley Technologies **(Booth 2218)** will showcase one of the industry's lowest-power oscillators—its model LP62 oven-controlled crystal oscillator (OCXO). Operating at frequencies from 10 to 50 MHz, the oscillator requires 350 mW typical startup power, but has low 135-mW steady-state power consumption when operating from a +3.3-V dc supply. It delivers +9-dBm typical output power into a 50-Ω load with −30 dBc harmonics and low phase noise. For sinusoidal outputs, the phase noise is typically −95 dBc/Hz offset 1 Hz from a 10-MHz carrier, −152 dBc/Hz offset 100 Hz from the same carrier, −162 dBc/Hz offset 1 kHz from the carrier, and −165 dBc/Hz offset 10 kHz from the 10-MHz carrier.

Wenzel Associates **(Booth 1792)** will show its ONYX Series OCXOs among its variety of low-noise oscillators and source modules. Available with output frequencies from 10 to 160 MHz, these oscillators maintain low phase noise even during rigorous vibration, such as in military systems. The phase noise is as low as −176 dBc/Hz. The OCXOs are supplied in PCB-mount housings measuring just 1.0 × 1.0 × 0.5 in. Additional suppliers of high-performance crystal oscillators expected at the 2018 IEEE IMS include Crystek Corp. **(Booth 1933)** and Greenray Industries **(Booth 2104)**

13. Kratos' high-speed indirect frequency synthesizer tunes from w to 18 GHz in 1 µs or less. *(Courtesy of Kratos General Microwave)*

A long-time supplier of components for commercial and military applications, Kratos General Microwave Corp. **(Booth 1416)**, will display examples of its large catalog of microwave through mmWave components, including attenuators, phase shifters, switches, and frequency synthesizers. Among its fast-switching indirect frequency synthesizers is model SF6218 *(Fig. 13)*, a compact unit with 1-µs frequency switching speed from 2 to 18 GHz. Well-suited for electronic-warfare (EW) and instrumentation applications, it tunes in 10-kHz steps via 21-bit parallel tuning control. The wideband frequency synthesizer, just one example of Kratos' extensive lineup, provides +10 dBm typical output power with –20 dBc harmonics. The phase noise is typically –90 dBc/Hz offset 1 kHz, –100 dBc offset 10 kHz, and –105 dBc offset 100 kHz from the carrier.

Ducommun **(Booth 1312)** will be in Philadelphia with samples of its high-frequency Gunn-based oscillators for microwave and mmWave systems. Its mechanically tuned OGF series Gunn oscillators, for example, cover waveguide frequency bands from 18 to 110 GHz. Among the higher-frequency units, model OGF-1205-01 tunes from 60 to 90 GHz with WR-15 waveguide and provides +5 dBm typical output power. Model OGF-1003-01 tunes from 75 to 110 GHz with WER-10 waveguide, generating +3 dBm typical output power across the band.

In contrast, Micro Lambda Wireless **(Booth 1503)** will show its wide range of microwave oscillators and frequency synthesizers based on yttrium-iron-garnet (YIG) technology. Among its different types of frequency synthesizers are the MLMS and MLSP series frequency synthesizers for PXI modular applications. With models available at tuning frequencies as high as 20 GHz, they can be installed into test systems to provide high-performance signal generation while occupying little volume. As an example, model MLSP-2080 tunes from 2 to 8 GHz in 1-kHz steps with phase noise of only –117 dBc/Hz offset 100 kHz from the carrier. The compact frequency synthesizer measures just 5 × 3 × 1 in.

BUILDING MATERIALS

Materials associated with high-frequency electronics design include adhesives, EM shielding, packaging, and printed-circuit-board (PCB) materials. A number of leading suppliers for each material category will be present with booths on the IMS exhibition floor, including Epoxy Technology **(Booth 2132)** showing a variety of adhesives for electronic circuits and systems. The company's EPO-TEK epoxy-based materials are used for critical product assembly applications. The RoHS-compliant materials also meet some of the most demanding quality requirements, including ISO 9001:2008 and MIL-STD-883/5011 for military and aerospace applications.

Rogers Corp. **(Booth 939)** will be at this year's IMS with samples of several of its latest high-performance circuit materials: AD300D laminates *(Fig. 14)* and IM Series laminates. The fourth-generation AD300D circuit materials extend the capabilities of the popular AD300 product line for RF and microwave circuit applications. These ceramic-filled, glass-reinforced, PTFE-based materials provide the outstanding stability and performance needed for mobile communications infrastructure applications, including 4G LTE and emerging 5G systems.

The AD300D laminates exhibit dielectric constant of 2.94 in the z-axis (thickness) at 10 GHz, tightly controlled within ±0.05. The laminates have low loss, with dissipation factor (Df) of 0.0021 at 10 GHz and outstanding passive-intermodulation (PIM) performance with −159 dBc for a 0.03-in. material thickness.

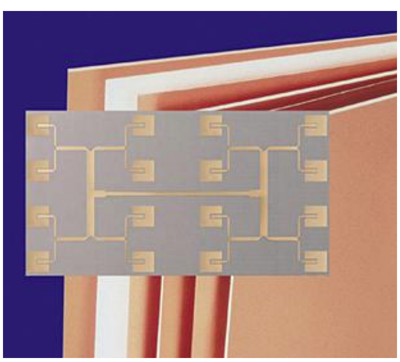

14. The 2018 IMS will be a launching pad for many new products, including these fourth-generation PCB materials for 4G and 5G wireless designs. *(Courtesy of Rogers Corp.)*

15. Visitors to the 2018 IMS in need of the latest test gear will find help with the 5G NR software upgrade to this popular signal analyzer. *(Courtesy of Anritsu Corp.)*

When even better PIM performance is needed, Rogers' IM Series high-frequency laminates are superior-PIM versions of the AD300D materials. They are well-suited for wireless base-station antennas where the most demanding PIM performance levels must be achieved. The IM Series laminates feature ultra-smooth electrodeposited copper foil cladding with excellent adhesion to the substrate materials. Additional materials suppliers at the exhibition include Materion Advanced Materials **(Booth 2315)**, Polyflon **(Booth 2214)**, and Taconic **(Booth 703)**.

TESTING LIMITS

For a show like the 2018 IEEE IMS, suppliers of test-and-measurement solutions usually have their hands full, since their customers come from both inside and outside the exhibition hall. The usual trends in test, to make accurate measurements in less time and for less expense, remain in 2018 with rapidly growing requirements for higher-frequency measurements in support of mmWave electronic devices and circuits in automotive radar and 5G wireless communications networks.

Anritsu Co. **(Booth 925)** recently introduced a number of 5G measurement software options for its versatile MS2850A signal analyzer *(Fig. 15)* that are compliant with the 3GPP 5G New Radio (5G NR) wireless standard. When equipped with the new software, the signal analyzer can be used to verify the transmit characteristics of 5G base stations, small cells, and mobile devices, along with existing wireless devices and satcom equipment. The analyzer is available in versions covering 9 kHz to 32 GHz and 9 kHz to 44.5 GHz. Using fast Fourier transform (FFT) technology, the analyzer is capable of analysis bandwidths as wide as 1 GHz with as much as 140-dB dynamic range.

The software can be used with the analyzer to test 5G systems at sub-6-GHz signals as well as at mmWave bands of 28 and 39 GHz (depending on instrument model version) according to the 5G NR standard. The software helps to speed what are traditionally complex and time-consuming measurements, such as transmit power, frequency error, and error-vector-magnitude (EVM) measurements.

Keysight Technologies **(Booth 1325)** is focused on solving the challenges associated with mmWave frequencies. The company will showcase several solutions for 5G, WLAN, radar/EW, and satcom applications, including a suite of software solutions utilized across the

product development workflow. Some of the solutions it will demonstrate include:

- **PathWave:** Transforms how test-and-measurement data is shared across the product development lifecycle. With PathWave, design, test, and manufacturing teams can improve handoff time, integrate new equipment faster, and scale resources.
- **5G NR Design Validation Testbed (featuring the Ball Aerospace phased array):** Designed to generate and analyze a variety of standards and custom waveforms, including 3GPP NR, pre-5G (5GTF), custom OFDM, and custom I/Q. This reference solution combines Keysight software and hardware to provide a flexible testbed for 5G research and development and design validation for 5G waveform generation and analysis *(Fig. 16)*.
- **110-GHz Network Analyzer:** Enables mmWave receiver characterization. This broadband mmWave solution can enhance device characterization and modeling for on-wafer and connectorized measurements.
- **Nonlinear Vector Network Analyzer (PNA-X):** Allows users to perform X-parameter measurements to characterize beamforming ICs, GaN amplifiers, and other devices. This solution is intended to simplify test setups and provide detailed insight into designing nonlinear components. The PNA-X Series network analyzer with NVNA (nonlinear VNA) accurately measures and displays the nonlinear behavior of the device under test (DUT) to deterministically design components, modules, and systems.

16. This 5G testbed for design validation can analyze the performance of a phased-array antenna in receive mode with a 3GPP NR signal in the presence of an unwanted interfering signal. *(Courtesy of Keysight Technologies)*

As a Gold Sponsor, National Instruments **(Booth 1825)** will also be on hand at the 2018 IEEE IMS exhibition with numerous samples of the powerful NI AWR Design Environment design and simulation software, as well as its variety

17. The S Series one-box tester reflects a trend of packing more measurement power into a smaller test space. This unit works to 20 GHz. *(Courtesy of Elite RF LLC)*

of measurement hardware solutions. In addition to exploring the use of the software on display at the booth, it will be part of a separate display for the MicroApps exhibition **(Booth 1457)** scheduled for Tuesday, June 12. MicroApps will include the use of design software to improve the efficiency of RF/microwave power amplifiers; help design multiple-input multiple-output (MIMO) antennas for IoT applications; create phased-array antennas for X-band systems; and develop hardware for automotive radar systems for ADAS applications.

Visitors to the Mini-Circuits' booth **(203)** may be surprised by the firm's strong presence in the test equipment market, with many different benchtop and modular measurement solutions. These include programmable switch matrices and multiple-channel attenuator systems, as well as some equipment that might not be found at many RF/microwave instrument suppliers, such as 75-Ω test systems that perform cable-television (CATV) equipment measurements and high-temperature operating-lifetime test systems.

Among its many instruments on display, Rohde & Schwarz USA (**Booth 649**) will show its affordable R&S FPC1500 spectrum analyzer, which also packs the functionality of a vector network analyzer (VNA) and a signal (tracking) generator into a single compact instrument. With a standard frequency limit of 1 GHz, it is keycode upgradeable to 3 GHz. It offers resolution bandwidths as fine as 1 Hz with a one-port VNA and Smith Chart display. It can even be remotely controlled via Wi-Fi using the appropriate test software. The versatile instrument is a good match for evaluating IoT products.

In addition to its amplifiers, Elite RF LLC **(Booth 307)** will demonstrate some of the instruments that can test them with its S Series of single-box test systems, with multiple functions in one box *(Fig. 17)*. Instrument systems such as the highest-frequency models in the line, the SA1241 and SPA1241, combine a spectrum analyzer, tracking generator, two-channel signal generator, four-channel oscilloscope, and pulsed/CW power meter in a standard rack-mount instrument enclosure. The tracking generator, oscilloscope, and spectrum analyzer extend to 12.4 GHz while the power meter is usable from 50 MHz to 20 GHz.

Additional suppliers of test-and-measurement solutions at the 2018 IEEE IMS include:

Berkeley Nucleonics Corp. **(Booth 1709)**, Boonton **(Booth 932)**, Copper Mountain Technologies **(Booth 1849)**, EM Research **(Booth 2230)**, Focus Microwaves **(Booth 2025)**, GGB Industries **(Booth 1317),** Holzworth Instrumentation **(Booth 1949)**, Maury Microwave Corp. **(Booth 1525)**, Mini-Circuits **(Booth 203)**, MKS Instrument Italy **(Booth 552)**, Noise XT **(Booth 1555)**, Noisecom **(Booth 932)**, OML Inc., **(Booth 1436)**, and Roos Instruments **(Booth 2137)**.

MANAGING mmWAVES

Millimeter-wave frequencies are gaining interest due to their growing importance for ADAS and 5G systems, and suppliers of mmWave components are expected to see more than their share of visitors at the 2018 IMS. A long-time mmWave component supplier, SAGE Millimeter **(Booth 1103)**, will show both active and passive components. Its model SAT-363-25028-C1 is a WR-28 orthomode transducer (OMT) that operates between 30 and 42 GHz (*Fig. 18*). It separates a circularly or elliptically polarized waveform into two linear, orthogonal waveforms. It can also

18. This orthomode transducer operates at millimeter-wave frequencies from 30 to 42 GHz and represents a growing number of mmWave products on display at the IEEE IMS. *(Courtesy of SAGE Millimeter)*

19. This active frequency multiplier creates signals from 71 to 86 GHz from input signals at one-fourth the frequencies. *(Courtesy of SAGE Millimeter)*

While many of these CAE software suppliers offer online seminars and educational tools on their websites, insights gained from staff members at an exhibition booth are usually worth the wait for that open computer display screen.

combine two linearly polarized waveforms into one circularly or elliptically polarized waveform.

The firm will also present its model SFA-713863415-12SF-S1 active ×4 frequency multiplier. It transforms inputs from 17.75 to 21.50 GHz to outputs from 71 to 86 GHz *(Fig. 19)*. The active multiplier boosts inputs at +5 dBm to outputs at +15 dBm, with low harmonics (−20 dBc). Input signals feed a female K connector while outputs are available at a WR-12 waveguide port.

Analog Devices **(Booth 1725)** will display its own mmWave solutions, such as the company's complete 24- to 44-GHz radio based on SiGe and 28-nm CMOS. The company will also demonstrate how its technology can enable 77-GHz automotive radar along with autonomous transportation systems.

In addition to mmWave products, Analog Devices plans to demonstrate a 7.125-GHz 5G signal chain. Furthermore, the company will showcase an expansion of its RadioVerse technology, as well as high-speed RF converters and aerospace/defense solutions. Technology exhibits include MEMS switches, RF switches, power detectors, GaN power amplifiers, synthesizers, new updates from the Linear/power management line, and more.

Getting back to mmWaves, additional suppliers of mmWave components at the 2018 IMS include Farran Technology **(Booth 2306)**, Flann Microwave **(Booth 2149)**, Millimeter Wave Products **(Booth 2203)**, Pasternack **(Booth 2133)**, TDK Corp. **(Booth 1207),** Teledyne **(Booth 525)**, UTE Microwave **(Booth 955)**, and Werbel Microwave LLC **(Booth 1857)**.

SAMPLING SOFTWARE

Finally, for those looking for the latest versions of RF/microwave design software at the 2018 IMS, the trick is to seize an open screen, since CAE suppliers are usually swamped with visitors checking to see what's new. In addition to its plethora of test software, Keysight Technologies **(Booth 1325)** will show its popular Advanced Design System (ADS) software in various options, including professional and student versions. National Instruments **(Booth 1825)** will also be on hand with its powerful suite of software design tools from Applied Wave Research (AWR), including Microwave Office, Visual System Simulator (VSS), and its AXIEM 3D planar EM simulator.

For all of its efforts in modeling 5G and automotive radar systems using its EM simulation tools, Remcom **(Booth 1917)** should draw a crowd on the exhibition floor. The software has proven its value to those involved with antenna design and placement, especially in the design of systems with MIMO antenna elements for emerging 5G wireless networks.

Additional CAE software suppliers worth a stop at the 2018 IMS include ANSYS **(Booth 1025)**, Cadence Design Systems **(Booth 1861)**, MathWorks **(Booth 2056)**, Modelithics **(Booth 1642)**, and Sonnet Software **(Booth 541).** While many of these CAE software suppliers offer online seminars and educational tools on their websites, insights gained from staff members at an exhibition booth are usually worth the wait for that open computer display screen. mw

MAKING MEASUREMENTS COUNT AT THE 2018 ARFTG

ABOUT TO MEET for the 91st time, the Automatic RF Techniques Group (ARFTG) has grown from an informal gathering of test-and-measurement professionals and concerned users of test equipment to a full-fledged measurement conference with technical presentations rivaling those of the 2018 IEEE IMS conference. The 91st ARFTG is a one-day event scheduled for Loews Hotel across from the Pennsylvania Convention Center on the last day of the IMS week (June 15), with technical presentations organized into five separate sessions and its own dedicated ARFTG exhibition area.

The technical forums provide coverage of the challenges in performing accurate characterization of modulated signals, especially as those signals reach toward millimeter-wave (mmWave) frequencies for 5G systems; large-signal measurements of the different building blocks needed for 5G networks, including GaN power amplifiers; the importance of calibrating test equipment and measurement systems for 5G applications; and the coming challenges in making measurements at mmWave frequencies.

In addition, the almost full-day interactive forum will address on-wafer measurements at mmWave frequencies; various techniques for measurements on materials; and the importance of calibration standards for measurement systems through 110 GHz. With the growing interest in mmWave frequencies, the 91st ARFTG is clearly tuned to the heart beat of the industry.

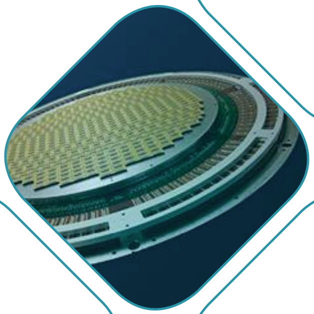

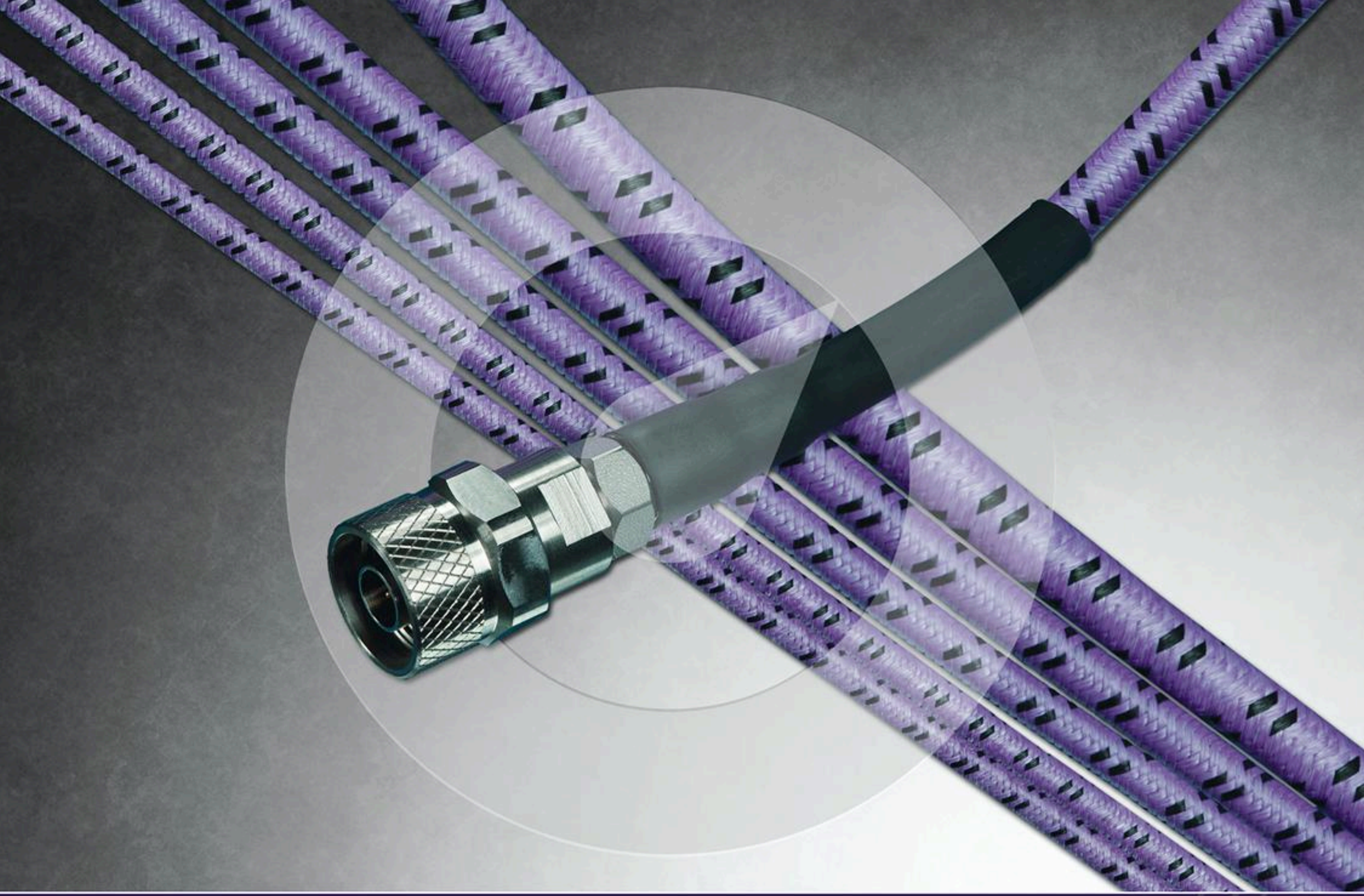

JACK BROWNE | Technical Contributor

Managing Limited Spectrum for Unlimited Applications

The wireless frequency spectrum extends to 300 GHz and beyond, but with the ever-growing number of wireless applications, that spectrum must be managed for its most efficient use.

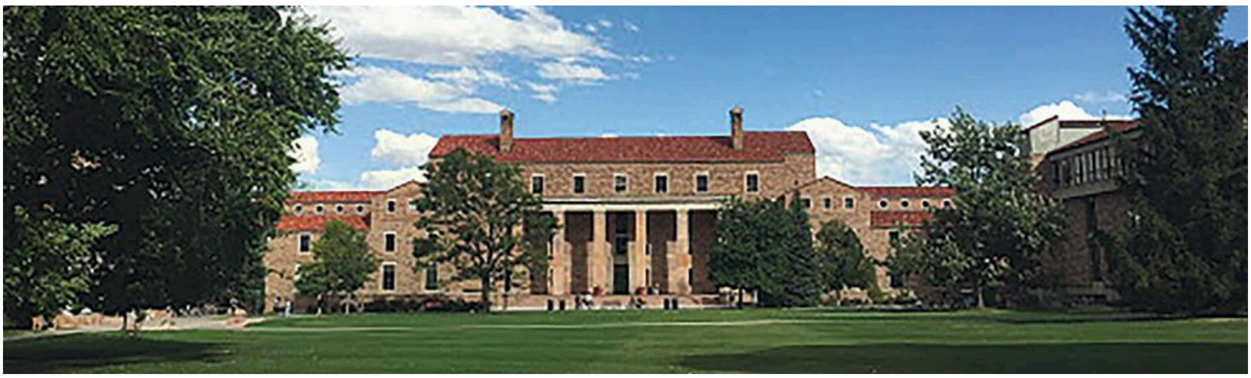

1. The NTIA is partnering with the University of Colorado Boulder on spectrum-management research over the course of a five-year R&D agreement. *(Courtesy of the University of Colorado Boulder)*

Frequency spectrum might seem unlimited, considering the wide range of radio frequencies from 9 kHz to 300 GHz. But with more people and things using radio spectrum, portions of it, including smartphones in 4G LTE and soon 5G wireless networks, billions of Internet of Things sensors (*see p. 118*), and in connected smart cars, even the millimeter-wave (mmWave) frequencies (30 GHz and above) are being used up.

Spectrum management is the process of getting the most efficient use of available radio frequencies and with minimum interference. It involves commercial and military management, at national and international levels. Spectrum management is an ongoing process, since the demand for frequency spectrum grows with the number of wireless devices. Can radio frequency spectrum run out? If not properly managed, it can. But with proper management, even 6G will be possible.

Spectrum management has been going on since radio waves were first used for AM and FM broadcast radios, maintaining signals for these radios in the ranges of 540 to 1600 kHz and 88 to 108 MHz, respectively. In the U.S., broadcast television services occupied VHF and UHF bands at roughly 54 to 806 MHz, and the radio spectrum allocation chart started to fill with these early commercial uses of electromagnetic (EM) energy and radio spectrum.

Today, the radio-spectrum allocation chart for the U.S. is a densely populated map of commercial, military, and government applications with rapidly shrinking sections of available bandwidth. The U.S. table of frequency allocations covers the radio spectrum from 9 kHz to 300 GHz. In addition to those early radio and television applications, frequency bands are filled by cellular telephones, wireless communications networks, Global Positioning System (GPS) satellites, vehicle collision-avoidance radars, satellite communications (satcom) systems, and a variety of defense-related systems, such electronic-warfare (EW), electronic intelligence (ELINT), radar, and surveillance systems. Each application has its own allocated portion of the frequency spectrum, designed for its optimum use, but also for minimum interference with existing applications using other portions of the radio spectrum.

ALLOCATING FREQUENCIES

The various frequency bands are assigned by the process of spectrum authorization, handled by different organizations in different locations. The National Telecommunications and Information Administration (NTIA) is the organization that manages the U.S. federal government's use of frequency spectrum, working with the Interdepartment Radio Advisory Committee (IRAC). The Federal Communications Commission (FCC) manages all domestic non-federal use of spectrum in the U.S.

Additional government organizations such as NASA work with these spectrum regulatory groups to ensure that spectrum will be available for present and future space-exploration missions. Internationally, the International Telecommunications Union (ITU) is part of the United Nations that manages terrestrial and satellite use of frequencies among different nations.

As spectrum continues to be consumed by different wireless applications, additional concepts have been proposed to ease the control of these organizations. This includes spectrum trading or sharing, in which a portion of bandwidth initially authorized for one type of application might also be used for a different application without need of authority from an organization like the FCC.

The FCC most recently issued a public notice (PN, May 1, 2018) on the feasibility of the licensed and unlicensed use or sharing the use of the frequencies between 3.7 to 4.2 GHz. The FCC notes that there's currently no federal allocation for the band from 3.7 to 4.2 GHz, and is hoping to explore the effects of having commercial licensed and unlicensed users possibly share the band with federal users.

For federal U.S. applications, the NTIA will work with a federal government group or agency to review the expected characteristics and specifications for a new wireless system to ensure that the new system can operate effectively without disrupting existing radio-frequency systems. If it appears that the new system is safe, the NTIA will issue a Certificate of Spectrum Support, followed by a frequency authorization to the proposing group or agency that makes it possible to use the new system on a specific frequency and bandwidth or band of frequencies.

It's then a matter for the proposing agency to put one or more of the new systems to use in the field. Therefore, actual use tests can be performed with available test equipment, such as signal generators and spectrum analyzers, to evaluate the effects of what might have been unforeseen problems (e.g., second- and third-harmonic interference from an antenna or signal source). The NTIA must review and approve any of these test results to ensure that the new application performs as expected and does not cause interference to existing applications. The NTIA works with guidance from other federal agencies, such as IRAC, as well as different federal departments like the U.S. Department of Transportation (DOT), as needed on spectrum-management issues.

GOING TO SCHOOL

As part of the U.S. Department of Commerce, the NTIA works with many researchers on maintaining the database needed for effective spectrum management. The NTIA recently announced a five-year R&D agreement with the University of Colorado Boulder to develop a wireless test bed that essentially uses the university's grounds (*Fig. 1*) as a laboratory for spectrum-management research. The NTIA and the university will benefit from the research, installing spectrum-monitoring sensors throughout the campus.

David Redl, Assistant Secretary of Commerce for Communications and Information and NTIA Administrator, says, "We're excited that ITS is moving forward with this important test-bed research that will provide analytics on how real-world spectrum sharing could work. The scientists and engineers working at ITS are experts in the field of spectrum measurement, and we expect the collaboration with CU to lead to new opportunities for government users to share spectrum with other agencies and commercial users." The test bed will help explore new wireless technologies, specifically how they occupy spectrum and interact with each other under real-world conditions.

Peter Mathys, Associate Professor in Electrical, Computer and Energy Engineering at the university, offers, "This will be a great motivator for students who use wireless devices on a daily basis but have little understanding of the underlying physical limitations associated with wireless technology. This testbed will enable measurement of the effects associated with the ever-growing demand for increased wireless communications."

For its part, the FCC works on developing new uses for frequency spectrum with state and local government users as well as private and business users. For any new application, the FCC will first issue a Type Acceptance that identifies the authorized frequency band and the performance parameters, such as maximum transmit-power and frequency-channel bandwidth. Following the Type Acceptance, the FCC will issue the user a radio license for that frequency or group of frequencies, and the user must go through testing of the new equipment according to the FCCs requirements and recommended test methods.

The FCC works closely with the NTIA in managing spectrum in all conditions, in peacetime as well as war. As part of a 2010 presidential advisory, the FCC is collaborating with the NTIA to "find" or make available a total of 500 MHz of federal and non-federal communications spectrum for mobile and fixed broadband wireless use by the year 2020.

On a global basis, the ITU has mapped the world's use of frequency spectrum into three main operating areas, and maintains a global Table

ULTRA-LOW PHASE NOISE

PHASE LOCKED REFERENCE TRANSLATORS (OCXO)

Frequency Option	Reference Frequency In (MHz)	Frequency Out (MHz)	Phase Noise @ 100 Hz Offset dBc/Hz (Max)	Model Number
Programmable	1, 5, 10, 20, 50	1000	-110	**LNFTP-1000-15**
Fixed (Dual Output)	10	120 / 240	-130 / -125	**LNFTD-10-120240-12**
Fixed	10	1000	-110	**LNFT-10-1000-15**

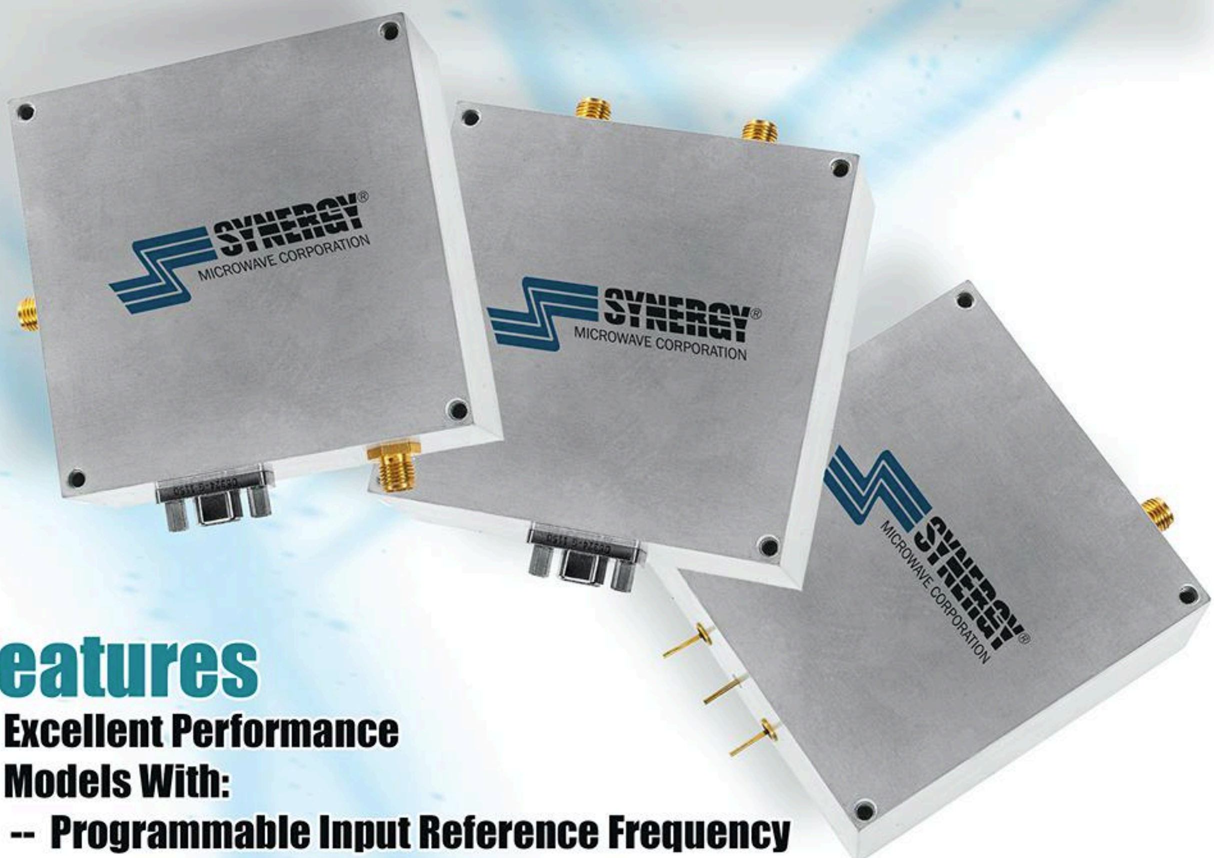

Features

-- **Excellent Performance**
-- **Models With:**
  -- **Programmable Input Reference Frequency**
  -- **Dual RF Output (Fundamental & X2)**
  -- **Fixed Output Frequency**

Applications

-- **Frequency Converters**
-- **Synthesizer Reference Multipliers**

Talk To Us About Your Custom Requirements.

SYNERGY®
MICROWAVE CORPORATION

Phone: (973) 881-8800 | Fax: (973) 881-8361
E-mail: sales@synergymwave.com
Web: WWW.SYNERGYMWAVE.COM
Mail: 201 McLean Boulevard, Paterson, NJ 07504

Visit us at the IMS Show Booth #409

of Allocations for the different nation members to follow. When new telecommunications designs or applications are developed, proposals for that new use of frequency spectrum must be submitted to the ITU. To assess the global need for spectrum management and any reorganization of the Table of Allocations, the ITU holds regular.

World Radiocommunications Conferences (WRCs) to invite new ideas for frequency-spectrum usage.

2. BroadbandUSA is an initiative and website organized by the NTIA to promote the use of broadband communications throughout the U.S. *(Courtesy of the NTIA)*

5G AND BEYOND

Much of the promise of 5G wireless networks depends on the availability of sufficient frequency bandwidth to support the many functions of this emerging wireless technology, and the NTIA will play a key role in finding the spectrum required for 5G in the U.S. What makes 5G somewhat unconventional is its use of scattered spectrum, at both lower and higher frequencies. For mmWave frequency access, for example, the NTIA has supported the FCC's Spectrum Frontiers program, collaborating on a means of sharing the 37-GHz frequency band between federal and non-federal users. Both agencies feel that if the 37-GHz effort is successful, it could serve as a model for spectrum sharing of other mmWave bands, especially those needed for short-haul links in support of high-data-rate communications in 5G wireless networks. The NTIA is also working very closely with the FCC on the use of the 24- and 28-GHz frequency bands, which are under consideration for use in emerging 5G wireless networks.

At lower frequencies, the FCC has proposed the possibility of reusing the 2.5-GHz spectrum currently allocated to the Educational Broadband Service for the lower bands of 5G networks. At the same time, the NTIA has proposed repurposing the band of frequencies from 3450 to 3550 MHz for commercial use, perhaps as part of coming 5G wireless networks.

While the FCC is responsible for safeguarding the interests of non-Federal users for existing frequency bands, the NTIA must also watch for any conflicts that can cause interference with government and military users. It must ensure that the frequencies and bandwidths consumed by an emerging application such as 5G do not "steal" needed bandwidth from military communications or radar systems.

Much of the work to be done by the NTIA and FCC in finding spectrum for 5G must weigh not only the available spectrum, but the state of technology out there that can support the use of any available frequencies. Since 5G is being designed to make use of lower, mid-range, and higher (mmWave) frequencies, the economy of components for each different frequency range will vary with the frequency, with the most expensive components at the highest frequencies. Still, agencies such as the NTIA and FCC have traditionally used spectrum management to encourage the development of new technologies and more practical solutions that would allow the economical use of mmWave frequencies even above 95 GHz.

In recent remarks to the CTIA on that organization's "Global Race to 5G" report, the NTIA's David J. Redl, confirmed the importance of 5G as more than just a new generation of wireless communications equipment: "5G and the technologies it will enable promise transformative changes that will improve healthcare, advance manufacturing, and benefit public safety."

Redl noted that maintaining a technological edge in 5G technology and modern communications in general is critical for the U.S. as a world leader. In addition to spectrum availability, security is one of the main concerns for the development of 5G wireless networks. Whereby the network and devices on that network can be made sufficiently secure to protect the information for users at all levels, from private citizens to the government and military users expected to share the many resources of 5G systems.

Along with its close ties to the FCC, the NTIA also works with many government organizations to promote effective use of frequency spectrum throughout the country. One of its newer initiatives, BroadbandUSA (*Fig. 2*), is aimed at helping communities throughout the U.S., no matter how remote, to develop the broadband communications capacity required for effective economic development, education, healthcare, and public safety. BroadbandUSA is expected to use webinars and other educational methods to reach citizens, and to encourage close coordination among federal agencies to promote broadband deployment and adoption. mw

JEFF HARRIS | Vice President of Portfolio Marketing, Keysight Technologies
www.keysight.com

Millimeter-Wave Automotive Radar Testing Must be Flexible

What are the keys to effective mmWave automotive radar? This article looks at the simulation, development, and manufacturing phases required for the design and test of these systems.

One of the most ambitious areas of automotive innovation is **autonomous driving**, where precision sensors provide input to real-time decision-making algorithms. Most autonomous driving strategies use some combination of a sensor set, including optical, LiDAR, and radar systems. Sensors can be deployed at different locations around the vehicle, with each being responsible for providing critical input information to decision-making algorithms.

The radar sensor is tasked with identifying and spatially locating mass-based obstacles. These can include other vehicles, bicyclists, pedestrians, animals, and even fixed obstacles. The key metrics when analyzing the performance of a radar sensor is how reliably it can resolve objects (range resolution), how much it can resolve velocity of objects (velocity resolution), and the size of the antennas that dictate placement.

1. Shown are typical automotive mmWave radar applications and mounting locations.

The first two parameters above are governed by the radar's bandwidth, while the third is governed by the radar's center frequency. Understanding the radar's set of responsibilities in an advanced driver assistance system (ADAS) is key to determining how to measure its performance.

In vehicles, radars are typically integrated in two main locations—either in the four corners or looking out the front of the vehicle *(Fig. 1)*. The corner-looking applications are typically for short-range applications, such as blind-spot detection, lane-change assist, and front/rear collision-warning alert. The front-looking applications are typically mid- to long-range applications, such as emergency braking systems and adaptive high-speed cruise control on highways.

FREQUENCY AND BANDWIDTH CHANGES RADAR TESTING

Initial automotive radars were in the 24-GHz band, but were limited to bandwidths of 250 MHz due to worldwide spectrum availability. The narrow bandwidth limited the radar's ability to resolve objects that were close to one another. Newer 77-GHz radars will offer 1 GHz of bandwidth, while 81-GHz systems will allow up to 4 GHz of bandwidth. These wider bandwidths will dramatically increase range and velocity resolution, and the higher center frequencies enable smaller profile antennas that open up new vehicle installation placement opportunities.

Transitioning from 24- to 81-GHz bandwidths results in 20X better performance in terms of range resolution and accuracy. The improvement in range resolution means that the 75-cm resolution at 24 GHz is as fine as 4 cm in an 81-GHz system, allowing for detection of bicyclists next to cars, people walking with pets, etc.

2. Looking at this bandwidth comparison, employing a 4-GHz bandwidth (right) enables two objects that are only 10 cm apart to be separated.

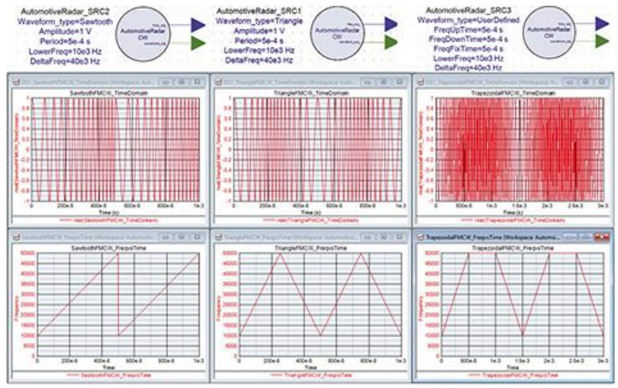

3. These FMCW signals were generated by the Keysight SystemVue W1908 Automotive Radar Library (from left to right: sawtooth, triangle, and custom FMCW waveforms).

Test comparisons between 1- and 4-GHz bandwidths highlight the difference *(Fig. 2)*. A 1-GHz bandwidth signal, shown on the left, is not able to distinguish between two side-by-side objects in the same manner as the 4-GHz bandwidth signal, shown on the right. If that were a man and his dog walking closely together and the dog suddenly jumps onto the road, only the 4-GHz bandwidth signal would detect both separately and provide the correct information to the driver or autonomous-vehicle system.

TEST CONSIDERATIONS FOR ADVANCED AUTOMOTIVE RADARS

Developing high-performing millimeter-waveform automotive radar requires minimizing propagation loss, phase noise, I/Q and frequency-response errors, and noise. Testing at mmWave frequencies, especially the 76- to 81-GHz band, demands a sophisticated test solution where the choice of instruments, cables, connectors, and accessories all matter to ensure signal accuracy and repeatability. Important considerations exist in the design, validation, and manufacturing test phases that could skew the outcomes.

DESIGN SIMULATION PHASE

Flexible, accurate signal generation is at the heart of good radar system design and test. This starts with an automotive radar simulation library that contains multiple models and reference designs. The library should include comprehensive tools for frequency-modulated-continuous-wave (FMCW) radar waveform generation, signal modulation, antenna modeling, channel simulation, and signal processing. Reference designs, such as multi-target range, speed measurement, and 3D scanning radar using antenna arrays, provide a starting point to implement design ideas into early simulations and prototyping. *Figure 3* shows samples of three different types of FMCW signals.

DEVELOPMENT PHASE

Once a simulated waveform is selected, a developer downloads it to an arbitrary waveform generator (AWG). AWGs are used to generate wide-bandwidth radar signals for automotive radar testing *(see table)*. The signals are upconverted to mmWave frequency bands to verify designs in preparation for real hardware testing. A typical test setup consists of an AWG, a vector signal generator (VSG), and an upconverter to generate an ideal reference signal (replace Tx LO/VCO) plus interference, clutter, and jamming signals (Rx Test).

HIGH-SPEED AWG FUNCTIONALITY AND BENEFITS TO TEST AUTOMOTIVE RADAR

High Speed AWG Functionality	Radar Testing Benefit
Extremely wide modulation bandwidth (e.g., dc to 32 GHz)	Discern targets that are close together Finer resolution of a given object
Instantaneous frequency hopping Overlapping pulses at different frequencies	Realistic simulation of multiple emitters transmitting simultaneously
Phase-coherent, multi-emitter, multi-channel pulse generation	Economical setup for testing multi-channel radar receivers
Repeatable phase from pulse-to-pulse and channel-to-channel, perfect frequency ramps	Repeatable results
Flexible modulation format	Develop new modulation schemes that are more tolerant to interference
No images or carrier feedthrough Flat magnitude and phase response (after calibration)	Testing your device and not the instrument

Once a design is complete, efficient and comprehensive test coverage during manufacturing increases reliability and reduces cost. During manufacturing test, the key is to create a scalable, reliable, accurate, and repeatable radar target simulator (RTS) solution.

Wide-bandwidth automotive radar signal analysis includes RF power, spectrum emissions, phase noise, frequency stability, and modulation quality. For this, a complete automotive radar signal-analysis system, such as the setup shown in *Figure 4*, is needed.

When measuring wide-bandwidth systems, it is vital to have measurement capabilities that go beyond the expected design. For instance, if testing 4-GHz bandwidth signals at 81 GHz, it is recommended to use a signal-analysis system that can analyze frequencies as high as 110 GHz and bandwidths as high as 5 GHz for extra design margin.

The other key metric is sensitivity. A displayed average noise level (DANL) that reaches −150 dBm/Hz allows developers to measure low-level and sensitive radar signals. The Keysight E8740A automotive radar signal-analysis and generation solution performs analysis and generation of automotive radar signals across full frequency ranges for 24-, 77-, and 79-GHz radar. It provides scalable analysis bandwidth that ranges from 2.5 to greater than 5 GHz, depending on test requirements.

MANUFACTURING

Once a design is complete, efficient and comprehensive test coverage during manufacturing increases reliability and reduces cost. During manufacturing test, the key is to create a scalable, reliable, accurate, and repeatable radar target simulator (RTS) solution.

At a minimum, the RTS should be able to apply time delay, Doppler frequency shift, and attenuation to simulate range, radial velocity, and radar cross-section (size of object) in a simulated test range. To be realistic, the RTS needs to be capable of testing at ranges as close as 1 m and as far as 450 m, and within speeds from zero to ±360 km/hour.

END-TO-END TESTING FOR mmWAVE AUTOMOTIVE RADARS

While optimizing all three parts of the development cycle are important, flexibility is the most critical aspect during the development phase. Testing is rarely static during this phase, as developers strive to precisely measure performance in the presence of a variety of realistic noise and jamming conditions—all of which need to be integrated.

Frequency coverage, measurement accuracy, and dynamic range of instruments make a huge difference in measurement efficacy. And most importantly, do not forget to implement a disciplined S-parameter and power calibration process to ensure that measurements remain accurate throughout your design, validation, and production phases.

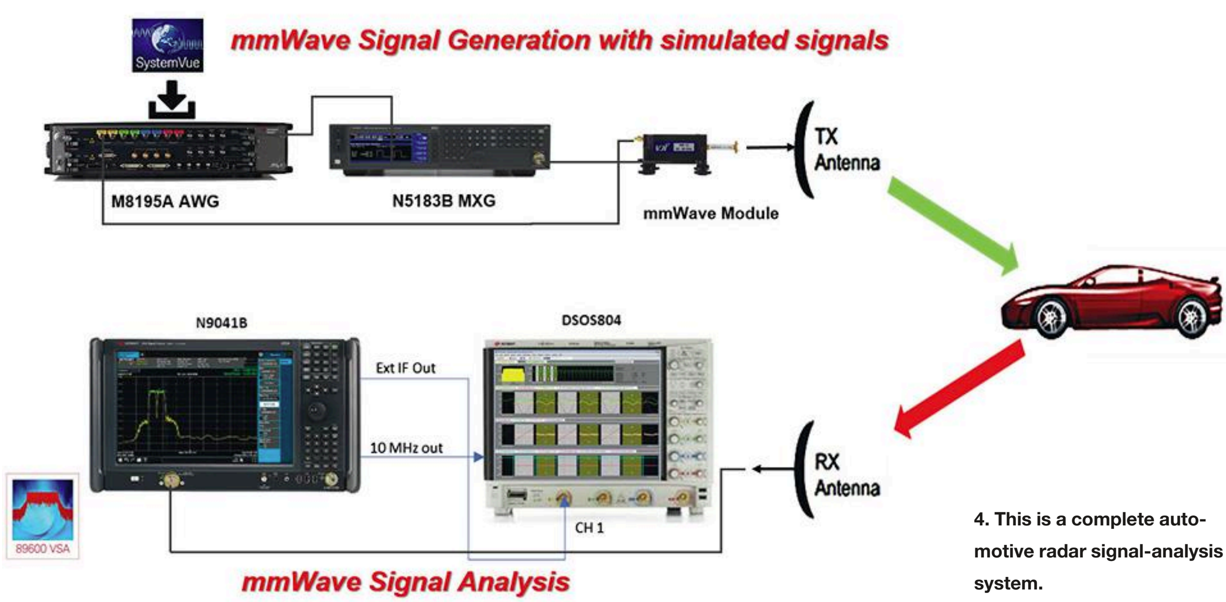

4. This is a complete automotive radar signal-analysis system.

KRYTAR®
Microwave Components & Instruments
DC to 67 GHz
IMS
Connecting Minds. Exchanging Ideas.
Visit KRYTAR
IMS2018
Booth #1203
Directional Couplers
to 67 GHz
3 dB 90° Hybrid Couplers
to 44 GHz
Directional Detectors
to 50 GHz
Double Arrow 3 dB 180°
Hybrid Couplers to 40 GHz
Detectors
Zero Bias
Schottky
Planar Doped
Barrier Planar
Tunnel Diode
Threshold Detectors
to 40 GHz
MLDD Power Divider/
Combiner to 45 GHz
RF & Microwave
Power Meter
100 KHz to 40 GHz
Adapters: DC to 67 GHz
In Series: SMA, 2.92 mm, 2.4 mm
Between Series: 2.29 mm to 2.4 mm
Coaxial
Terminations
to 67 GHz
Broadband Limiters
Pin-Pin Diode
Pin-Schottky Diode to 18 GHz
43 Years of Excellence
KRYTAR
Since 1975
MIL Qualified Components Available
KRYTAR® 1288 Anvilwood Ave. Sunnyvale, CA 94089
Toll Free: (877) 734-5999 • Fax: (408) 734-3017 • sales@krytar.com
www.krytar.com lists complete specifications and application ideas for all products

AHMED A. IBRAHIM | Assistant Professor, Communication and Electronic Department, Faculty of Engineering, Minia University, Minia, Egypt and University Pierre and Marie Curie, Sorbonne University, Paris VI, France

MAHMOUD A. ABDALLA | Assistant Professor, Electronic Engineering Department, Electrical Engineering branch, MTC College Cairo, Egypt

ADEL B. ABDEL-RAHMAN | Assistant Professor, Communication and Electronic Department, Faculty of Engineering, South Valley University, Qena, Egypt

Wireless Bandpass Filters Build on Metamaterials

These second- and third-order bandpass filters leverage metamaterial resonators for low passband insertion loss and high out-of-band rejection for wireless applications at 2.4 GHz.

Microwave bandpass filters (BPFs) are essential for maintaining separate channels in wireless communications systems. As such systems become more compact, BPFs must meet more demanding requirements for smaller size, lower insertion loss, higher out-of-band rejection (selectivity), and lower cost. Several techniques are used to design microwave BPFs,[1-4] although the authors have developed an approach that delivers BPFs with extremely low passband insertion loss in smaller-than-conventional sizes. The secret lies in the use of metamaterials.

The cutoff points for the rejection bands of a BPF are located by attenuation poles or transmission zeros at finite frequencies. This can be done with different design approaches. For example, cross-coupling between nonadjacent resonators allows for creation of alternative signal paths from filter input to output ports, so that a complete transmission zero can be introduced at certain frequencies.[4-10] Hence, many filter designs incorporate transmission-line zeros.[11-13]

Another important choice in the design of a filter regards the physical elements, which will impact the filter response and size. Open-loop resonators have often been used in microwave filter design.[14-18] The open-loop resonator is constructed by adding half-wave-length microstrip lines with a certain coupling structure to achieve the required filter performance. Three types of coupling methods are used in these filters: electric coupling, magnetic coupling, and mixed coupling.[19-21]

For microstrip open-loop resonator filters, several attempts have been made to reduce the resonator size by changing its structure, such as by using an open-loop folded half-wavelength resonator,[21,22] modified shapes,[19,23] and defected ground structures (DGSs).[24-28] However, employing DGS requires double ground processing, which further complicates the filter design.

Artificial dielectric metamaterial (composite) structures have been shown to exhibit novel electromagnetic (EM) properties. Studies revealed that the same EM properties at microwave frequency bands cannot be obtained with conventional materials. Metamaterials are single-negative (SNG) material (in terms of permittivity or permeability) or double-negative (DNG) media.[29-31]

Metamaterials have been realized employing either composite-right-left-handed transmission lines (CRLH) or split-ring resonators (SRRs) or as complementary split ring resonators (CSRRs).[29-31] CRLH transmission lines (TLs) which are realized by periodically loading a conventional TL with series capacitors and shunt inductors, are non-resonant structures. They have been suggested for use in to many filters.[32-35]

SRRs were originally proposed by Pendry et al.[36] Depending on the employment configuration of SRRs, they have been used to represent SNG metamaterial. SRRs have been applied for microstrip BPFs to achieve the filter compactness because these resonators can be designed with dimensions smaller than the signal wavelength at their resonant frequency.[37-39] Also, the compactness of an SRR-based filter is achieved due to the capacitive coupling introduced between the inner and outer rings.[40-42] On top of that, coupled metamaterial SRRs have been used to introduce high-selectivity BPFs.[43-46]

To better understand the design of SRR-based BPFs, the designs of SRR BPFs of two different orders will be presented, with objectives of achieving compact sizes with high out-of-band rejection (high selectivity). Commercial computer-aided-engineering (CAE) software was used for the full-wave performance simulations of the filters, CST Microwave Studio software from CST *(www.cst.com)*, with simulations validated by measurements of fabricated prototype filters.

SYNTHESIZING A FILTER

It's possible to synthesize coupled filters using an optimization technique. Although other coupling techniques are known, the optimization method is also effective. Filter synthesis is based on extracting the desired coupling coefficient between resonators and the external quality factor at the input and the output resonator. The transmission function $S_{21}(\omega')$ is given by refs. 8 and 9 and the following equations:

$$|S_{21}(\omega')|^2 = 1/[1 + \varepsilon^2 F_N^2(\omega')] \quad (1)$$

$$\varepsilon = [10^{R/10} - 1]^{-1/2} \quad (2)$$

$$F_N(\omega') = \cosh[\Sigma_{n=1}^{N} \cosh^{-1}(x_n)] \quad (3)$$

$$x_n = (\omega' - 1/\omega_n')/(1 - \omega'/\omega_n') \quad (4)$$

where ω' is the variable angular frequency, R is return loss, and ω_n' is the location of the nth transmission zero.

Fig. 1 illustrates a network of multiple coupled-loss resonators. The coupling coefficient between resonators i and j is denoted by $M_{ij} = M_{ji}$. The scattering parameters of the filter are calculated by eqs. 5 through 8[7,8]:

$$S_{21} = -2j/(R_1R_2)^{0.5}[A^{-1}]_{N1} \quad (5)$$

$$S_{11} = 1 + 2jR_1[A^{-1}]_{11} \quad (6)$$

$$[A] = [\omega'U - jR + M] \quad (7)$$

$$\omega' = (\omega_0/\Delta\omega)[(\omega/\omega_0) - (\omega_0/\omega)] \quad (8)$$

where R_1 is the internal resistance exiting from resonator 1 and R_2 is considered the load at the output that's connected with resonator N. Parameter [U] is the identity matrix; R is a matrix with

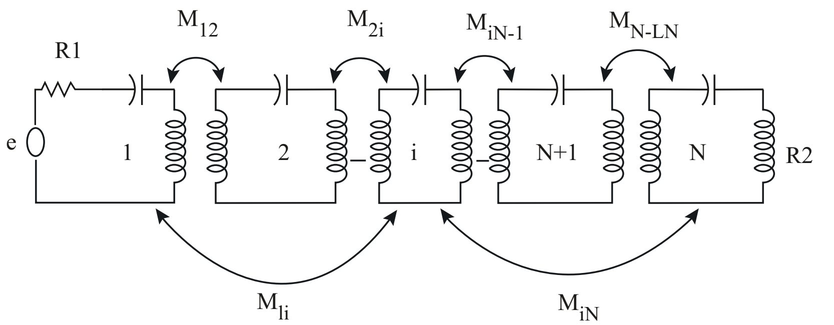

1. This simple schematic diagram shows a BPF with a number of coupled resonators.

only nonzero elements of $R_{11} = R_1$ and $R_{NN} = R_2$; and M is a symmetric square coupling matrix. Also, ω' is the normalized angular frequency and ω_0 is the center angular frequency of the filter. The sequence of filter analysis, comparison with the desired performance, and modification of the design parameters is performed iteratively until the optimum filter performance is achieved. The objective function is based on the optimization technique[8] illustrated by Eq. 9:

$$K = \Sigma^N_{i=1}|S_{11}(\omega'_{zi})|^2$$

$$+ \Sigma^P_{i=1}|S_{21}(\omega'_{pi})|^2$$

$$+[|S_{11}(\omega' = 1)| - \varepsilon/(1 + \varepsilon^2)^{0.5}]^2 \quad (9)$$

where ω'_{zi} and ω'_{pi} are the zeros and poles, respectively, of the filtering function F_N, which is assumed to have P poles and N zeros.

SECOND-ORDER BPF

To put Eqs. 5 to 9 to work, a second-order coupled SRR BPF was designed and fabricated according to a target set of specifications. These include a center frequency of 2.4 GHz, a passband 150 MHz, resulting in a fractional bandwidth (FBW) of $BW/f_0 = 0.058$. The SRR BPF will be designed for a minimum return loss of 20 dB. The proposed filter synthesis for the fundamental mode is based on the coupling matrix and external quality factor extraction using Eqs. 5 to 9. A coupling matrix (M) to realize the chosen topology was optimized and extracted as:

$$M = \begin{bmatrix} 0 & 1.6583 \\ 1.6583 & 0 \end{bmatrix} \quad (10)$$

The external quality factors are $q_1 = q_2 = 1.5$ and, hence, the actual external quality factors at input and output, $Q_{ei} = Q_{eo}$, can be established by Eq. 11:

$$Q = q/FBW \quad (11)$$

The actual (denormalized) coupling matrix becomes:

$$m = FBW \times M \rightarrow m \begin{bmatrix} 0 & 0.0967 \\ 0.0967 & 0 \end{bmatrix} \quad (12a)$$

$$Q_{ei} = Q_{eo} - 12.51 \quad (12b)$$

According to the coupling matrix and external quality-factor extraction, the physical structure of the coupled resonator filter is realized as a second-order filter using full-wave EM simulation. A prototype filter was fabricated in a microstrip configuration with RO6010 circuit material from Rogers Corp *(www.rogerscorp.com)*. The circuit material has a dielectric constant (Dk) of 10.2 in the z-axis (thickness) at 10 GHz, dielectric loss tangent of 0.0027, and thickness (h) of 1.27 mm. Two 50-Ω microstrip transmission lines are added at the filter ends. *Fig. 2* shows the 2D layout of the second-order coupled SRR resonator filter.

The simulated (full wave) and theoretical (circuit implementation) trans-

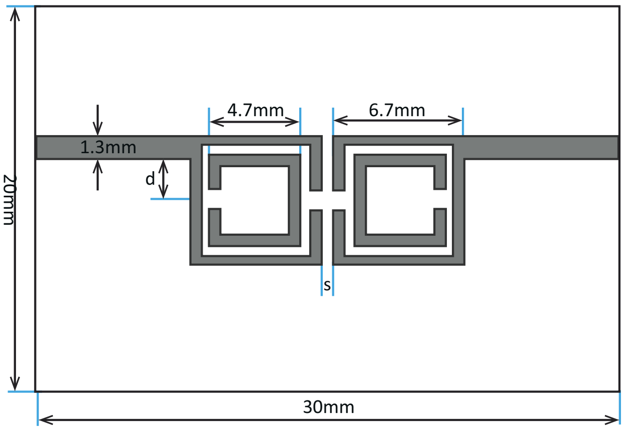

2. This two-dimensional (2D) layout represents a second-order coupled SRR filter.

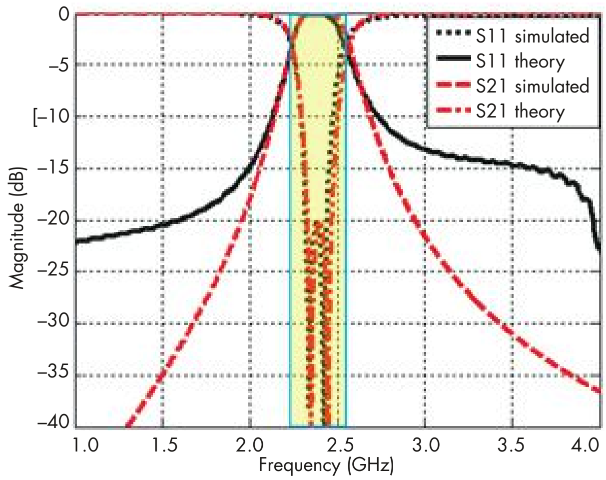

3. By applying theory and computer simulations, the insertion and return losses can be found for the second-order coupled SRR filter.

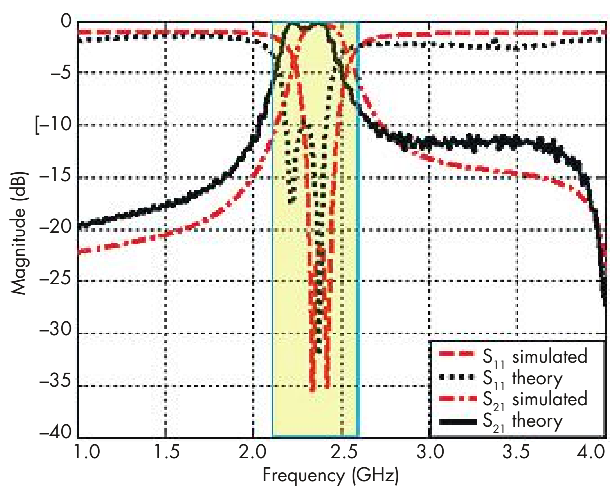

5. The simulated and measured losses of the second-order coupled SRR filter can be compared here.

mission and reflection coefficients of the coupled SRR filter are plotted in *Fig. 3*. It's obvious that the center frequency of the filter equals 2.4 GHz with bandwidth of 150 MHz. Within the passband, the filter has transmission coefficient (S_{21}) close to –0.5 dB and reflection coefficient of –20 dB.

As *Fig. 3* shows, there's good agreement between the theoretical optimized performance (employing Eqs. 5 and 6) and the full-wave simulation. The results are well-matched within the BPF passbands (2.1 to 2.7 GHz). However, above 3 GHz, a deviation exists between the prototype and simulation results. This can be claimed as a limitation of the lumped-element components used in the circuit calculations compared to the precision of the full-wave simulation. The deviation does not impact the results, however, and does not predict the presence of transmission zeros in the BPF design.

Fig. 4 shows a prototype of the BPF, while *Fig. 5* shows measured S-parameters for the BPF. The center frequency is at 2.3 GHz, with bandwidth from 2.1 to 2.6 GHz. The filter achieves return loss of about –10 dB within the passband. Insertion loss of less than 0.8 dB is one deviation in the measured results that does not exist in the simulated performance. The observed frequency shift of about 100 MHz between measured and simulated results may be a result of the imperfect full-wave simulation and variations in fabrication accuracy, which cannot be totally avoided.

For the third-order BPF, the specifications include a center frequency (f_0) of 2.4 GHz, bandwidth (BW) of 300 MHz (the FBW is BW/f_0 = 0.125), return loss of better than 15 dB, and one single transmission zero at only 50 MHz after the upper cutoff frequency (2.6 GHz). This transmission zero increases the filter selectivity compared to the previous design.

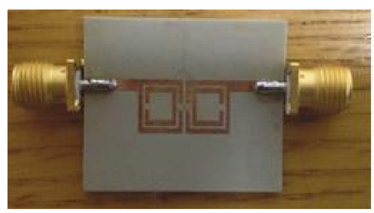

4. The second-order coupled SRR filter was fabricated on commercial circuit laminate material, with coaxial connectors attached for testing.

As explained in ref. 8, this optimization technique can produce equal transmission zeros according to (N – 2), where N is the number of resonators used. Therefore, to have one transmission zero, the proposed filter in this stage is designed as a third-order coupled resonator. It's worth noting that the position of the transmission zero is explained by the type of cross-coupling between the third resonator and the two original ones. Also, the specific value of the transmission zero was specified in the optimization equation ended by the coupling matrix. This approach is explained in detail in ref. 4, with the optimization technique described in ref. 8.

Fig. 6 shows the equivalent circuit of the trisection cross-coupled filter. The resonator circuit is a LC resonant tank.

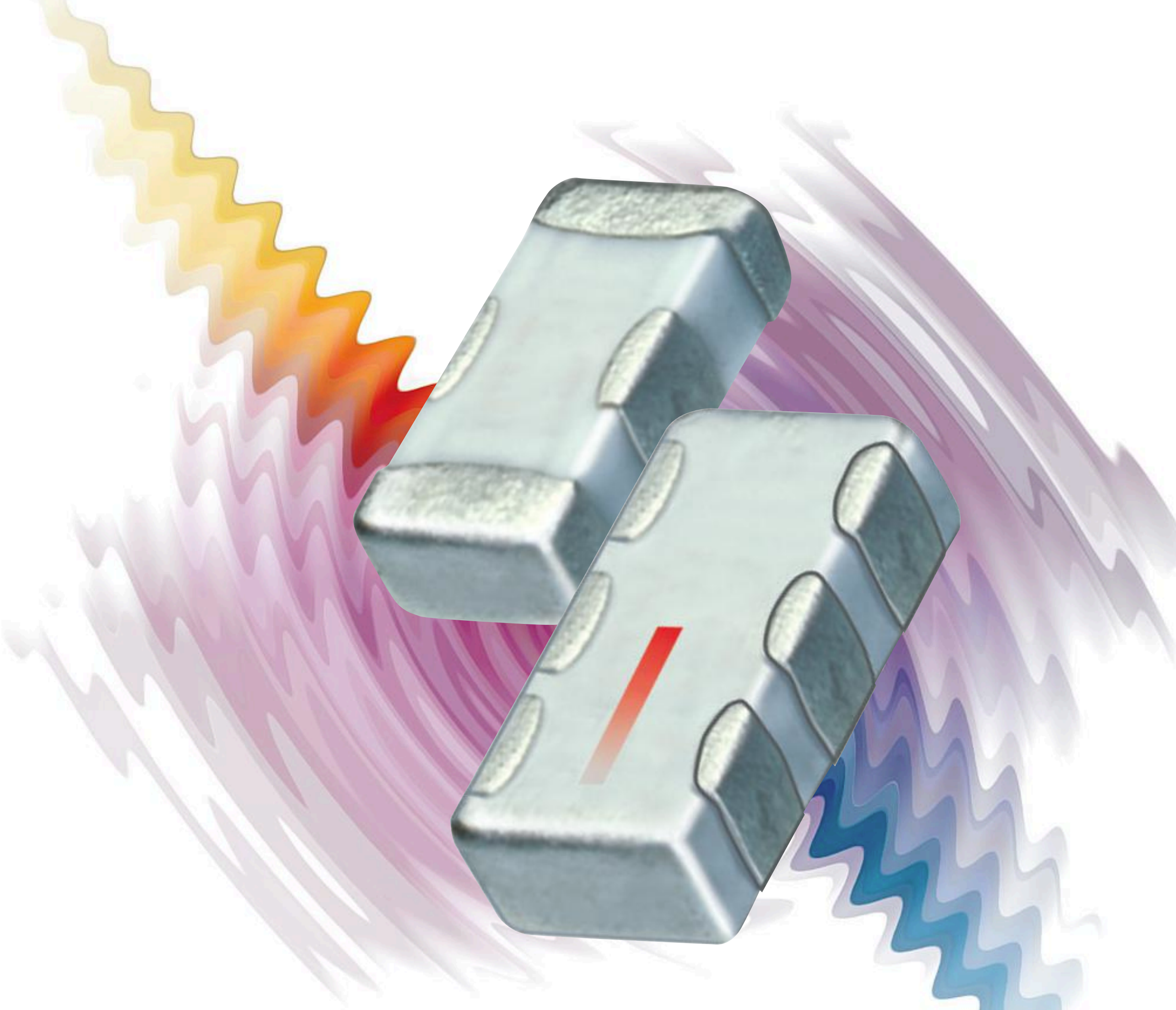

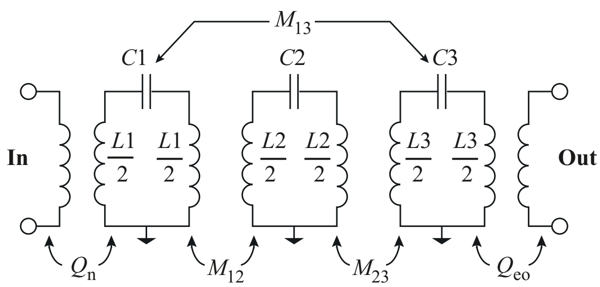

6. This is an equivalent circuit of the trisection, cross-coupled third-order SRR filter.

Coupling coefficients M_{12} and M_{23} are considered as the coupling between adjacent resonators. Also, the cross-coupling is given by M_{13}. Parameters Q_{ei} and Q_{eo} are the input and output external quality factors, respectively.

The filter design procedures can be summarized in two steps:

1. By controlling the coupling between resonators and the external quality factor, a bandwidth of 300 MHz is achieved.
2. The location of the transmission zero is specified at 2.61 GHz

Based on the previous optimization technique of extracting the coupling matrix and the external quality factor, coupling matrix (M), which is validated for the chosen topology, is optimized and extracted using the matrix of Eq. 13:

$$M = \begin{bmatrix} -0.1566 & 0.6727 & -0.7747 \\ 0.6727 & 0.7595 & 0.6727 \\ -0.7747 & 0.6727 & -0.1566 \end{bmatrix} \quad (13)$$

The external quality factors are $q_1 = q_2 = 1.009$. The actual (denormalized) coupling matrix becomes:

$$m = \begin{bmatrix} 0.0195 & 0.0841 & -0.0968 \\ 0.0841 & 0.0949 & 0.0841 \\ -0.0968 & 0.0841 & -0.0195 \end{bmatrix} \quad (14)$$

The actual external quality factors at input and output are $Q_{ei} = Q_{eo} = 8.072$.

The third-order coupled resonator filter performance is confirmed by using a full-wave EM simulation. *Fig. 7* shows the 2D layout of the third-order coupled SRR BPF. The filter consists of three SRR resonators; two are direct-coupled to each other and the third cross-coupled with them.

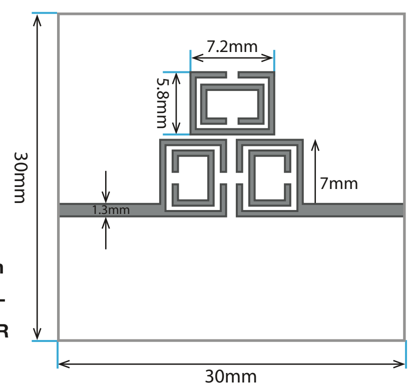

7. The 2D layout represents the circuit pattern for the trisection, cross-coupled third-order SRR filter.

Fig. 8 presents a comparison between the full-wave simulated scattering parameter magnitudes of the filter and theory, which depends on filter syntheses using the optimization technique. It's clear that the filter center frequency is 2.4 GHz and the filter bandwidth equals 300 MHz. There's a single transmission zero at 2.61 GHz, with this transmission zero due to cross-coupling between the resonators. Within its passband, the filter has insertion loss (S_{21}) close to 0.3 dB and return loss of 15 dB. As *Fig. 8* shows, good agreement was achieved between simulation and theory.

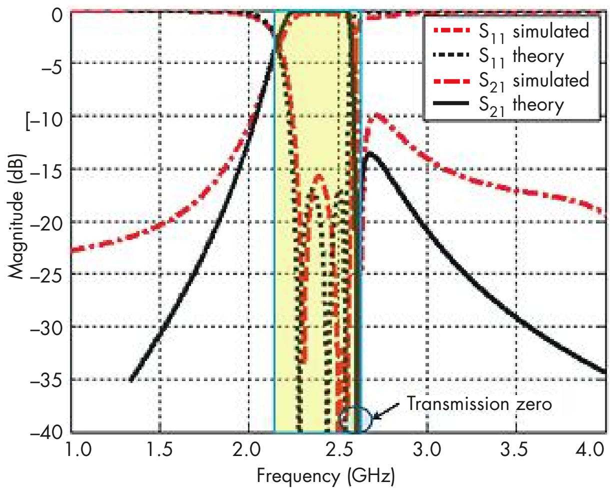

8. Theory and computer simulations for the third-order coupled-resonator SRR filter can be compared here.

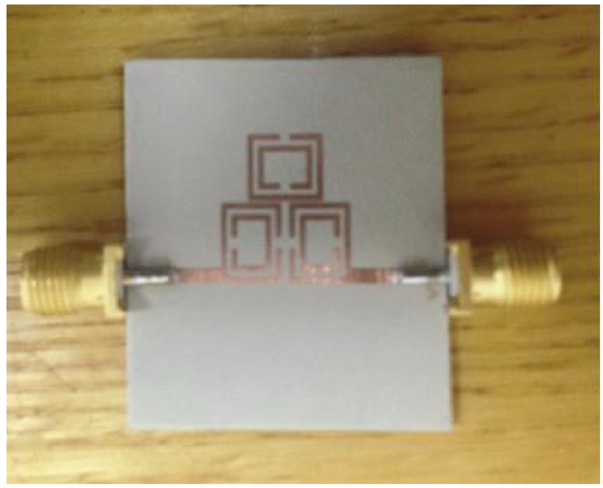

9. The photograph shows the third-order SRR filter, fabricated on commercial circuit material.

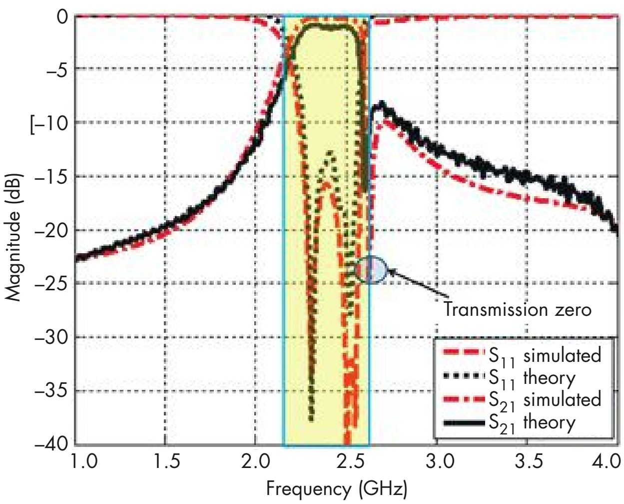

10. Compared are measured and simulated S-parameters for the third-order BPF.

Fig. 9 shows a photograph of the fabricated third-order BPF, while *Fig. 10* provides simulated and measured scattering parameter magnitudes for the filter. The measured results illustrate that the center frequency is about 2.4 GHz, with almost 15-dB return loss, close to 0.7-dB insertion loss, and with transmission zero at 2.61 GHz. This is about 0.3-dB greater measured insertion loss than the simulated value. The *table* compares results for some recently published filter designs.

These second- and third-order BPFs both have passbands around a center frequency of 2.4 GHz. Both are based on SRR resonators to achieve compact size (only 3 × 2 cm), and the third-order filter provides the added bonus of high out-of-band rejection for suppression of signals outside of the channel of interest. Whether simulated or measured, the filters provide performance levels in close agreement. mw

REFERENCES

1. David M. Pozar, *Microwave Engineering,* Wiley, New York, 2011.
2. G. L. Jones, G. Matthaei, and Leo Young, *Microwave Filters Impedance-Matching Networks and Coupling Structures,* Artech House, Norwood, MA, 1985.
3. R. J. Cameron, C. M. Kudsia, and R. R. Mansour, *Microwave Filters for Communication Systems: Fundamentals, Design, and Applications,* Wiley, New York, 2007.
4. J. S. Hong, *Microstrip Filters for RF/Microwave Applications,* 2nd ed., Wiley, New York, 2011.
5. Ralph Levy, Richard V. Snyder, and George Matthaei, "Design of Microwave Filters," *IEEE Transactions on Microwave Theory and Techniques,* Vol. 50, No. 3, 2002, pp. 783-793.
6. J. A. Ruiz-Cruz, C. Wang, and K. A. Zaki, "Advances in microwave filter design techniques," *Microwave Journal,* Vol. 51, No. 11, November 2008, pp. 26–44.
7. J. Lee and K. Sarabandi, "Synthesizing Microwave Resonator Filters," *IEEE Microwave Magazine,* Vol. 10, No. 1, 2009, pp. 57 - 65.
8. S. Amari, "Synthesis of Cross-Coupled Resonator Filters Using an Analytical Gradient-Based Optimization Technique," *IEEE Transactions on Microwave Theory & Techniques,* Vol. 48, No. 9, September 2000, pp. 1559-1564.
9. F. Seyfert and S. Billa, "General synthesis techniques for coupled resonator networks," *IEEE Microwave Magazine,* Vol. 8, No. 5, October 2007, pp. 98–104.
10. J. Uhm, J. Lee, I. Yom, and J. Kim, "General coupling matrix synthesis method for microwave resonator filters of arbitrary topology," *ETRI Journal,* Vol. 28, No. 2, 2006, pp. 223–226.
11. C.-M. Tsai, S.-Y. Lee, and C.-C. Tsai, "Performance of a planar filter using a zero-degree feed structure," *IEEE Transactions on Microwave Theory & Techniques,* Vol. 50, No. 10, October 2002, pp. 2362–2367.
12. W. Xue, C.-H. Liang, X.-W. Dai, and J.-W. Fan, "Design of Miniature Planar Dual-Band Filter With 0º Feed Structures," *Progress in Electromagnetics Research,* Vol. PIER 77, 2007, pp. 493–499.
13. Pu-Hua Deng and Jen-Tse Tsai, "Design of Microstrip Cross-Coupled Bandpass Filter With Multiple Independent Designable Transmission Zeros Using Branch-Line Resonators," *IEEE Microwave and Wireless Components Letters,* Vol. 23, No. 5, 2013, pp. 249 -251.
14. Jia-Sheng Hong, H. Shaman, and Young-Hoon Chun, "Dual-Mode Microstrip Open-Loop Resonators and Filters," *IEEE Transactions on Microwave Theory & Techniques,* Vol. 55, No. 8, 2007, pp. 1764-1770.
15. Mahmoud A. Abdalla, Aser M. Ahmed, and A.M.M.Allam, "A Multiband Filter for Wireless and RFID Applications," ICET 2014, Cairo, Egypt, pp. 1-4.
16. P. Mondal and M. K. Mandal, "Design of Dual-Band Bandpass Filters Using Stub-Loaded Open-Loop Resonators, *IEEE Transactions on Microwave Theory & Techniques,* Vol. 56, No. 1, 2008, pp. 150-155.
17. M. Hayati, L. Noori, and A. Adinehvand, "Compact dual-band bandpass filter using open loop resonator for multimode WLANs," *Electronics Letters,* Vol. 48, No. 10, 2012, pp. 573-574.
18. Chang-Soo Ahn, Juseop Lee, and Young-Sik Kim, "Design flexibility of an open-loop resonator filter using similarity transformation of coupling matrix," *IEEE Microwave and Wireless Components Letters,* Vol. 15, No. 4, 2005, pp. 262-264.

(Continued on page 117)

COMPARING FILTER DESIGNS

Source	Center frequency (GHz)	Bandwidth (MHz)	Insertion loss/return loss (dB)	Size (mm^2)
This article	2.4	300	0.7/15	15×13
Ref. 13	2	120	2.6/8	33×35
Ref. 21	10.5	420	0.4/20	7×7
Ref. 22	2	200	1.2/20	48×48
Ref. 23	1	100	0.8/18	18×18

DR. JIŘI POLIVKA, PH.D. | Consulting Engineer, Spacek Labs Inc., 212 East Gutierrez St., Santa Barbara, CA 93101;
(805) 564-4404, E-mail: jiripol@yahoo.com, *www.spaceklabs.com*

NOISE Can Tell Much About Material

When used as a test signal, noise and the field it produces can be quite handy in characterizing the quality and moisture content of different material solids.

Noise can hide details, but it can also reveal them. If properly used, noise will tell a great deal about a device under test (DUT), including when a DUT is raw material. For example, the Microwave Noise Field (MNF) test method has the capability to test different objects that can move, as well as objects with granular or irregular composition. When properly applied, the MNF method can provide precise analysis of different types of materials to help optimize the use of those materials in industrial applications.

The MNF method, also known as active radiometry, is a means of using noise rather than continuous-wave (CW) test signals when measuring the insertion loss of different materials.[1-3] The DUT or material to be tested is placed between a noise source and a radiometer antenna. The noise field is random with low coherence so that interference effects are negligible close to the radiators.

In addition, a DUT can move within the noise field without invalidating the measurements. A DUT being characterized in the noise field of the MNF method might even be considered as an object surrounded by white light, with little or no effects on the object from the white light.[4]

For measurements using the MNF method, the power level of the radiated noise in the noise field is very low, with noise measurements typically at nanowatt (nW) levels. A microwave radiometer is required as a detector to determine such low noise levels. The use of wideband noise for device or material testing has certain advantages over the use of measurements performed with CW test signals. In contrast to the MNF method, measurements performed with CW test signals require that a DUT be located in the far-field zone of the test signals, and that the DUT not move at all during testing.

Low-cost radiometers have been designed with the same low-noise block downconverters (LNBs) often found in satellite television receivers. Such LNBs are stable enough for measurement purposes, with good low-noise characteristics. In addition, the C- and Ku-band frequencies used for satellite television reception are internationally protected and managed communications frequency bands, preventing the generation of man-made signals (other than satellite-television signals) within those frequency bands.

TEST SETUP AND PERFORMANCE

Fig. 1 shows a typical test arrangement for measuring the insertion loss of a DUT placed between a noise radiator and a radiometer antenna. Any propagation loss due to the short distance between the noise radiator and the antenna must be included in the loss measurements. The typical maximum amount of loss that can be measured with such a setup is 40 to 50 dB. Therefore, the test setup can be mounted on a laboratory bench, and the distance between the noise radiometer and the antenna is preferably less than 30 cm (1 ft.) when using Ku-band components.

A typical microwave noise radiator

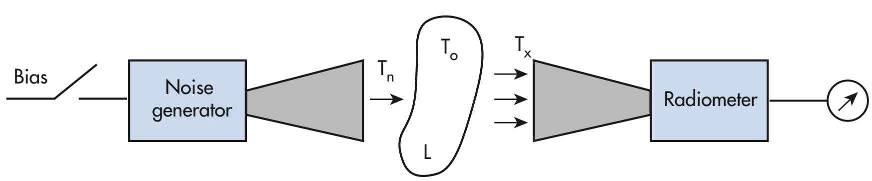

1. The block diagram shows the functions of a basic radiometer to determine the EM loss of an object.

(MNR) with an avalanche-diode noise source is characterized by an excess noise ratio (ENR) of 30 dB. The ENR (Eq. 1, in degrees Kelvin) quantifies the noise produced at the output of a DUT by its noise temperature (T_x) above the ambient temperature (To) of the test setup:

$$T_x = ENR \times T_o \quad (1)$$

An ENR of 30 dB means that for a typical T_o of 300 K, the T_x is 300,000 K.

The noise power, P_n, (in W) can be found from Eq. 2:

$$P_n = kT_xB \quad (2)$$

where k is Boltzmann's constant (1.38×10^{-23} J/K); B is the noise bandwidth of the system (in Hz), and T_x is the noise temperature (for this case 3×10^5 K). A typical dipole or waveguide-horn noise radiator has a noise bandwidth of several gigahertz, but radiometers with satellite LNBs typically have noise bandwidths of 1.0 to 1.5 GHz or 10^9 Hz. Using Eq. 2, it is possible to estimate the radiated noise power for such a radiometer:

$$P_n = kT_xB$$

$$= 1.38 \times 10^{-23}(3 \times 10^5)10^9$$

$$= 4 \times 10^{-9} \text{ W or } 4 \text{ nW}$$

Fig. 2 presents the range of DUT loss (in dB) that can be measured with a noise radiator with ENRs of 15 and 30 dB, and a radiometer with various temperature resolutions.

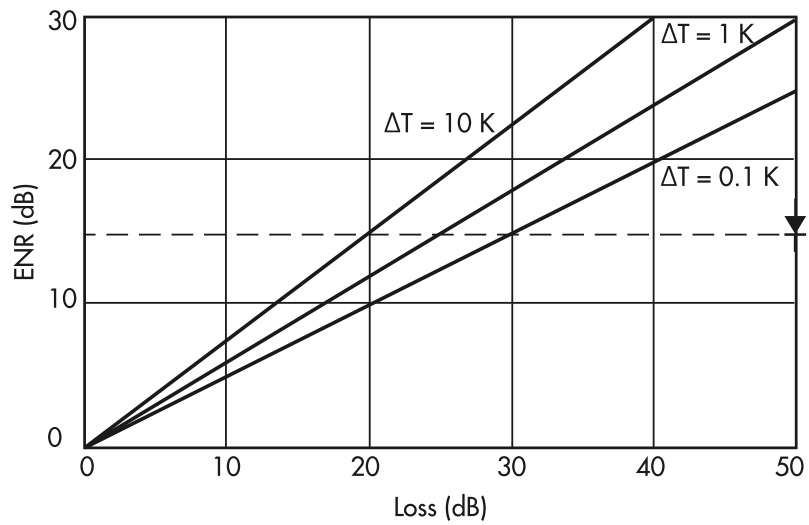

2. The curves demonstrate the measurable loss in a system such as that represented in Fig. 1.

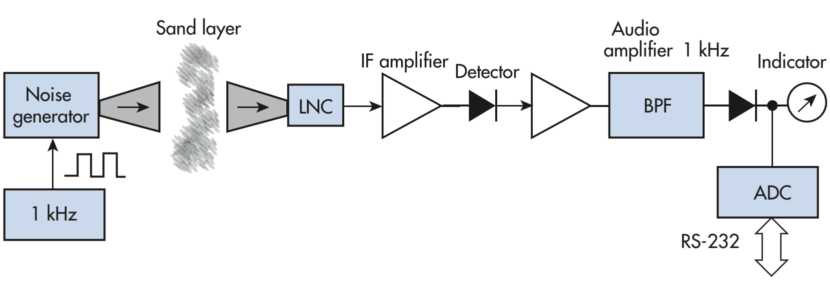

3. This block diagram represents a system that can measure the loss of a moving object by using noise.

Typical microwave radiometers with satellite LNBs consist of the LNB, an intermediate-frequency (IF) amplifier, and an IF detector *(Fig. 3)*. With an RF bandwidth of 1.0 to 1.5 GHz and noise figure of 1 to 2 dB, the temperature resolution1 can be found from Eq. 3:

$$dT = T_{sn}/(B\tau)^{0.5} \quad (3)$$

where dT is the minimum detectable temperature step (in degrees K); T_{sn} is the radiometer noise temperature (including the antenna noise temperature if pointed off target);

B is the predetection bandwidth; and τ is the post-detector smoothing time constant (in seconds). For the frequencies and values mentioned previously, the T_{sn} is around 350 to 400 K (the radiometer antenna typically sees an ambient temperature wall if the noise radiator is off); B = 1 GHz; and τ can be set to 1 s.

By plugging values into Eq. 3, it becomes

$$dT = 400/[(10 \times e^9)(1)]^{0.5} = 0.12 \text{ K}$$

Since simple radiometers are not completely temperature stable, a value of 0.5 to 1.0 K can be used for the value of dT to account for the instabilities.

To improve system resolution and stability, keying is performed with the noise radiator output, and the corresponding ac component for a particular keyed noise input. *Fig. 3* shows a noise-detection system that makes use of noise keying. An audio noise keying frequency, such as 1 kHz, can be used as the keying signal. For the MNF test setup, a sound level meter was connected to the radiometer output, to indicate the loss in dB for the noise keying signals.

With the use of keying, the loss measurement range exceeded 40 dB. The test system response was also tested with a calibrated waveguide attenuator connected between the noise source and the horn antenna to confirm system "linearity" for levels above 40 dB.

Fig. 3 shows the schematic diagram of a practical noise-field measurement system that has been used to measure moisture in sand and to detect flaws in wooden planks, in plywood, in rubber-tire sidewalls, as well as to identify wet spots in paper and fabrics. *Fig. 4* plots a comparison of measurements of moisture-based loss in sand, using CW test signals and noise field data.

The plots showing the influence of increased moisture on increased loss are quite similar. However, using a CW test signal at 10 GHz (at a wavelength, λ, of 3 cm) is not practical, since the sand layer must be fixed and cannot move to allow the use of a CW test signal. Using a noise field for such measurements is greatly preferred since the measurement data are not impacted by any movement of the sample material under test. *Fig. 5* shows a photograph of the experimental MNF test setup, with keying circuit for the noise radiator, the radiometer, its analog indicator, and the logarithmic sound-level meter.

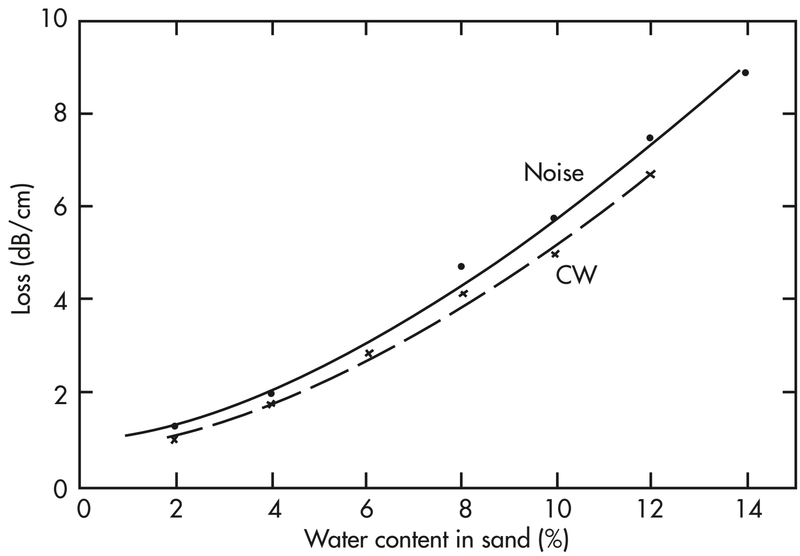

4. Loss in sand increases as a function of water content, shown for a wavelength of about 3 cm.

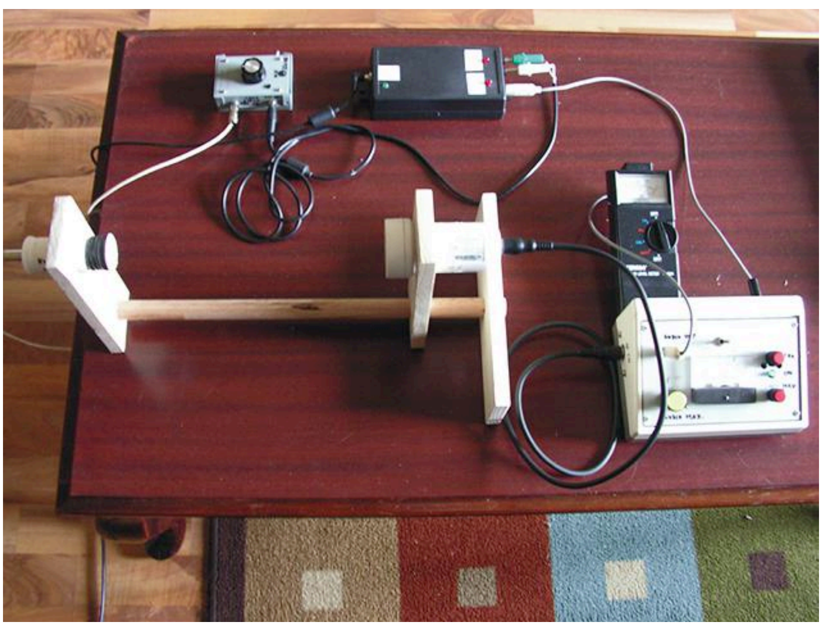

5. This experimental setup includes a keying circuit for the noise radiator, the radiometer, its analog indicator, and the logarithmic sound-level meter.

USEFUL APPLICATIONS

The first application of the MNF method was described in ref. 2 for the measurement of loss due to the moisture content of sand. Figure 4 shows a calibration curve for conventional CW test signals and for noise-based measurements on sand moisture levels from 0 to 14% (sand cannot be moister than this).

The industrial MNF system performed measurements on sand moving on a conveyor belt. A sand layer approximately 3 cm thick was maintained with a steel ruler on the rubber conveyor belt. Some loss, about 4 dB, in the system was discounted to account for measurement variations. However, sand movement within the system did not affect the measurement of the sand-moisture value, providing that some integration was performed for smoothing.

In this measurement system, noise keying at 1 kHz was used, with antennas set 15 cm apart. The Ku-band system, named Scout-1, has been used in several concrete-mixing plants since 1990 as a means of measuring moisture content of moving materials.[5] A similar system was designed for use at C-band frequencies to measure the moisture content of wood chips and wooden planks in a wood-drying plant and in an incinerator.

In 2014, the Czech Technical University, Institute of Materials, sought a method to detect flaws in the sidewalls of rubber tires for a rubber tire manufacturer. The manufacturer used a sidewall-looking camera to detect sidewall thickening or thinning. Samples with marked flaws were tested in the setup shown

in Fig. 5, at Ku-band frequencies, to confirm the known flaws as well as to identify whether additional, unseen flaws were present. The rubber tire company then declined to cooperate. Apparently, the MNF system detected more flaws than the rubber tire manufacturer expected to be found. For noise measurements performed on the rubber sidewalls, typical loss was 10 dB on average, with flaws increasing the loss by 3 to 5 dB.

The test setup shown in Fig. 5 was also used to measure the moisture content of wood planks with 1 in. thickness. Cracks and knots in the planks were readily indicated with the MNF method. Also, fiber orientation and moisture were detected by moving planks or plywood by hand between the antennas. The typical loss measured for a dry plank was 10 dB. Flaws and moist spots added 3 to 5 dB to the loss measurements, while knots and cracks in the wood reduced the loss measurements by as much as 3 dB.

Other researchers have used the MNF method to test granular and irregular-shaped materials. In addition to Ku- and C-band frequencies, they have performed wideband sweeps from 1 to 10 GHz as well as measurements around 94 GHz.[6]

Most LNBs are designed to receive one polarization. But some can receive two orthogonally polarized signals by electrically switching signal polarization with a voltage of 13 or 15 V dc. A linearly polarized signal can be used to distinguish between fibrous materials such as wood or plywood, and a polarization difference can indicate flaws and irregularities in tested samples.

In contrast to attempting to detect weak signal changes (in polarization) in the presence of a strong primary test signal when detecting the results of Mie forward-scatter during material measurements, the MNF test setup was used to identify changes in polarization during testing (i.e., changes in the shapes of the materials being measured). The MNF system was able to easily identify several round objects used to create the Mie forward scatter conditions, including metal rods and plastic rods and tubes.

Metal objects exhibited the greatest on-axis loss, while dielectric materials exhibited two symmetrical peaks with maximum on-axis loss. Most objects measured by the dual-polarization MNF system caused off-axis peaks in the field intensity, as expected according to Mie forward-scattering field theory.

Since the discovery of the MNF method, a number of applications have been evaluated for the technique much like those described here. Basic features have been presented in ref. 1, although not a great deal of feedback resulted in response. The use of the MNF method for industrial material testing features the benefit of the technique's simplicity and the capability of moving the material or DUT during testing, which is not possible when testing with microwave CW signals. The test approach can gauge loss of more than 40 dB for a material of interest while using extremely low-noise test power levels, leading to the possibility of using the MNF method for analysis in medicine and biology as well as for material research. mw

REFERENCES

1. Jiri Polivka, "Noise Can Be Good, Too," *Microwave Journal*, March 2004, pp.66-78.
2. Jiri Polivka, "Microwave Radiometry in Measuring Sand Moisture," 3rd International Workshop on Electromagnetic Wave Interaction with Water and Moist Substances, Athens, GA, April 11-13, 1999.
3. Jiri Polivka, "An Overview of Microwave Sensor Technology," *High Frequency Electronics*, April 2007, pp. 32-42.
4. Jiri Polivka, P. Fiala, and J. Machač, "Microwave Noise Field Behaves Like White Light," *Progress in Electromagnetic Research*, Vol. 111, 2011, pp. 311-330.
5. "Scout-1" sand-moisture measuring system; more details available at *www.ok1icz.cz*.
6. B. Kapilevich and B. Litvak, "Noise Versus Coherency in MM-Wave and Microwave Scattering from Inhomogeneous Materials," Progress in Electromagnetic Research B, Vol. 28, 2011, pp. 35-54.

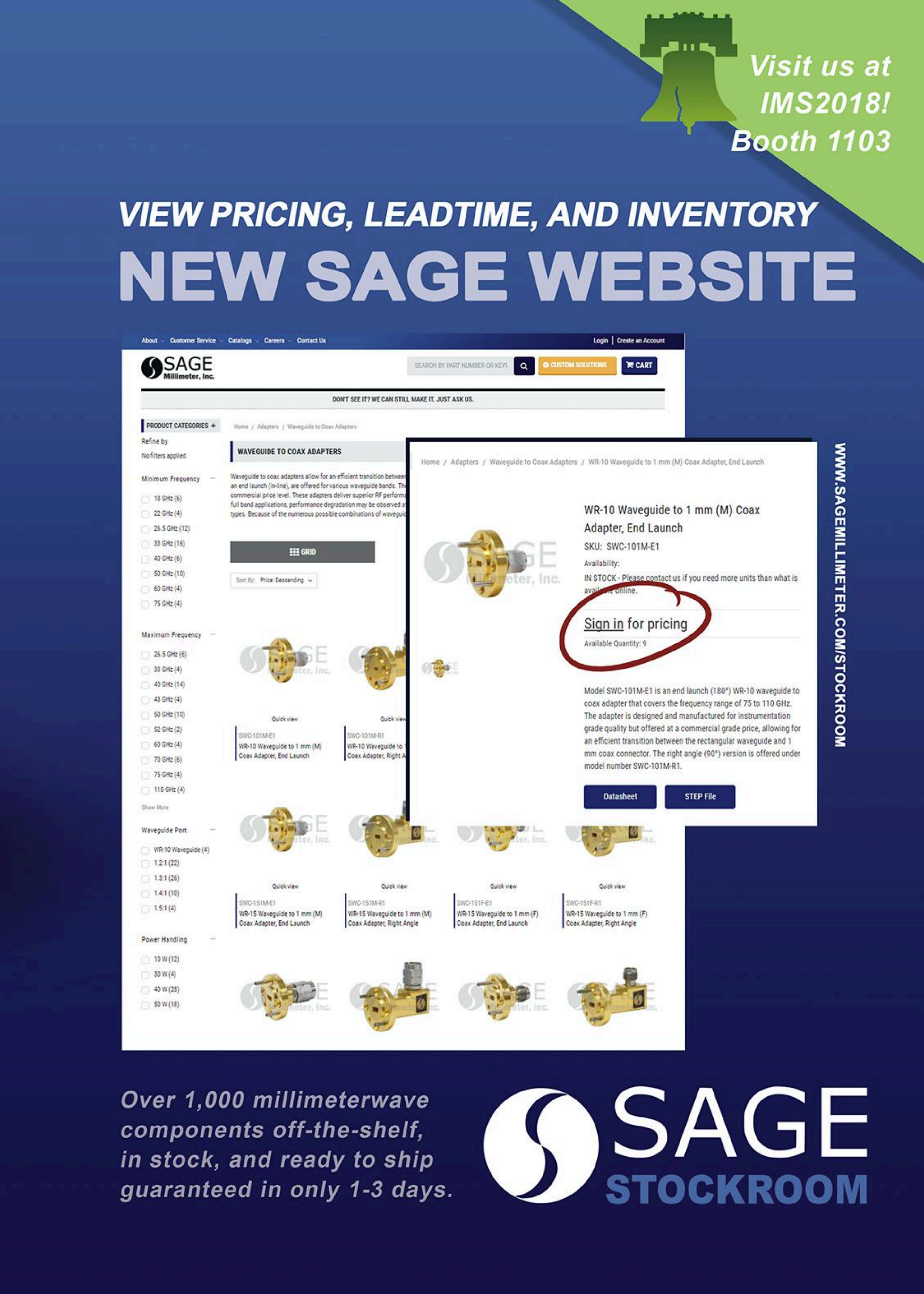

Visit us at IMS2018! Booth 1103
VIEW PRICING, LEADTIME, AND INVENTORY
NEW SAGE WEBSITE
WWW.SAGEMILLIMETER.COM/STOCKROOM
WAVEGUIDE TO COAX ADAPTERS
WR-10 Waveguide to 1 mm (M) Coax Adapter, End Launch
SKU: SWC-101M-E1
Sign in for pricing
Available Quantity: 9
Model SWC-101M-E1 is an end launch (180°) WR-10 waveguide to coax adapter that covers the frequency range of 75 to 110 GHz. The adapter is designed and manufactured for instrumentation grade quality but offered at a commercial grade price, allowing for an efficient transition between the rectangular waveguide and 1 mm coax connector. The right angle (90°) version is offered under model number SWC-101M-R1.
Datasheet
STEP File
Over 1,000 millimeterwave components off-the-shelf, in stock, and ready to ship guaranteed in only 1-3 days.
SAGE STOCKROOM

Design Feature

SWETHA G M | Research Engineer, Center for Research in Space Science and Technology, ECE Department of PES University, Bengaluru, India

HEMAVATHY K | Junior Research Fellow, Crucible of Research and Innovation Center, PES University, Bengaluru, India

S. NATARAJAN | Professor and Key Resource Person, Department of Information Science and Engineering, PES Institute of Technology, Behgaluru, India

V. SAMBASIVA RAO | Director, Centre for Research in Space Science and Technology, PES University, Bengaluru, India and Professor, ECE Department of PES University, Bengaluru, India (and keeper of S-band satellite ground station at PES University for interested students)

Overcome Message Collisions in Satellite Automatic ID Systems

A technique based on blind source separation can help maritime vessels gain meaningful guidance from satellite-based signals—even when they overlap.

Ocean-going ships rely on various types of signals from space satellites for guidance. At times, maritime vessels can struggle to resolve overlapped Gaussian minimum shift keying (GMSK) signals as part of the Space-Based Automatic Identification System (SB-AIS).

Fortunately, a practical technique based on the use of blind source separation (BSS) can resolve overlapped SB-AIS signals. It implements an independent component analysis (ICA) method to extract component values from the mixture of AIS signals received by a satellite receiver from different ship sources. Tracking component signals can be accomplished by estimating mixing components and accumulating a set of mixed GMSK signals. In fact, the approach is robust enough to receive transmitted symbol sequences despite different Doppler shifts in the received signals.

Use of the satellite-based AIS is required by the International Maritime Organization (IMO) for guidance of ships of class 300 tons and larger when on the high seas. The AIS is designed to avoid collisions between ships and used for terrestrial applications.[1] It employs self-organized time-division multiple access (SOTDMA) as an access scheme. AIS transceivers in each ship continually transmit each vessel's key data, such as its identification (ID) code, position, course, and speed toward other nearby ships.[2,3]

It also transmits ship details to the AIS stations along coast lines using the VHF maritime frequency band. AIS transponders transmit and receive data at 9.6 kb/s[4] using GMSK frequency modulation (FM) over the two frequency channels of 161.975 MHz and 162.025 MHz of 25-kHz (Class A) bandwidth. Each SOTDMA frame has one-minute duration that's divided into 2250 time slots. The transmission power (for Class A transponders) is 12.5 W.[4]

MESSAGE…RECEIVED?

Conventional VHF communication between a ship and the shore or one ship to another ship is constrained by the horizon, typically to 40 nautical miles.[5] The limitation of terrestrial coverage is overcome by the SB-AIS.[6] In the SB-AIS system, low-earth-orbit (LEO) satellites receive AIS signals from various ships located over a wide area on the Earth. The allocation of AIS message slots is self-coordinated within a limited area referred to as a cell. During the visibility of the satellite to a ship, several such organized cells are covered simultaneously. AIS messages sent in the same time space from various self-coordinated regions will be received by a satellite at the same time, resulting in the collision of AIS messages.

AIS messages sent in adjacent time slots from different organized areas may also overlap partly because of the different path distances.[7] This causes serious signal interference at the spacecraft. Hence, there's a total reduction in the probability of detection of the AIS messages when the satellite passes over areas with high traffic density.

The main challenge is to overcome the interference between messages received from various organized areas and to

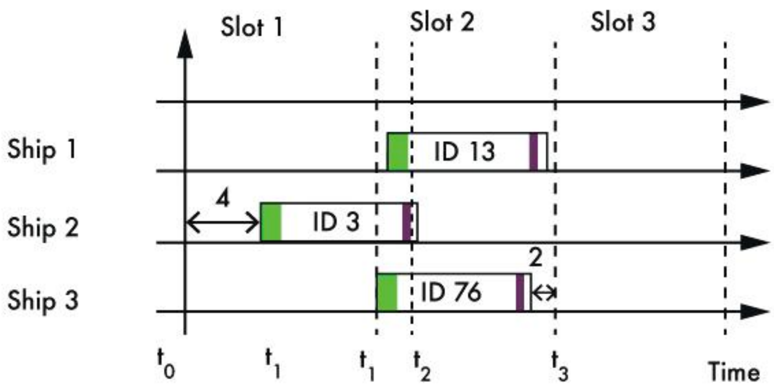

1. This plot presents examples of timing collisions among the communications to satellite for three different ships.

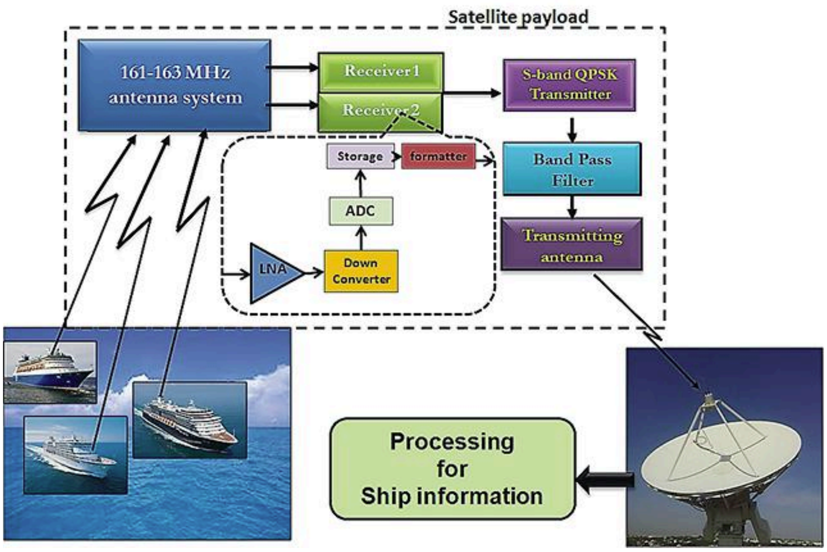

2. The block diagram represents a satellite-based AIS.

extract individual ship data. Fortunately, a technique with a signal-separation algorithm can be used to separate the overlapped GMSK signals. It successfully mitigates the slot collision problem associated with the received mixed AIS signals under maximum Doppler shifts/ time delay due to different path-loss conditions.

Signals transmitted from the AIS systems onboard ships in a satellite antenna's coverage zone are received by the satellite receiver onboard a LEO satellite. Signals transmitted by ships in different areas within the same time slot result in the collision of AIS messages.[8] The signals transmitted within each slot are received by the satellite with different amplitudes, time delays, and different Doppler frequency shifts due to the spatial separation of the ships. *Fig. 1* depicts the slot collision of AIS messages.

As per statistical observations, the probability of receiving more than three ship signals in each slot at the satellite simultaneously is quite low.[2] For this reason, three signals are simulated to test the effectiveness of the proposed signal separation technique. At each time instant, the received signal is a mixture of AIS messages with a certain amplitude ratio. This ratio depends on received power level and channel characteristics. Equation 1 gives the received mixed signal X at each instant of time as a mixture of three ship signals (S_1, S_2, and S_3) with different amplitude ratio. The amplitude ratios associated with S_1, S_2, and S_3 are taken as A_1, A_2, and A_3, respectively:

$$A_1S_1 + A_2S_2 + A_3S_3 \quad (1)$$

Fig. 2 presents a schematic diagram of the proposed advanced SB-AIS architecture. Three ships are assumed to be transmitting in a time slot in the satellite visible zone. The transmitted signals are received by three VHF monopole antennas mounted onboard a LEO satellite. The three VHF antennas are placed with spatial separations equal to fractional wavelengths of the transmitted frequencies. The mixtures of the three signals are received by three separate high-sensitivity VHF receivers onboard the LEO satellite, frequency-downconverted, digitized, and multiplexed into a single data stream and stored using a solid-state recorder (SSR).

During the satellite visibility period, the stored digital data is transmitted to ground by quadrature-phase-shift-keying (QPSK) modulation of an S- or X-band carrier. At the ground station, the received compound signal is demodulated, demultiplexed, and processed using the proposed signal separation algorithm to extract individual ship data.

The AIS transmitter part of the AIS transceiver placed onboard the ship includes AIS message and SOTDMA formatter and Gaussian-minimum-shift-keying (GMSK) modulation. Its 256-bit data form a data packet for transmission in each 26.6-ms slot *(Fig. 3)*. *Table 1* describes the bit size, timing, and functionality of each frame of the data packet. The carrier is GMSK-modulated with the formatted AIS data stream.

GMSK is a modulation technique that prefilters the incoming signal using a Gaussian pulse-shaping filter and per-

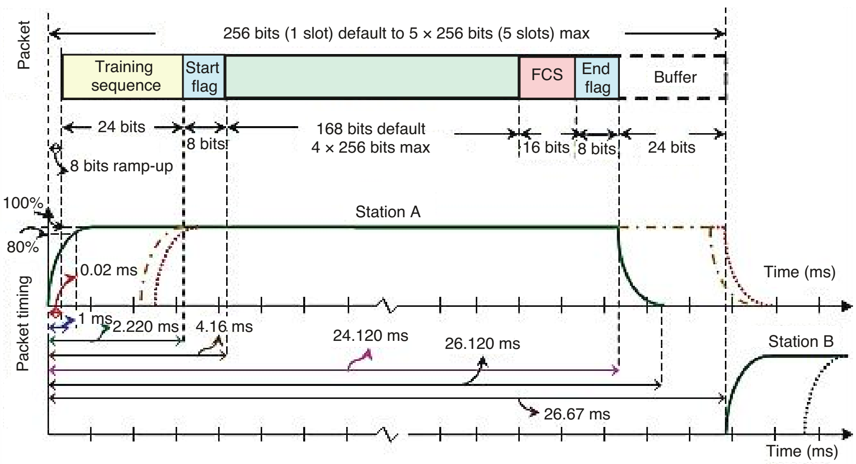

3. This is the structure of an AIS data packet.

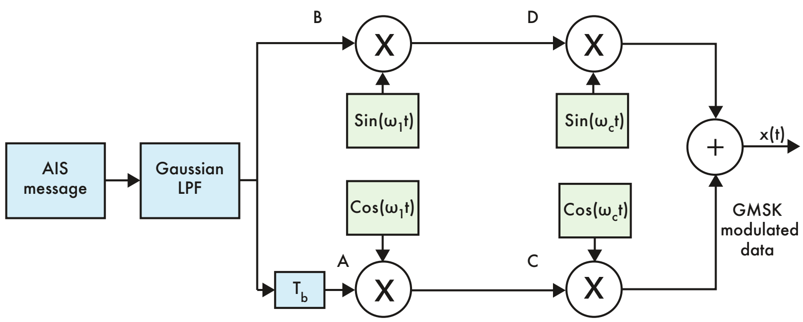

4. This block diagram represents a GMSK modulator unit.

TABLE 1: AIS DATA PACKET FUNCTIONALITY		
Packet data	**Length**	**Functionality**
Ramp	8 b	Switch-on time for AIS transceiver, 1 ms long
Training sequence	24 b	Necessary for synchronization
Start flag	8 b	In accordance with high-level data link control (HDLC) (HDLC) protocol, "7E" in Hex or "01111110" in binary
Data	168 b	data for the packet
FCS	16 b	In accordance with the HDLC, CRC-16-CCITT used over all data bits
End flag	8 b	Same as start flag
Buffer	24 b	Bit stuffing, distance delays, repeater delay and jitter
Ramp	8 b	Switch on time for AIS transceiver, 1 ms long
Training sequence	24 b	Necessary for synchronization
Start flag	8 b	Start flag in accordance with HDLC protocol, "7E" in Hex or "01111110" in binary
Data	168 b	Data for the packet
FCS	16 b	In accordance with the HDLC, CRC-16-CCITT used over all data bits
End flag	8 b	Same as start flag
Buffer	24 b	Bit stuffing, distance delays, repeater delay, and jitter

forms MSK modulation.[9] The bandwidth of the filter is chosen based on BT value, which is the product of the premodulation Gaussian filter bandwidth (B) and bit period (T).[10] *Fig. 4* presents a block schematic diagram of the GMSK modulator.

The AIS channel access scheme is based on SOTDMA, in which total transmission time for each AIS frame is 1 min and contains 2250 slots. Each AIS slot contains 256 bits of formatted data that's transmitted within 26.6 ms. AIS-enabled ships continuously synchronize themselves with GPS time in order to avoid slot collisions. Slot selection of each AIS station is randomized within a defined interval. The SOTDMA channel access scheme is shown in *Fig. 5*. When a station changes its slot location, new location and timeout for the same are announced beforehand. As a result, new slot location, including modified ship slot and new slot for ships in radio visibility, will be received by all vessels in a coverage area.

LOTS OF SLOTS

According to IMO, a minimum of 2000 time slots per minute is the reporting capacity of AIS-equipped ships. When the slots are shared in the SOTDMA broadcast mode, it overloads the system by 400-500%. In the case of communication between the ships within a range of 8 to 10 nautical miles, throughput is 100%. When the system gets overloaded, the preference is given to nearer rather than farther targets.

The proposed onboard receiver architecture contains three VHF monopole antennas, three receivers—each consisting of a low-noise amplifier (LNA), frequency downconverter, intermediate-frequency (IF) automatic-gain-control (AGC) amplifier—and an analog-to-digital converter (ADC). The three outputs are multiplexed and stored onboard the SSR. An S/X-band transmitting unit facilitates data transmission during the ground-station visibility period. *Fig. 6* gives an overview of an onboard AIS

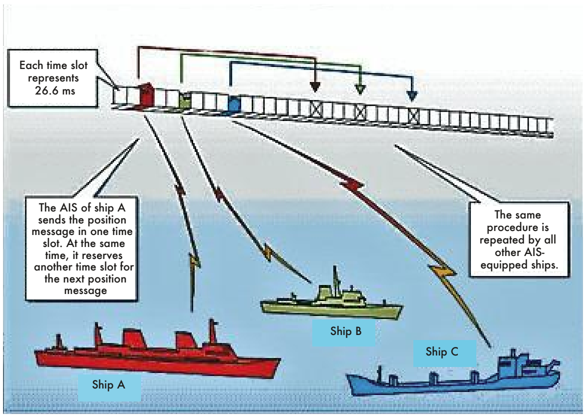

5. Shown is an SOTDMA channel scheme for three ships communicating with a satellite.

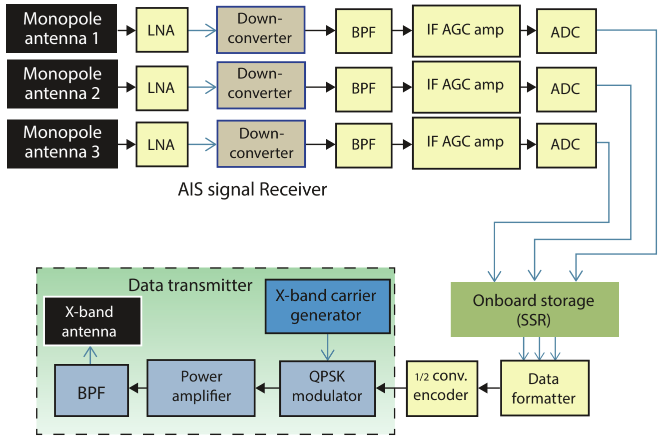

6. The components on board an AIS include frequency downconverters, filters, and amplifiers of several kinds.

receiver and transmitter architecture. As *Fig. 7* shows, three monopole antennas designed for VHF are mounted on three corners of the Earth-visible panel of the satellite. Each antenna output is connected to a dedicated receiver.

The signals received by the three dedicated receivers are passed through individual LNAs, downconverters, and bandpass filters (BPFs) to reach a baseband frequency of 480 kHz. The downconverted signals are digitized by an ADC, which samples the input analog signal at a rate of 10 times the baseband signal frequency (4800 kHz). The digitized data streams are multiplexed and then stored within an SSR.

During the period during which the satellite is visible to Earth, the stored or real-time data is QPSK-modulated on an S- or X-band carrier, depending on spectrum availability. The modulated carrier is transmitted by an S- or X-band antenna. An antenna designed for transmitting an S/X-band QPSK modulated carrier is mounted on the Earth-visible panel of the satellite. The antenna is designed with a beamwidth of about 130 deg.

The three mixed signals (X_1, X_2, and X_3) are received from the three monopole antennas. The ratio of each ship transmitted signal S_1, S_2, and S_3 in a mixture X_i ($i = 1, 2, 3$) is based on the channel characteristics and received power level. The ratio vectors of each mixed signal differ from the others based on the antenna placements from each other. Mathematically, the three mixed signals X_1, X_2, and X_3 received by the three monopole antennas are expressed by Eqs. 2 through 4:

$$X_1 = A_{11}S_1 + A_{12}S_2 + A_{13}S_3 \quad (2)$$

$$X_2 = A_{21}S_1 + A_{22}S_2 + A_{23}S_3 \quad (3)$$

$$X_3 = A_{31}S_1 + A_{32}S_2 + A_{33}S_3 \quad (4)$$

For this model, three antennas separated by fractional wavelengths of the frequencies of interest are mounted on the satellite. Three receivers will receive the mixed signals with their relative phase differences. *Fig. 8* shows the configuration of the ground station. The ground station receives the signals transmitted by satellite, demodulates

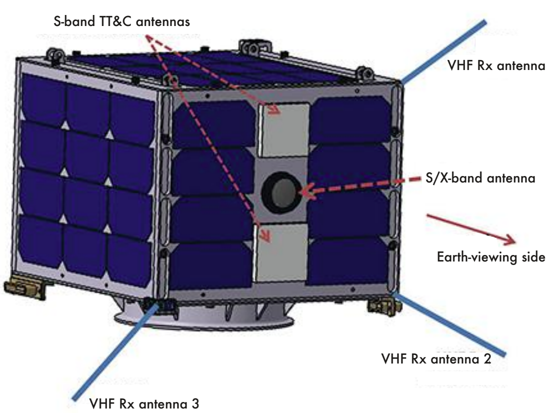

7. Antennas of different frequencies are configured on an AIS satellite.

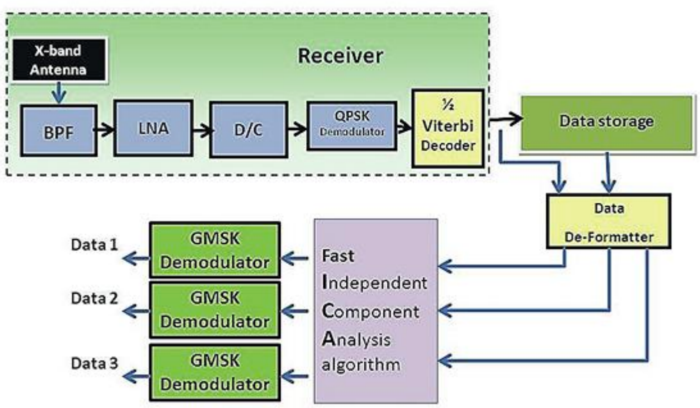

8. This is a block diagram of the ground station for a self-correcting AIS setup.

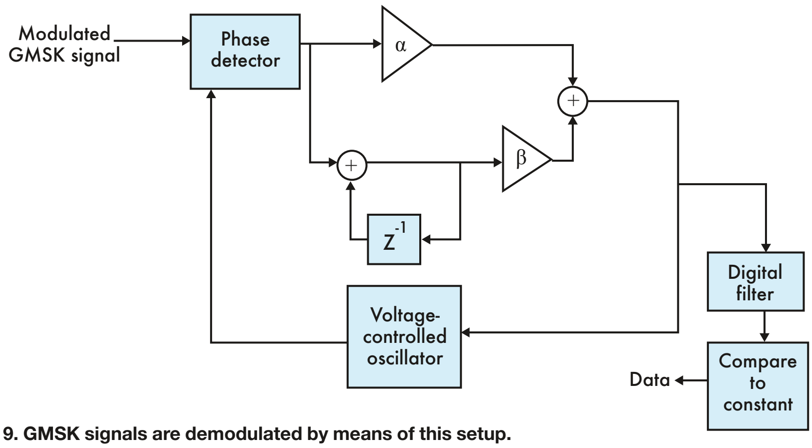

9. GMSK signals are demodulated by means of this setup.

them, demultiplexes them, and applies the signal separation algorithm to separate the signals, which are further GMSK-demodulated to discover individual ship data.

The received S/X-band signals pass through a receiver with an LNA and then downconverted to a 480-kHz IF. The IF signal is demodulated, Viterbi decoded, and demultiplexed to get the three signals X_1, X_2, and X_3. The three signals are separated using the Fast ICA Technique detailed subsequently in this article. The recovered ship-transmitted signals S_1, S_2, and S_3 are in modulated form with a carrier frequency of 480 kHz. The data is recovered using independent GMSK demodulators.

Demodulation of the GMSK signals is performed using the digital phase-locked loop (DPLL) shown in *Fig. 9*.[12] It consists of a phase detector, proportional-integral loop filter, and voltage-controlled oscillator (VCO).

The two inputs to the phase detector are the input and the output of the VCO. The phase detector is a digital multiplier that generates an error signal proportional to the phase error between the input signal and the output of the VCO. The type 1 loop filter, a π-controller, is part of the PLL's means of tracking phase and frequency. The π-controller consists of two arms: a proportional arm and an integral arm as indicated by the transfer function of a type 1 loop filter in Eq. 5:[12]

$$F_s = K_p + K_I/s \qquad (5)$$

where the proportional arm gain (K_p) produces the signal for small values of phase error. Parameter β controls the proportional gain.

The integral arm gain (K_I) produces the response proportional to changes in the frequency and maintains the DC bias. The α parameter controls the proportional gain. The output frequency of the VCO is controlled by the input error voltage. The VCO output frequency increases from free-running oscillator frequency (under zero input voltage) continuously until the output frequency of the VCO is equal to the input signal frequency.

Fast "Independent Component Analysis (ICA)"is a powerful BSS technique[13,14] to separate and recover the source signals S_1, S_2, and S_3 from the mixed antennas' signals X_1, X_2, and X_3. The modulated signal has a property of non-Gaussian distribution and is statistically independent. According to central limit theorem, due to the mixing of signal vector S by mixing matrix A, the mixed signal possesses a Gaussian distribution and the signal components are correlated. Fast ICA[15] is a signal-processing technique that processes the ship signal data in the mixed signal by de-correlating the mixed data and maximizing the non-Gaussianity.

The relationships between mixed signals X_1, X_2, and X_3 and modulated ship signals S_1, S_2, and S_3 in terms of matrices can be expressed as in Eq. 6:[16]

$$X = A * S \qquad (6)$$

where:

$$X = \begin{bmatrix} X_1 \\ X_2 \\ X_3 \end{bmatrix}$$

$$A = \begin{bmatrix} A_{11} & A_{12} & A_{13} \\ A_{21} & A_{22} & A_{23} \\ A_{31} & A_{32} & A_{33} \end{bmatrix}$$

and

$$S = \begin{bmatrix} S_1 \\ S_2 \\ S_3 \end{bmatrix}$$

Vector **X** is preprocessed by centering and sphering (for de-correlation).[17]

The Fast ICA process locates the mixing matrix A and performs A – 1 processing to recover the ship-signal vector Y, expressed mathematically by Eq. 7:

$$\mathbf{Y} = \mathbf{W}^*\mathbf{X} \qquad (7)$$

where:

$$\mathbf{W} = (w_1, w_2, w_3)^T = A^{-1}$$

is the unmixing matrix. The objective function is based on maximizing the non-Gaussianity in the mixed signals to recover the ship data as given by Eq. 8:[15]

$$J_G(Y_i) = [E\{G(Y_i)\} - E\{G(\gamma)\}]^2 \qquad (8)$$

where G is the cubic function given by $G(u) = u^3$; Y_i is the ith sample of the mixed-signal vector; and γ is the random Gaussian variable of zero mean and unit variance. To obtain the recovered signal vector Y, the objective function $J_G(Y_i)$ must be maximized.

Based on the signal projection pursuit direction, to find one independent modulated ship signal under the constraint:

$$\|w_i\|^2 = 1 \text{ for } i = 1, 2, 3$$

Eq. 8 is rewritten as Eq. 9:[15]

$$J_G(w_i) = [E\{G(w_i^T X)\} - E\{G(\gamma)\}]^2 \quad (9)$$

According to the Kuhn-Tucker condition, the local maxima of the function $J_G(w_i)$ under the norm constraint are at places where Eq. 10 is satisfied:

$$E\{Xg(w_i^T X)\} - \beta w_i = 0 \quad (10)$$

where $g = G'$; $\beta = E\{w_0^T X g(w_0^T X)\}$; and w_0 is the value of w at optimum.

Considering Eq. 10 as a function of (w_i) given in Eq. 11:[15]

$$f(w_i) = E\{Xg(w_i^T X)\} - \beta w_i \quad (11)$$

After solving Eqs. 10 and 11 via the Newton Raphson method, an iterative equation given by Eq. 12 yields:

$$w_i(n+1) = w_i(n) - f(w_i) f'(w_i) \quad (12)$$

The Jacobian matrix $f'(w_i)$ can be obtained as in Eq. 13:

$$f'(w_i) = E\{XX^T g'(w_i^T X)\} - \beta I \quad (13)$$

As a result, the weighting update is given by Eq. 14:[15]

$$w_i(n+1) = w_i(n) - [E\{Xg(w_i^T X)\} - \beta w_i]/[E\{XX^T g'(w_i^T X)\} - \beta I] \quad (14)$$

For a fixed convergence of Newton's method, converging factor μ is added to the equation, resulting in Eq. 15:[15]

$$w_i(n+1) = w_i(n) - \mu[E\{Xg(w_i^T X)\} - \beta w_i]/[E\{XX^T g'(w_i^T X)\} - \beta I] \quad (15)$$

where μ is a step-size parameter that changes dynamically with the iteration count. The value of μ ranges from 0.001 to 1.[15]

Considering flexible convergence and solving Eq. 15 by pre-multiplying it with $[\beta - E\{g'(w_i^T X)\}]$ yields Eq. 16:

$$w_i(n+1) = E\{Xg(w_i^T X)\} - E\{g'(w_i^T X)\} w_i \quad (16)$$

To estimate all of the independent ship data signals, Eq. 16[15] is iterated for all values of i = 1, 2, 3.

Once all independent weighting vectors w_i are estimated, to prevent different weights converging to the same estimated ship signal, decorrelation of the weighting vector w_1, w_2, and w_3 after every iteration is carried out. A symmetric decorrelation technique is carried out for this purpose. A two-step algorithm for the symmetric method is:

Step 1: Normalization of the updated weight as in Eq. 17:

$$W_{norm}(n+1) = W(n+1)/[\|W(n+1)W^T(n+1)\|]^{0.5} \quad (17)$$

Step 2: Repeat Eq. 18 until reaching convergence:

$$W^+ = (3/2)W_{norm} - (1/2)W_{norm}W_{norm}^TW_{norm} \quad (18)$$

The updated weighting vector (W^+) is the unmixing matrix obtained through the Fast ICA procedure. The matrix is used in Eq. 7 to obtain the estimated signal vector Y transmitted by a ship.

IMPLEMENTING THE ALGORITHM

The flowchart in *Fig 10* explains the steps involved in implementing the Fast ICA algorithm as MATLAB m-code.

Step1: Obtain the mixed signals X_1, X_2, and X_3 from the receiver unit.

(Continued on page 137)

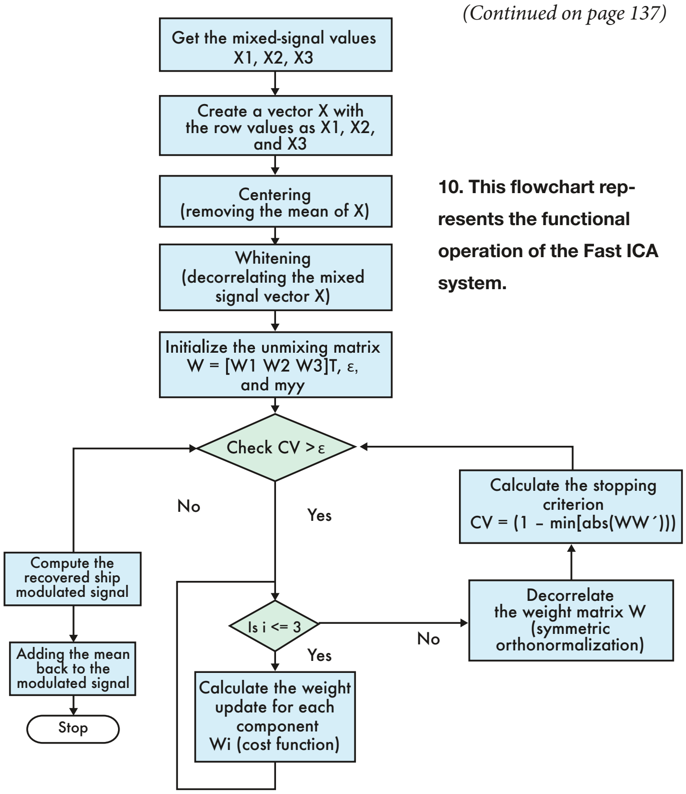

10. This flowchart represents the functional operation of the Fast ICA system.

ROB RUTKOWSKI | Digital Marketing Specialist, Bliley Technologies
www.bliley.com

What's the Difference Between OCXOs and TCXOs?

Oven-controlled and temperature-compensated crystal oscillators seem to be similar heat-related devices, but they have distinct characteristics and applications.

Oven-controlled crystal oscillators (OCXOs) and temperature-compensated crystal oscillators (TCXOs) are often confused—and for good reason. From a layman's perspective, both "oven-controlled" and "temperature-compensated" imply the use of heat or temperature to help control the frequency output of a crystal oscillator.

While this may be true, quite a few characteristic differences exist between OCXOs and TCXOs. In this article, we'll discuss OCXOs and TCXOs and what makes them different from each other. We'll also get into the common application uses for each type.

OVEN-CONTROLLED CRYSTAL OSCILLATORS (OCXOS)

OCXOs are used in applications that require a very high degree of frequency stability. Sometimes these oscillators may even be referred to as temperature-stabilized crystal oscillators, or simply crystal ovens. Just don't get excited about cooking any pizzas in this type of oven.

While crystal oscillators show a high degree of stability even when the outside temperature is varied over a significant range, some applications require even higher levels of temperature stability. In these applications, OCXOs may provide the required solution.

THE POWER TO CONTROL TEMPERATURE

It's still sometimes necessary to ensure an even better degree of stability. This can be achieved by placing the crystal in a thermally insulated container with a thermostatically controlled heater.

By heating the crystal to a temperature above that which would normally be encountered within the electronic equipment, the crystal's temperature can be maintained at a constant temperature. This results in a far greater degree of temperature stability. Additionally, the crystal in the OCXO will be cut to ensure that its temperature stability is optimized for the internal operating temperature *(see figure)*.

Quartz crystals such as these are cut to ensure that temperature stability is optimized for the OCXO's internal operating temperature.

The internal temperature for a crystal oven is commonly run at about 75°C. It needs to be above the highest temperature likely to be encountered, or else the temperature control will not work.

The typical specification for an OCXO might be $\pm 5 \times 10^{-8}$ per degree Celsius (0.05 ppm). A non-oven-controlled oscillator, on the other hand, may be between 10 and 100 times poorer.

To ensure that the optimum overall accuracy is maintained, combating elements such as aging of the crystal itself may be required as well as a periodic calibration of the OCXO. Typical calibration periods may be on the order of six months to a year, but the actual period will depend on the OCXO itself and the requirements of the application in which it is being used.

MORE PHYSICAL ABILITIES OF AN OCXO

OCXOs are physically much larger than a simple crystal oscillator. This is because they:

- Incorporate the crystal oscillator itself
- Contain a heater
- Contain control circuitry
- House thermal insulation around the crystal oscillator

Typically, the heater will run from a different supply to the oscillator. The supply for the OCXO's heater may be quite current-hungry. Some units may require an amp or so upon warm-up. This figure will reduce as the temperature inside the OCXO rises and less heat is needed. As you might imagine, the temperature is thermostatically controlled.

TEMPERATURE-COMPENSATED CRYSTAL OSCILLATORS (TCXOS)

A standard TCXO has quite a few performance qualities and can even completely solve the two major problems with quartz crystals. Here are some of the most common performance characteristics of TCXOs:

TCXO PPM performance: The TCXO temperature performance is better than that of a normal crystal oscillator. Figures of between 10 and 40 times improvement can often be seen. Figures of better than ±1.5 ppm over a 0 to 70°C temperature range are difficult to achieve, though. That's because they fall into a high-precision category, where costs increase significantly.

Power dissipation: The power dissipation of a TCXO will be greater than an ordinary oscillator due to the additional circuitry required. In addition, the cost is greater. One should also remember that it takes a short while after startup for the oscillator to stabilize (and hopefully stay stabilized). This may be on the order of 100 ms, or possibly longer, depending on the design.

TCXO package: TCXOs come in a variety of packages, depending on the way they have been designed and the requirements of the end user. The most common form of construction is to build the circuit on a small printed circuit board (PCB) that can be housed in a plated metal package. This then becomes suitable for mounting onto the main circuit board of the overall equipment. Since the crystal itself is sealed, this means that sealing of the overall TCXO package is not critical, or even required for most applications.

Note: Package sizes such as 5 × 3.2 × 1.5 mm or 5 × 3.5 × 1 mm are widely used for TCXOs; smaller packages are available if required.

Output format and level: With many TCXOs being used to drive digital circuits, most of the small oscillator packages produce what is termed a clipped sine wave. This is suitable for driving a logic circuit, although in many cases it's wise to put it through a logic buffer to ensure it's sufficiently square. Often the output is an open collector circuit. If a sine wave output is required, this must be chosen at the outset; it will limit the choice available.

Power requirements: Actual power requirements will be predicated on the device. Many operate from supplies of 3 V and may draw as little as 2 mA, although this will depend on the general type, the manufacturer, and the particular device chosen.

4 COMMON TYPES OF TCXOS

Although TCXOs are normally referred to in this manner, occasionally more detailed descriptions are used. Consequently, a variety of techniques can be used to provide the temperature compensation.

ADTCXO: This is an analog digital TCXO, widely used in cell phones. ADTCXOs leverage analog technology to provide temperature correction to the oscillator. It has the advantage that changes take place slowly and no phase jumps are experienced, as is the case with some all-digital types.

DTCXO: As you probably surmised, this is a digital TCXO. A DTCXO begins with a temperature sensor. Logic and mathematical functions use digital circuitry along with a lookup table. The resulting digital correction figure is converted to an analog signal using a digital-to-analog converter (DAC).

DCXO: This is a form of oscillator where any correction is calculated by the host processor within the equipment. In this way, the TCXO is not a separate entity, but the processing is incorporated within that of the overall equipment. This can help save costs in some instances.

MCXO: This form of TCXO uses a microprocessor to provide a considerably increased level of processing to deliver more accurate compensation under a variety of circumstances. While performance is a little better, costs are above those of the other forms.

TCXOs are widely used where accurate frequency sources are needed. They are less expensive and smaller than OCXOs. As such, they offer an ideal solution for many portable units requiring a reasonably accurate source. mw

defense electronics

A Special Section to INFORMA'S DESIGN ENGINEERING & SOURCING GROUP MAY 2018

JACK BROWNE | Technical Contributor

COTS Test Gear Tunes Radar Systems

A detailed application note explains how to generate the many different and simultaneous target signals needed to exercise modern radar systems. *(Courtesy of Rohde & Schwarz)*

RADAR SYSTEMS are invaluable tools/weapons for every modern military force, whether on the ground or in the air. Given the complexity of modern radar, though, they are not easy to test or maintain.

However, a leading high-frequency test-and-measurement instrument maker, Rohde & Schwarz, has compiled various ways to evaluate radars, using commercial-off-the-shelf (COTS) test equipment that might already be sitting in a laboratory for high-frequency component testing. The company has collected its radar target generation guidance in a new, 41-page application note, "Real-time Radar Target Generation," available for free download from the company's website *(www.rohde-schwarz.com)*.

Standard RF/microwave test equipment can be used to perform elaborator measurements on many different radar systems. Rather than building one-of-a-kind test systems with fiber-optic delay lines and digital RF memories (DRFMs) to simulate delays in reflections from radar targets, the application note shows how to use "standard" test equipment to generate multiple radar target echoes for testing radar systems to 40 GHz. The approach combines two of the company's workhorse microwave test instruments—the R&S FSW signal and spectrum analyzer and the R&S SMW vector signal generator—to accomplish the RTG and radar system testing.

The application note provides performance information on the different COTS test equipment used for the radar testing, along with a bibliography that contains additional information sources for the types of tests used to evaluate military and automotive radar systems as well as frequency-agile radar systems. In addition, the application note provides example instrument settings for performing different radar tests, including coexistence testing of airport radars with Long Term Evolution (LTE) wireless communications networks. de

Two-Channel Radio Links Battlefield Users

THE LATEST two-way portable radio from Harris Corp., the AN/PRC-163 Army Radio, is designed as much for the battlefield as for the modern world. The rugged and lightweight radio *(see figure)* employs a software-defined-radio (SDR) architecture for ease of use and to allow interoperation with other radio designs, such as satellite-communications (satcom) systems and even Android civilian smartphones.

The AN/PRC-163 can transmit and receive information through combinations of mobile ad-hoc networks, satcom systems, and VHF/UHF line-of-sight (LoS) communications methods. The radio is based on U.S. Special Operations Command (SOCOM) requirements with size, weight, and power (SWaP) optimized to benefit multiple

The latest portable tactical radio from Harris Corp., the AN/PRC-163, is designed to connect to various communications technologies and systems. *(Courtesy of Harris Corp.)*

(Continued on page 94)

Some Advances Aid Both Commercial and Military Designs

THE GAP BETWEEN what's commercial and what's military electronics is no longer so wide. At one time, radar simply meant military. Radar, an acronym for radio-based detection and ranging, was developed during the 1930s and put to work during World War II, and has been part of the battlefield in many shapes, ways, and forms ever since. But radar can do much more than detect enemy targets. It has been part of weather forecasting since the late 1980s, and will soon be considered standard equipment in advanced driver-assistance systems (ADAS) as part of vehicular electronic safety systems.

But perhaps the area of electronic equipment where the gap between commercial and military performance is narrowest is in communications. Certainly, 5G wireless phones will be designed and built to be disposable, as consumer electronic products that are perhaps replaced once a year. They will be no match for the ruggedness of tactical radios used on the battlefield. But in terms of performance, it may be hard to tell the difference between the best military radio and a 5G phone.

President Trump has already explained the importance of the U.S. being a world leader in the development of 5G wireless communications networks and equipment. 5G phones will have all of the capabilities of military radios, with voice, video, and data communications, and they will be capable of reaching satellites for connections when needed. But they will also use mmWave frequencies when data rates of 1 Gb/s or more are needed, rates which even now would be considered impressive for most computers.

5G phones and networks may come to represent the ultimate in what mixed-signal electronics technology can do for modern communications—surpassing what even the best military radios can accomplish for a fraction of the cost. But, the military may also come to use those same 5G phones, or at least the networks, and President Trump has stressed the importance of securing those 5G networks. Commercial and military electronic systems designers have learned a great deal from each other over the years, and 5G technology may be where they finally come to meet! de

Jack Browne, Technical Contributor

Two-Channel Radio Links Battlefield Users

(Continued from page 91)

mission needs (for example, less weight for a soldier to carry into battle). The radio includes a module expansion slot to add capabilities as needed for future requirements.

"The AN/PRC-163 Army Radio's future-proof design and software-defined architecture provides superior capabilities today and enables fast field upgrades for emerging capabilities," says Chris Young, president, Harris Communication Systems. "That upgradeability, coupled with ease of use and interoperability, makes it a clear choice for the Army's network modernization."

BACN Technology Becomes USAF Program of Record

The U.S. Air Force has upgraded the status of BACN communications technology to POR for greater availability to its troops.

THE IMPORTANCE OF Battlefield Airborne Communications Node (BACN) systems for maintaining tactical communications in RF-challenging environments, such as mountainous regions, was not lost on the U.S. Air Force and its managers at the Wright Patterson Air Force Base. The BACN system technology has been transitioned from its status as Joint Urgent Operational Need to a more permanent status of Program of Record (POR). The system technology has actually proved its value to pilots and warfighters for more than a decade, and the change in status marks a more effective and permanent approach to the technology for a greater number of users.

This change of status allows BACN to be used in more than just its initial Central Command applications. With the POR status, the technology will be available during training and to a greater number of warriors as an effective communications tools in mountainous regions. Requests for BACN-equipped aircraft have grown steadily since the development of BACN technology in 2008.

"We've been constantly analyzing the size of the fleets, and building the best schedules to maximize coverage since day one," says Lt. Col. Tim Helfrich, BACN's materiel leader. "We have a small team that weighs aircraft downtime and operational needs against coverage requests. Every BACN-equipped aircraft is always in theater." ■

Relay Handles Harsh Inductive Loads

POWER SWITCHING for aerospace, defense, and marine applications can take its toll when connected to high-power motors. Fortunately, the latest relay from TE Connectivity, its CII FC-335 series relay, is designed for harsh inductive power-switching applications, including the loads in lamps and motors. With a 35-A/28-V dc resistive load rating, the mid-range relay handles much higher capacity loads than most comparable mid-range relays on the market.

"What sets this relay apart from other similar devices on the market is its 35-A resistive rating for both 28-V dc and 115-V ac loads. Until TE released this product, the highest current rating available in this configuration was 25 A," says Randy Biddix, product manager for CII relays at TE Connectivity. "This gives customers additional current switching headroom in their applications."

The CII FC-335 series relays are built in accordance with MIL-PRF-6106 standards to meet or exceed the requirements of switching applications in power distribution, fuel pumps, guidance and navigation systems, weapons systems, and ground support equipment. The relays feature an all-welded construction for increased durability compared to solder-sealed relays. They are constructed with double-make contacts to share a load across two sets of contacts for increased reliability. The relays are available in solder-hook or terminal-block configurations, as well as 28-V dc and 115-V ac coils configurations. ■

This mid-range relay has been designed for rigorous power-switching applications in aerospace, defense, and marine systems.

Aethercomm Earns Quality Management Certification

AETHERCOMM HAS successfully achieved certification to the new AS9100 Rev D Quality Management System standard. The certification is provided by DNV GL, a leading certification organization. The AS9100 Aerospace standard is one of the better-known quality standards within the industry serving the U.S. Department of Defense (DoD). By acquiring this certification, Aethercomm has demonstrated the company's long-term commitment to quality and excellence.

Aethercomm is a designer and builder of RF/microwave power amplifiers and subsystems for use in radar, electronic-warfare (EW), communications, and test systems for commercial and military users. The company has shipped more than 300,000 RF/microwave amplifiers over the past 19 years, many for use in harsh environments.

The model SSPA 0.020-6.000-70 is an example of a recent product development, a solid-state power amplifier (SSPA) based on GaN technology capable of 70 W saturated output power from 20 MHz to 6 GHz. The compact unit measures 5.0 × 5.0 × 2.0 in. and is suitable for both commercial and military systems. ■

Glass-Fabric Tape Provides Extreme Masking Protection

DW 500 is a silicon rubber-impregnated glass fabric tape that provides masking protection during the plasma and flame spraying of aircraft engine components.

DW 500 from DeWAL (a Rogers Corp. company) is a silicon rubber-impregnated glass fabric tape that has been designed to provide masking protection during the plasma and flame spraying of aircraft engine components and turbo charger wear components. It uses a glass cloth backing for excellent thermal resistance along with a high-temperature silicone adhesive. The masking tape is designed to withstand grit blast and plasma spray while protecting engine parts from overspray and splash. ■

MARK STANLEY | Product Manager, Epec Engineered Technologies, 174 Duchaine Blvd., New Bedford, MA 02745;
(888) 995-5171, (508) 995-5171, *www.epectec.com*

Tapping into Tactical Targeting Network Technology

This wideband, high-speed, and secure networking technology has been developed for users moving at high speeds to enlist Internet Protocol communications for military engagements.

TO SAY that data is an important part of modern life may be a bit of an understatement. In an ever-more digital world, data is everywhere. During the past two years, more data was created than during the history of the planet leading to that two-year period. And by as soon as 2020, approximately 1.7 MB of new information (data) will be created per second for every living person on the planet.

On its own, data is largely meaningless. It can be considered digital noise, a series of 1's and 0's. Value comes from specific, targeted, and critical data that can be placed in the hands of those who need it the most at precisely the right moment, allowing them to extract and use the data for meaningful results. All of this raises a larger issue of security, particularly in terms of military- and defense-based environments.

Civilians are certainly aware of some of the dangers they face in terms of data security, with consequences such as fraud and identity theft looming should their personal data fall into the wrong hands. Even greater dangers await for cases of insufficient data security on the battlefield. Lives are at stake when data is being transmitted from an aircraft traveling in excess of 1000 mph to command crews on the ground. For something as essential as national security, nothing can be left to chance in terms of the reliability and security of critical data. These are the types of concerns that Tactical Targeting Network Technology (TTNT) were designed to address.

WHAT EXACTLY IS TTNT?

TTNT is a very specific type of waveform technology intended to meet a pressing need for high-throughput, anti-jam, low-latency, and quick-network-join waveforms for Internet Protocol (IP) connectivity as it relates to the Global Information Grid. Essentially, it's a way to deliver the fastest and most secure ad hoc mesh network for instantly and accurately sharing voice, video, and data between two points, especially for fast-moving users. The architecture of the technology is based largely on the Joint Airborne Network-Tactical Edge (JAN-TE) capabilities document, which itself was based on the Time Sensitive Target Networking Technology requirements of the Tactical Data Link Transformation Capability Document.

This type of technology offers a wide range of benefits, particularly in terms of defense and government applications. Not only does it provide a low-latency, ad hoc, IP-based network functionality, but it can successfully do so for more than 200 users at any given time. The connection itself is also "self-forming" and "self-healing." That means communicating platforms/users can automatically join and leave the network without any type of advanced planning, which can be a hurdle for the use of other types of networking options. Such network access is very beneficial for situations where multiple aircraft might be in communication with each other, as well as with crews on the ground.

TTNT is designed for secure, high-speed communications by users moving at high speeds. It enables instant and secure sharing of voice, video, and data between radios at relative speeds to Mach 8, or about 6138 mph. This capability is beneficial when two high-speed aircraft must be in secure communications with each other, even when they are moving in different directions. Beyond the speed of the users, the volume of data for TTNT is significant, with a specification of 10 Mb/s at a distance of 300 nautical miles.

TTNT has been developed to protect data in a number of ways, including increasing the chances that the data will be seen by means of prioritization. Using an advanced statistical priority-based multiple-access (SPMA) protocol, TTNT sends critical data first; lower-priority data is not transmitted in a communication until absolutely needed.

Additional benefits of TTNT include a strong "anti-jam" feature that's particularly useful in a contested environment. The technology employs a multiple-hop relay and automatic routing techniques to extend the reach of a secure communications system beyond line of sight, along with the fact that the platform itself allows for the simultaneous transmission and reception of as many as four different data streams at one time.

These capabilities of TTNT make it an essential part of modern defense and military landscapes, in no small part because of the way it satisfies the U.S. Department of Defense's (DoD) Air-

MMIC AMPLIFIERS

50 MHz to 26.5 GHz

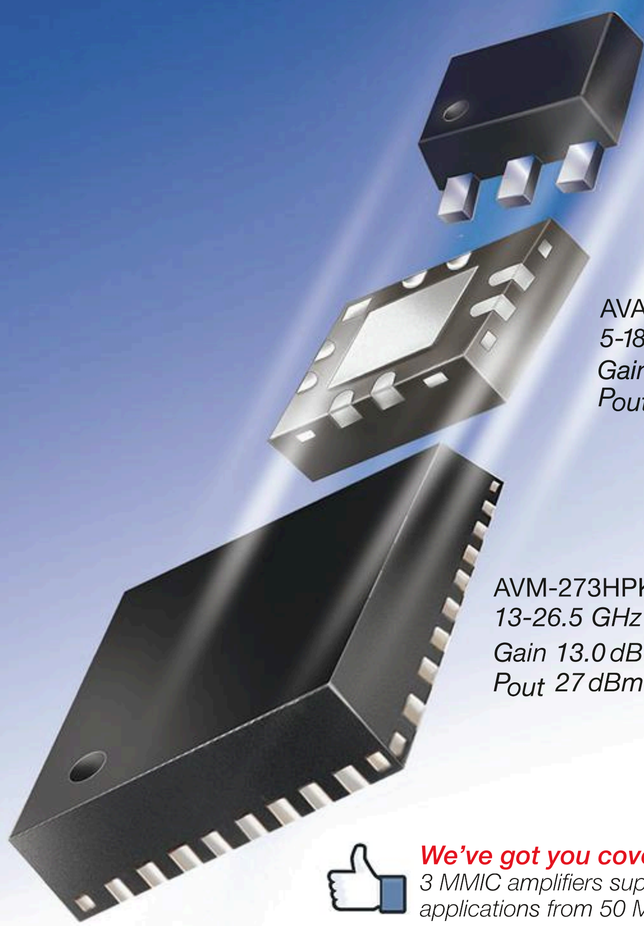

PHA-1+
0.05-6 GHz
$1.99 ea. (qty. 20)
Gain 13.5 dB
P_{out} 22 dBm

AVA-183A+
5-18 GHz
$7.95 ea. (qty. 20)
Gain 14.0 dB
P_{out} 19 dBm

AVM-273HPK+
13-26.5 GHz
$36.90 ea. (qty. 10)
Gain 13.0 dB
P_{out} 27 dBm

We've got you covered!
3 MMIC amplifiers support the whole gamut of applications from 50 MHz all the way up to 26.5 GHz!

Mini-Circuits' AVM-273HPK+ wideband microwave MMIC amplifier supports applications from 13 to 26.5 GHz with up to 0.5W output power, 13 dB gain, ±1 dB gain flatness and 58 dB reverse isolation. The amplifier comes supplied with a voltage sequencing and DC control module providing reverse voltage protection in one tiny package to simplify your circuit design. This model is an ideal buffer amplifier for P2P radios, military EW and radar, DBS, VSAT and more!

The AVA-183A+ delivers 14 dB gain with excellent gain flatness (±1.0 dB) from 5 to 18 GHz, 38 dB isolation, and 19 dBm power handling. It is unconditionally stable and an ideal LO driver amplifier. Internal DC blocks, bias tee, and microwave coupling capacitor simplify external circuits, minimizing your design time.

The PHA-1+ uses E-PHEMT technology to offer ultra-high dynamic range, low noise, and excellent IP3 performance, making it ideal for LTE, and TD-SCDMA. Good input and output return loss across almost 7 octaves extend its use to CATV, wireless LANs, and base station infrastructure.

Visit minicircuits.com for full specs, performance curves, and free data! These models are in stock and ready to ship today!

Modelithics® Vendor Partner

FREE X-Parameters-Based Non-Linear Simulation Models for ADS

https://www.modelithics.com/MVP/MiniCircuits

Mini-Circuits®

www.minicircuits.com P.O. Box 350166, Brooklyn, NY 11235-0003 (718) 934-4500 sales@minicircuits.com 478 rev S

Visit us at the IMS Show Booth #203

borne Networking requirements. Those requirements outline a strong need for how the three segments of the DoD's Global Information Grid—space, airborne, and terrestrial users—communicate with one another via IP-enabled network nodes. Due to almost a full decade of U. S. government investment and demonstrated applications in nearly every airborne platform in the U.S. Air Force and Navy, TTNT has already proven to be a viable means of providing secure, high-speed communications between rapidly moving radio systems.

APPLICATIONS FOR TTNT

Although TTNT has been designed for a particular group of (government and defense) users, the communications technology actually has a wide range of possible applications because of the viability and flexibility of the basic concept. For example, in 2005, the U.S. Defense Advanced Research Projects Agency (DARPA) successfully demonstrated the core technology by connecting tactical aircraft and ground communications nodes under a wide range of circumstances. These featured support for various applications that included, but are not limited to:

• Standard internet-based communications techniques such as e-mail, Internet chat, and internet access for aircraft that were already in the air.

• Voice over Internet protocol (VoIP), which transmits voice information over a data connection as an alternative to traditional telephone service.

• Support for the transmission of still images from both an aircraft to users on the ground, as well as from users on the ground to an in-flight aircraft.

• Support for the transmission of streaming, full-motion video from airborne aircraft to users on the ground.

• Enabling sophisticated aircraft procedures, such as implemented by the Joint Precision Approach and Landing System (JPALS) and the Automated Aerial Refueling System (AARS).

By design, TTNT has allowed tactical aircraft to quickly acquire time-sensitive assets that were in motion at high speeds, enabling network-centric sensor technologies to correlate information among multiple platforms, significantly increasing the accuracy in locating targets of interest *(see figure)*.

TTNT is a secure, high-speed networking communications technology that's designed for point-to-point links on the move, such as fighter aircraft and ground networking nodes.

Using TTNT and secure voice, video, and data, a ground commander could not only instantly identify support aircraft, but also correlate other critical information for the attack, including the amount and availability of fuel and ammunition. It would all be accurate, actionable, and real-time information that a ground commander could use to make the best possible decisions in response to the attack.

In the sky, a similar example would take place in the cockpit of a fighter jet. A pilot could use information from his/her own aircraft as well as information shared via TTNT from the ground to see an enemy fighter jet aircraft approaching from the rear faster than a radar warning receiver (RWR) could identify on its own. Of course, TTNT is more than a means of sharing data in the fastest, most secure way possible. It's also about ensuring the data gets to those who can make the best use of it, and who can keep people in potentially dangerous environments as safe as possible.

Of course, TTNT is not without its challenges. Developments in new technologies will be needed to make TTNT a practical and realizable technology. Broadband hardware components for systems using TTNT include power amplifiers, antennas, and transceivers compatible with existing Joint Tactical Radio System (JTRS) hardware. While TTNT is compatible with some existing hardware (since it's largely a new networking protocol), widespread implementation would require vast amounts of new hardware.

The TTNT network process as it relates to hardware begins with a particular user or radio system entering the range of the network. At that point, it receives a welcome signal and transmits verification information to the nearest hardware node on the ground. Subsequently, the user entering the TTNT network is connected to the nearest node and to other nodes in the area for transmission and reception of information. Upon leaving the range of the network, the user is automatically disconnected and the relevant IP address is deleted from the IP table.

For a secure communications network system to support TTNT, its hardware must be compatible. Any component that's not compatible with TTNT must be replaced or updated. The DoD has been working on this compatibility effort since 2006, when a document was issued that mandated the integration of TTNT into MIDS-JTRS designs.

Equally as important as the technology needed for current-day TTNT will be the technology needed to help it evolve. Without that support, TTNT could go the way of Link 16 technology. Link 16 data links are still used to transmit trend-sensing data between tactical aircraft, but they lack support for certain DARPA technologies, such as Advanced Tactical Targeting Technology (AT3). TTNT was developed in part to replace Link 16, but it must be fully supported to make that possible. de

JASON BAST | Principal Product Manager with Mercury Systems' Microelectronics Security Solutions Group, 7217, 3601 East University Ave., Phoenix, AZ 85034; (602) 437-1520

PHILIP FULMER | Director of Product Marketing for the Advanced Microelectronics Solutions group at Mercury Systems, 85 Nicholson Lane, San Jose, CA 95134; (669) 226-5823

Classic SiP Tech Repels Modern Threats

For the rugged operating conditions required by defense applications, SiP packaging technology still has more than a few miles left for squeezing advanced functionality in small spaces.

CHOICE OF packaging technology can often determine an electronic technology's ultimate effectiveness in a defense-related application. Once considered highly advanced, system-in-package (SiP) technology is no longer at the forefront of microelectronic packaging.

But, while other applications may seek to leverage the latest and greatest packaging technologies, military system architects cannot leverage new packaging technologies without clear evidence of military-grade reliability. In fact, by using a four-pronged approach, it is possible to modernize a proven, existing packaging technology—SiP—to power military applications in the most threatening environments.

SiP technology is still a valid approach for miniaturizing defense microelectronics, but other packaging options now crowd the scene *(Fig. 1)*. Semiconductor manufacturers and outsourced assembly and test (OSAT) providers have made tremendous progress in the commercialization of through-silicon-via (TSV) technology to interconnect multiple devices in compact form factors. The technology has matured sufficiently such that logic, memory, RF devices, sensors, and passive components are often integrated in a single package. While it would appear that the defense community would widely adopt TSV technology as its next packaging technology, there are still strong needs for SiP devices.

The performance benefits of TSV technology are well-established at commercial operating temperatures (0° to +70°C). Yet, military missions are not restricted to such a narrow operating temperature range.

In addition to temperature extremes—from −55 to +125°C—military electronics are also exposed to harsh thermal shock conditions from one temperature extreme to the other. Typical operating environments also include high altitudes, severe mechanical shock, vibration, and exposure to moisture. With all of these less-than-ideal operating conditions, military microelectronics are expected to perform flawlessly for years and even decades while being subjected to these operating environments.

Yes, the defense community must embrace commercial technologies to support military interests. However, this cannot be done without caution. For a military system architect, the decision to implement a new technology can lead to catastrophic consequences. Thus, the need arises for systematic evaluation of new technologies in realistic application environments. Furthermore, the perfect storm of worst-case environmental conditions must be an evaluation criterion. A quick review of the literature using any search engine quickly reveals that TSV technology has not yet matured to the levels required for predictable, long-term reliability in military application scenarios.

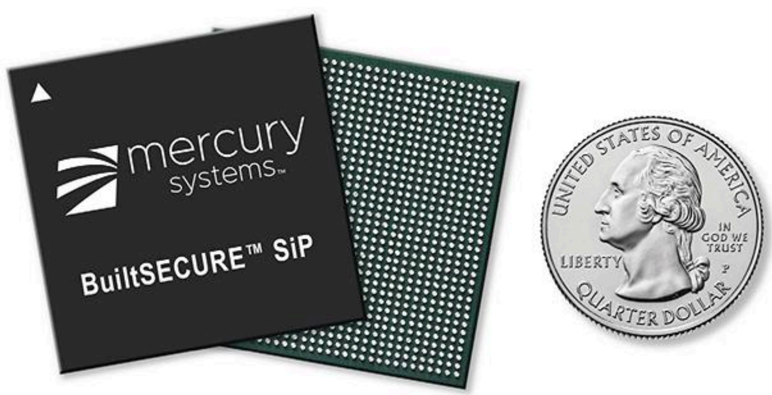

1. The small size of modern SiP technologies allows for extreme miniaturization of digital microelectronics capable of handling defense operating temperatures and conditions.

Before proceeding further, it is worthwhile discussing the spectrum of possibilities regarding the concept of an SiP device. Many manufacturers refer to an SiP device as a two-dimensional (2D) array containing a central processing unit (CPU) and memory, where interconnections between the devices are optimized for performance.

Best-of-breed SiP manufacturers will leverage three-dimensional (3D) stacking technologies (not to confused with TSV technology) to minimize the 2D footprints of their devices *(Fig. 2)*. Even fewer suppliers can apply multiple device interconnection technologies, such as wire bonding, surface-mount devices, and flip-chip devices, on the same design. Unlike a packaged device created with TSV technology, SiP devices can be rapidly prototyped and customized for specific program requirements.

While TSV technology is not suitable in forward-deployed military applications, it is worth questioning the fundamental assumption that tried-and-true SiP technology is no longer valuable for leading-edge defense applications. How can SiP technology be modernized to deliver the performance requirements demanded by our modern military forces? Four new SiP attributes are proposed: agile customization, advanced thermal management, embedded security, and trusted manufacturing.

AGILE CUSTOMIZATION

In years past, the defense industry converged on a single processor, the PowerPC, for military applications. Device scaling according to Moore's Law has enabled tremendous processing advances while reducing size, weight, and power consumption since the PowerPC was state-of-the-art.

Today, military system architects can choose from a wide range of processors and field-programmable gate arrays (FPGAs) to address different processing requirements. There is no universal combination of processor and memory that addresses every military application at present. Just as TSV technology can incorporate additional functionality beyond a processor and memory, SiP technology also embeds sensors and passive components, in addition to power-management circuitry.

Modern SiP devices must be developed by manufacturers capable of supporting rapid prototyping for new programs while sustaining production of a wide variety of legacy devices. Time to market, from concept development to production, must occur in less than one year to meet aggressive program schedules. The "one-size-fits-all" approach of the past must be replaced by agile customization for tomorrow.

THERMAL MANAGEMENT

Modern military computing systems process multiple, parallel data streams from a number of different sensor systems. Design rules for each device technology node continue to shrink. The processing demands placed on these compact devices are resulting in higher power densities, increasing the challenges for effectively dissipating the amount of heat generated. In applications where space constraints do not exist, discrete devices can dissipate heat via any combination of radiation, conduction, and convection.

When these devices are embedded within a ruggedized SiP device, thermal-management considerations cannot be avoided. Further complicating this scenario, it is distinctly possible that more than one processor, whether FPGA or GPU, must be embedded within the packaged device *(Fig. 3)*.

Next-generation SiP technology requires the manufacturer to dissipate a minimum of 100 W power without negatively impacting size, weight, and power (SWaP) or performance. Advanced thermal and mechanical modeling using highly sophisticated design tools maximizes thermal performance of a

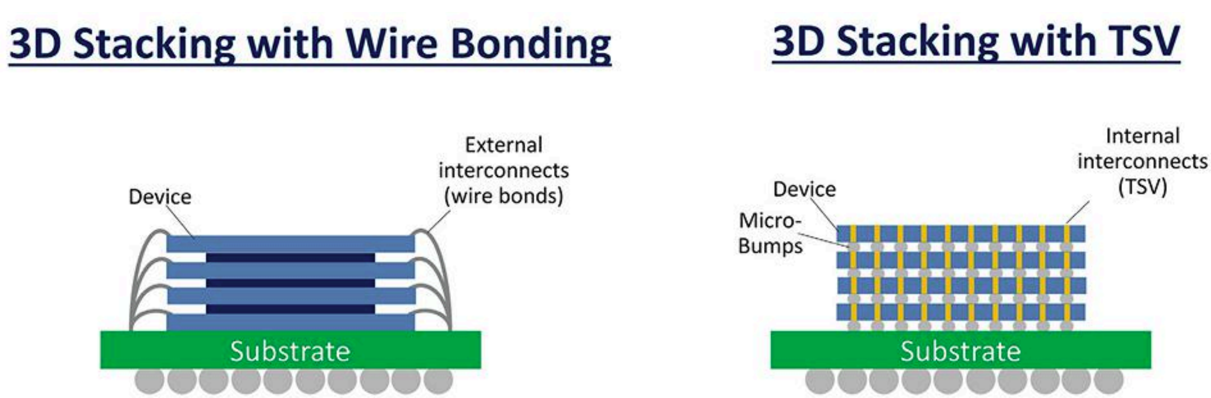

2. The 3D stacking in modern SiP enclosures makes it possible to squeeze a great deal of functionality within a small package size without sacrificing reliability.

Addressing the future needs of the defense market requires SiP manufacturers to take a holistic perspective to embedding trust within the cadence of daily operations. Supply-chain monitoring, particularly for critical components, ensures the authenticity of all procured parts.

packaged device. Predictable and reliable performance in environmental conditions simulating actual military environments is a prerequisite for SiP devices.

EMBEDDED SECURITY

Our military forces must maintain a strategic and tactical edge in global operations. The technology enabling these advantages must be protected at all costs. Yet it is unavoidable that many of the most advanced computing systems will be deployed in environments where platform capture is a possibility. Adversaries gaining access to these strategic technologies will leverage any tactic to understand the performance and construction of these devices, in addition to decrypting any stored data.

Although security features are typically not associated with SiP technology, embedding security within a SiP device is critical to protect the interests of our military forces. Achieving this ambitious goal of embedded security requires the intersection of two disciplines unfamiliar with each other: security architectures and microelectronics packaging. The typical defense microelectronics packaging supplier only achieves this objective through partnerships forged with security subject matter experts.

TRUSTED MANUFACTURING

Commercial microelectronics are manufactured in locations optimized to produce the highest volume of product per unit time with maximum cost efficiency. Nearly all electronic components today are manufactured outside the borders of the United States. As such, it is nearly impossible to guarantee that an adversary has not introduced bypass mechanisms into these devices to alter performance in life-or-death missions. Other supply-chain attacks may be more subtle. As an example, the introduction of counterfeit materials into the manufacturing process of a defense computing system can compromise mission performance.

Addressing the future needs of the defense market requires SiP manufacturers to take a holistic perspective to embedding trust within the cadence of daily operations. Supply-chain monitoring, particularly for critical components, ensures the authenticity of all procured parts.

The manufacturing environment must be monitored to make sure that manufacturing and quality procedures are rigorously followed without exception. The backgrounds of all employees directly or indirectly related to device manufacturing should be fully vetted. Finally, the network infrastructure containing valuable design and manufacturing records requires protection from cyberattacks through a vigilant cybersecurity program. The establishment of a trusted manufacturing center is not a trivial task, but manufacturers creating such centers of excellence will quickly realize the benefits.

By successfully incorporating agile customization, advanced thermal management, embedded security, and trusted manufacturing, SiP technology can be extended to address the requirements of modern military forces. Strategically designed enhancements based on application-specific requirements can deliver tangible benefits, as this example shows. Introducing these incremental innovations to proven technologies also offers affordability benefits, since there's no need to replace existing design and manufacturing equipment. de

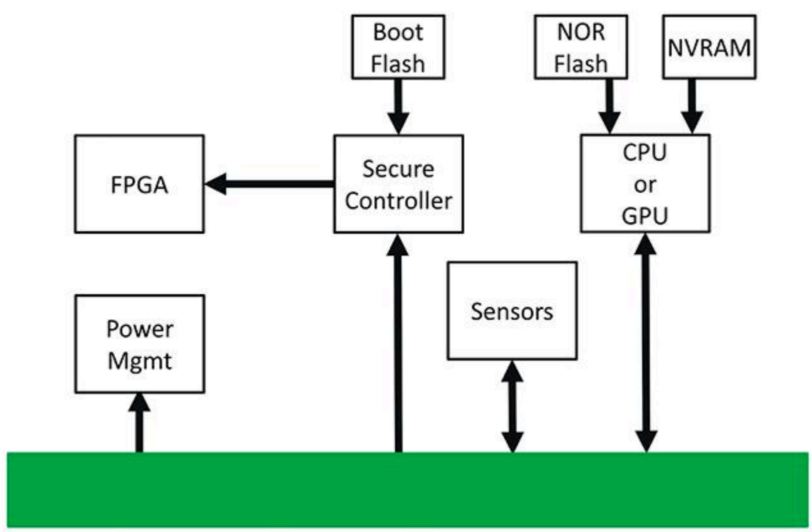

3. This block diagram is one example of the number of functions that can be contained in a miniature SiP housing.

JACK BROWNE | Technical Contributor

Radio Modules Make Upper C-Band Links

These interchangeable frequency modules turn this "smart" portable radio into a versatile unlicensed communications tool for use from 5.1 to 5.9 GHz.

UNLICENSED COMMUNICATIONS in industrial-scientific-medical (ISM) frequency bands have long been of interest to defense/military users as a way to add bandwidth when and where needed for particular applications. The latest frequency modules for the MPU5 mobile ad hoc networking (MANET) "smart" radios from Persistent Systems, LLC transform those radios into powerful, portable radios for use at upper C-band frequencies from 5.1 to 5.9 GHz within the unlicensed ISM band. This opens the door not only to defense contractors, but portable radio specifiers of all kinds to consider their needs for reliable voice, text, video, and data communications with these robust modular radios.

The Wave Relay MPU5 radios *(Fig. 1)* are as much computers as portable radios, each powered by an Android operating system. Like computers, the radios enable connection of external USB devices; the radios also have enough computer background to form and create self-healing networks with other radios and computer devices. The latest radio modules *(Fig. 2)* operate from 5.1 to 6.0 GHz with three independent antenna chains, each contributing more than 1.3 W transmit power to total 4 W transmit power.

The frequency modules support all multiple-input, multiple-output (MIMO) antenna modes with standard frequency accuracy of ±4 ppm. They support binary-phase-shift-keying (BPSK), quadrature-phase-shift-keying (QPSK), 16-state quadrature-amplitude-modulation (16QAM), and 64-state QAM (64QAM) modulation formats. As with the other frequency modules, the latest upper-C-band frequency modules are designed for operating temperatures from −40 to +85°C.

1. The modular MPU5 radios work with additional plug-in frequency modules to cover different frequency bands from L-band through upper-C-band frequencies.

2. The latest frequency modules for the MPU5 MANET radios support operation at unlicensed ISM frequencies, in the upper C-band range of 5.1 to 5.9 GHz.

POWERFUL PORTABLE RADIOS

Whether at C-band or lower frequencies, the MPU5 radios can monitor as many as 16 voice channels, with two channels active at any time. With their integrated radio-over-Internet-Protocol (RoIP) functionality, the radios can identify and connect to other radios via a tether cable to the audio input of the non-MPU5 radio. This networks the legacy analog voice from a third-party radio and makes the digital audio available as a resource to anyone on the MPU5 network.

The radios can view multiple video streams simultaneously; high-definition (HD) video input and output ports simplify connections to external cameras and HDMI-compatible displays, respectively. As data links, the radios can achieve 100-Mb/s and more throughout, and incorporate a variety of data connection points, including USB On-the-Go connections, RS-232 serial port, and Ethernet port. A Standard Charging Port (SDP) rated for 500 mA and voltages from 8 to 28 V dc helps to maintain battery power.

The latest, C-band frequency modules open additional frequencies for the MPU5 radio. The radio's Android OS helps an operator optimize available bandwidth, with software-definable channel bandwidths of 5, 10, and 20 MHz. Whether for defense use or other applications, the radios are well protected by numerous Suite B algorithm and encryption features.

The modules provide the links needed for a number of applications without human operators, including for Internet of Things (IoT) devices, unmanned aerial vehicles (UAVs), and vehicle-to-vehicle (V2V) and machine-to-machine (M2M) communications. However, with their flexibility and capabilities, it may be difficult to get these radios away from human operators, whether involved in commercial or military applications. de

PERSISTENT SYSTEMS, LLC, 303 5th Ave., New York, NY 10016; (212) 561-5895, www.persistentsystems.com

Amplifier Module Hits 100 W from 2 to 6 GHz

Model BME2969-100 is a solid-state amplifier module capable of 100 W saturated output power from 2 to 6 GHz. It measures 7.75 × 3.5 × 1.75 in. and weighs about 3 lbs. The Class AB linear amplifier is designed for operating temperatures from –40 to +65ºC and power supply of +28.5 V dc and has 600 W power consumption (20% typical efficiency). It delivers 59-dB typical gain with ±3-dB gain flatness across the frequency range, with typical second harmonics of –15 dBc and typical third harmonics of –20 dBc. Typical spurious levels are –60 dBc. The amplifier is fully protected against open and short circuits and is supplied with SMA input connectors and TNC output connectors.

COMTECH PST,
105 Baylis Rd., Melville, NY 11747; (631) 777-8900, www.comtechpst.com

Stacked Capacitors Handle High Temperatures

SMPS stacked capacitors feature multilayer ceramic capacitor (MLCC) construction with high-temperature solder to handle operating environments to +200ºC. Well-suited for space and aerospace applications, the SMX-style capacitors are supplied in a capacitance range of 100 pF to 340 µF and a voltage range of 25 to 1000 V dc for use in hostile environments. The capacitors have a temperature coefficient of 0 ±30 ppm/ºC from –55 to +200ºC.

AVX CORP.
One AVX Blvd., Fountain Inn, SC 29644-9039; (864) 967-2150, www.avx.com

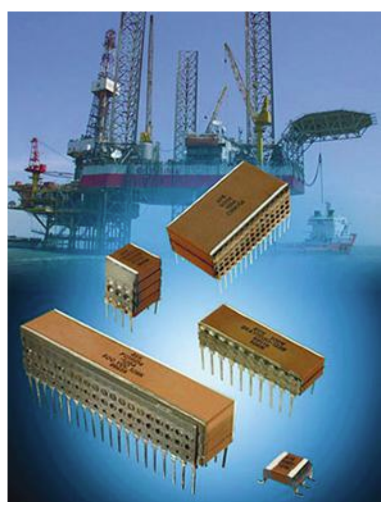

Cables Make Connections from DC to 18 GHz

The 6 Series of GORE-FLIGHT microwave cable assemblies are light in weight but durable in performance for a wide range of interconnect applications from dc to 18 GHz. The cable assemblies meet MIL-T-81490 requirements with minimum shielding effectiveness (SE) of 90 dB. They are available with different diameter cables, with maximum VSWR of 1.40:1 and typical VSWR of 1.25:1 through 18 GHz. The impedance is maintained to 50 ±1 Ω with insertion loss of no more than 0.384 dB through 18 GHz for any of the cable types.

W. L. GORE & ASSOCIATES, INC.,
1901 Barksdale Rd., Newark, DE 19711; (866) 271-5954, www.gore.com

Compact Amplifiers Boost Communications Ranges

Though the AR-20 tactical radio booster amplifier weighs just 1 lb., 10 oz., the fully automatic, band-switching VHF/UHF device provides 20 W output power from 30 to 512 MHz. It offers multiple dc supply options for flexibility, including operation from a single battery or 12/24-V vehicle supply. A built-in low-noise amplifier (LNA) can be switched on and off from the front panel. The booster amplifier provides 20 W output power when fed with a 1- or 2-W radio input signal.

AR MODULAR RF,
21222 30th Dr. SE, Ste. 200, Bothell, WA 98021; (425) 485-9000, www.arworld.us

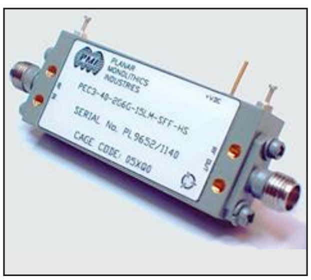

Limiting Amplifier Gains 1.85 to 6.25 GHz

Model PEC3-40-2G6G-15LM-SFF-HS is a limiting amplifier with minimum gain of 35 dB from 1.85 to 6.25 GHz. The gain remains flat within ±2.5 dB across the frequency range. The limiting amplifier delivers output of +15 dBm when fed with inputs from –15 to +17 dBm. Maximum noise figure is 6 dB. Measuring 1.91 × 0.78 × 0.36 in. with SMA female connectors, the limiting amplifier operates on supply voltages of +10.8 to +13.2 V dc.

PLANAR MONOLITHICS INDUSTRIES INC.,
7311-F Grove Rd., Frederick, MD 21704; (301) 662-5019, www.pmi-rf.com

GaN Bidirectional Amplifier Energizes 30 to 2700 MHz

Model TTRM120 is a wideband, GaN-based bidirectional amplifier (BDA) designed for use from 30 to 2700 MHz. It provides more than 8 W of transmit power in a compact housing measuring just 3.25 × 2.42 × 0.54 in. The efficient GaN BDA consumes only 24 W dc power with a wide dc input power range of +11 to +28 V dc. It produces more than 2 W of linear 16-state quadrature-amplitude-modulation (16QAM) output signals with less than 9% error vector magnitude (EVM). Switching between transmit and receive modes takes place in less than 1 μs, and can be performed manually.

TRIAD RF SYSTEMS INC.,
11 Harts Lane, Ste. 1, East Brunswick, NJ 08816; (855) 558-1001;
E-mail: sales@triadrf.com, www.triadrf.com

BE CERTAIN That Your IC is Compliant

Multichip packages and systems-on-a-chip (SoCs) are widely used to satisfy the demand for high-performing electronic devices. And with emerging applications requiring higher operating frequencies, the circuits used for these applications are becoming more complex. One factor to account for is the large amount of parasitic emissions that can be generated by such complex integrated circuits (ICs). In the application note, "Integrated Circuits (ICs) and Component EMC Testing," AR RF/Microwave Instrumentation discusses techniques that can be utilized to test ICs for electromagnetic compatibility (EMC) and electromagnetic interference (EMI).

The application note explains the fundamentals for both EMI and EMC testing. Essentially, EMI (emissions) testing determines the RF interference that's radiated or conducted from a component. Emissions from a component can cause nearby components/equipment to malfunction. EMC (susceptibility) testing determines the immunity of a component/device to external RF interference conducted or radiated into that component/device.

Following that discussion is an explanation of the TEM cell test method. It's used to measure the emissions or immunity of an IC from 150 kHz to 1 GHz. The document notes that either a two-port TEM cell or a one-port TEM cell can be used.

AR RF/Microwave Instrumentation, 160 Schoolhouse Rd., Souderton, PA 18964; (215) 723-8181; www.arworld.us

The note breaks down two standard test methods: the bulk current injection (BCI) method and direct power injection (DPI) method. The BCI method determines the immunity of an IC in the presence of conducted RF disturbances. And the DPI method determines the immunity of an IC as a function of the effective power transmitted to the circuit. Illustrations of both test setups are presented.

Another point highlighted in the app note is that cable harnesses and/or printed-circuit-board (PCB) traces can form efficient antennas. Thus, an IC receives unwanted RF energy through the pins that are connected to the wires of cables. That means the EM immunity of an IC can be characterized by conducted RF disturbance (i.e., RF forward power) rather than field parameters. Lastly, the document mentions specific AR amplifiers that can be used for BCI and DPI component testing, as well as the company's emcware test software.

CONNECTED CARS BANK ON the Right Hardware Components

WHILE THE INTERNET OF THINGS (IoT) has impacted many industries, nowhere is it more evident than in the automotive industry. This point can be proven by the rise of connected cars, which provide consumers with enhanced entertainment and safety features. But for connected cars to be a reality, the right hardware components are needed. In the white paper, "The Connected Car Market: Amphenol RF Solutions," Amphenol RF explains the significance of connected cars before discussing some of the hardware components that enable this technology.

The white paper notes that connected-car technology is increasingly being incorporated into consumer products. In terms of numbers, the global connected-car market penetration is 8.0% in 2018, with that number expected to rise to 19.3% by 2021. A quarter of a billion connected cars are projected to be on the road by 2020.

Amphenol RF, 4 Old Newtown Rd., Danbury, CT 06810; (800) 627-7100; www.amphenolrf.com

After that opening, the discussion surrounds the importance of the connected car, with an emphasis on entertainment and safety. One point brought out is that various forms of advanced driver-assistance systems (ADAS) are already implemented in many popular cars on the road. Automotive manufacturers also intend to implement additional ADAS technology into consumer vehicles in the near future. Furthermore, the white paper talks about both LiDAR and vehicle-to-everything (V2X) technologies.

Later on, the paper examines the hardware components of connected cars. It notes that while software will play an important role in connected cars of the future, hardware is equally vital to this industry. Examination of the connected-car hardware components then leads to a discussion of the FAKRA standard, which has been adopted as a global standard. FAKRA and other industry standards like USCAR have helped to reduce the costs associated with RF interconnections by optimizing electrical and mechanical performance in telematics applications.

Afterward, the white paper mentions Amphenol RF's earlier generations of FAKRA connectors (Gen 1.0 to 3.0). In addition, Gen 4.0 will play an integral role in the move to autonomous vehicles, according to the paper. 6.0-GHz FAKRA connectors are discussed as well.

BILL ROSAS | Signal Microwave
www.signalmicrowave.com

Transparentize Connections for 5G and WiGig Testing

As applications reach higher frequencies, the right tools are needed to develop effective connector interfaces.

Critical to many new projects is a transparent interface to the board—one that you do not even notice is there. This connector-to-board interface is referred to as the board "launch," where the RF energy transitions from the connector to the board. *Figure 1* shows a typical design with 2.92-mm interface 40-GHz connectors on the edge of the board.

For designers moving to higher frequencies, i.e., into the 20-GHz range and higher, it will no longer suffice to just treat an SMA connector as a lumped 50-Ω element and mechanically join it to the printed-circuit board (PCB) using a standard footprint. For these designs, it's now common to use 3D electromagnetic (EM) software tools, such as that supplied by COMSOL *(www.comsol.com).*

3D TOOLS AVAILABLE TO DESIGNERS

Designing a connector-to-board launch design is getting easier thanks to 3D EM software tools that have been available for years. Recently increased support from microwave connector suppliers is available as well.

Many microwave connector companies now provide 3D models of higher-frequency connectors that can be imported into 3D EM software tools. Some of these firms provide such models in a format that's only compatible with a specific 3D EM software package. A fee may also be charged to receive the model. Signal Microwave *(www.signalmicrowave.com)* models, on the other hand, are generic and can be used in any of the 3D EM software packages.

PCB material information is also available in many 3D solver packages. Signal Microwave goes beyond that by supplying reference designs for common high-frequency board materials. These reference designs, which are optimized by Signal Microwave, come in a common CAD format and can be imported into many 3D software tools. Customers are able to start with these reference designs and evaluate them using their own software tools. The design can then be used as is, or modified to better fit the customer's requirements for final performance.

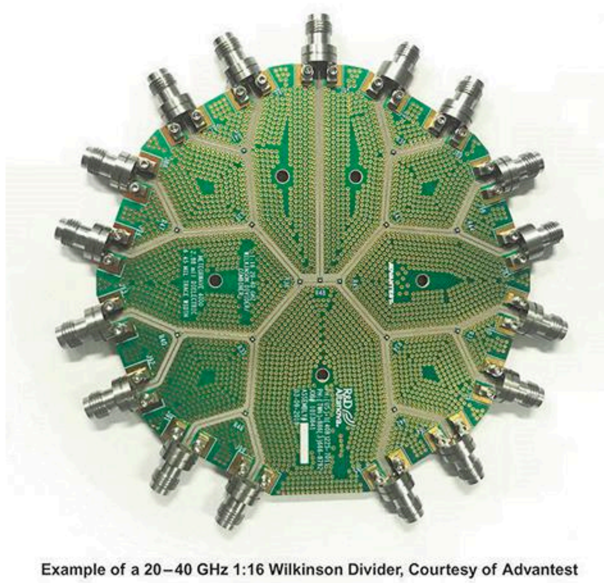

1. Shown is a 1:16 Wilkinson divider design that utilizes 2.92-mm connectors.

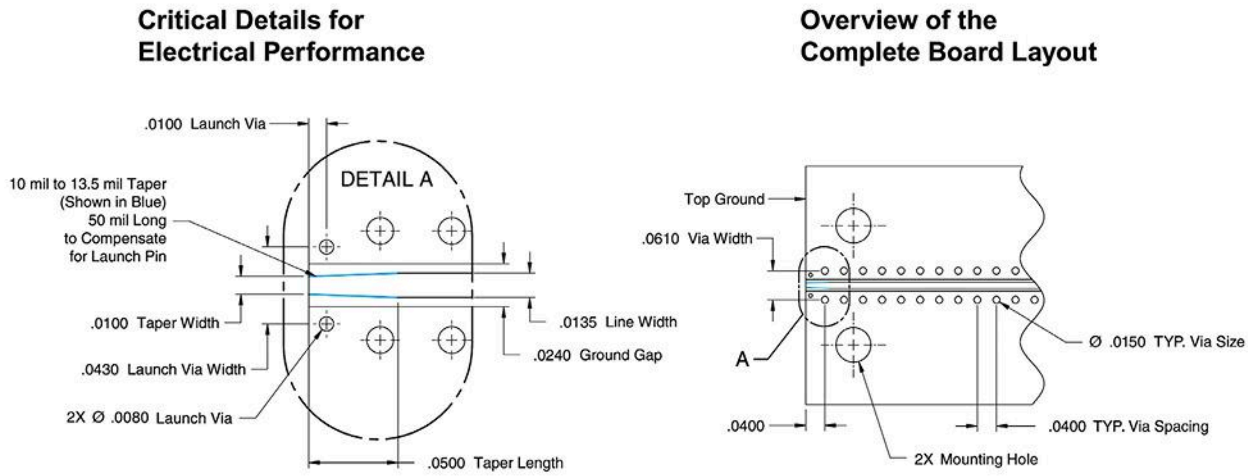

2. Critical details of a 70-GHz bandwidth launch design are revealed in this design.

THE NEED FOR 3D MODELS

In 2D circuit simulators, the components on a PCB that operate at high frequencies can be modeled using S-parameters. This is not the case with a coaxial-connector-to-PCB transition. The transmission-line geometry in a connector is coaxial (circular). On a board, however, this geometry is planar. Correctly modeling how these two transmission-line types directly interact requires a 3D EM solver to address the complexities of the change in transmission-line mode from coaxial to planar.

DESIGNS START WITH THE BOARD MATERIAL

Connectors are compatible with a wide range of board thicknesses and dielectric constants. The purpose of the board will determine the combination of board material, dielectric constant, and dielectric thickness requirements. The common board materials being used in the industry for high-frequency designs range in thicknesses from 4 mils (0.004 in.) to 12 mils (0.012 in.) with relative dielectric constants in the range of 3.0 to 3.5. Looking at these parameters, today's high-frequency connector geometry matches up well.

Here is a quick checklist of required knowledge before starting the actual design:

- List of components and features on the board
- Determine line widths to match
- Determine loss and power requirements
- Choose a transmission-line structure
- Choose a suitable substrate
- Choose a suitable connector

DESIGN EXAMPLE

Figure 2 shows a 70-GHz bandwidth launch design of a grounded coplanar-waveguide (GCPW) transition between a Signal Microwave ELF67-001 connector and an 8-mil-thick Rogers RO4003 PCB.

Key elements of the design include:

- Via size, placement, and spacing
- Circuit ground spacing to match the connector
- Signal-line width to create a 50-Ω transmission line
- Compensation of the signal line (taper) to account for the connector pin

HOW TO SET UP THE SIMULATION

Figure 3 illustrates a short transmission-line structure with 3D models of the connector on either side. Signal Microwave supplies 3D models of the launch portion of its board-mount connectors. COMSOL Multiphysics software, a 3D modeling package, has many of these models in its library along with common board materials. Using such a structure, it's easy to set up a two-port simulation model that can be used to optimize board designs.

Creating a through line with connectors on either end and creating the ports at the end of each connector simulation model will allow for the simulation of a structure that can be measured. The most efficient way to optimize the transition is by defining the ports as close as possible on either side of the section to be optimized. This would require creating a port in the transmission line of the board.

The domain between the inner and outer conductor of the edge-launch connector is filled with dielectric. Here, that dielectric is Neoflon, which has a dielectric constant of 2.5. All metal parts, including the edge-launch connectors, GCPW, metalized vias, and ground plane, are modeled as *Perfect Electric Conductor* (PEC) for low-frequency prototypes.

To consider loss factors and surface roughness at higher frequencies, the lossless PEC condition is replaced by *Transition Boundary Condition* and

Impedance Boundary Condition. The entire modeling domain is defined by *Scattering Boundary Condition*, which represents an open space.

The physics-controlled mesh is chosen to get all domains meshed with a tetrahedral mesh; maximum element size is five elements per wavelength so that the wave is well-resolved. The maximum mesh size is automatically scaled by the material properties in the dielectric substrate. The parts in the edge-launch connectors are meshed manually with a finer resolution to provide good resolution of the curved surfaces.

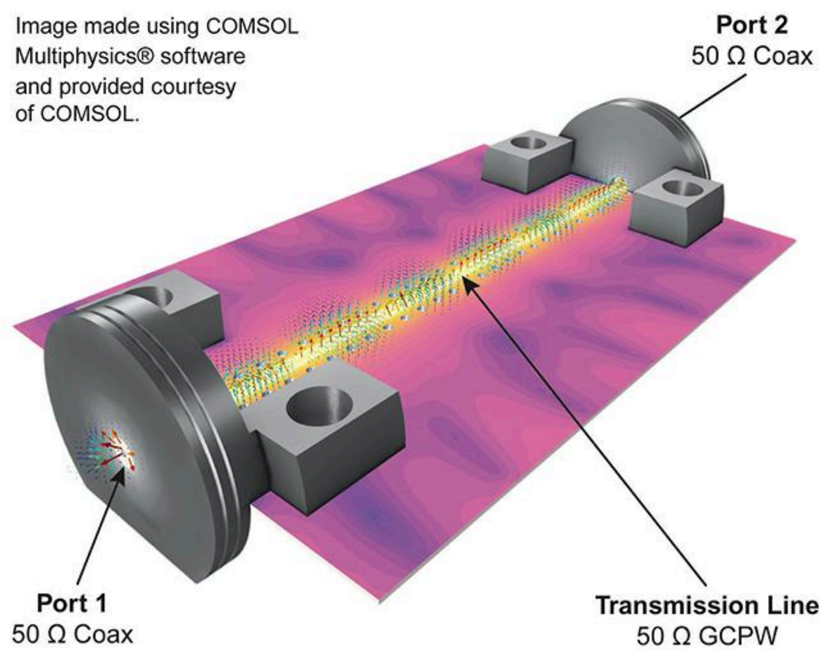

3. This is a model of a transmission line structure with connectors, created using COMSOL Multiphysics software. *(Courtesy of COMSOL)*

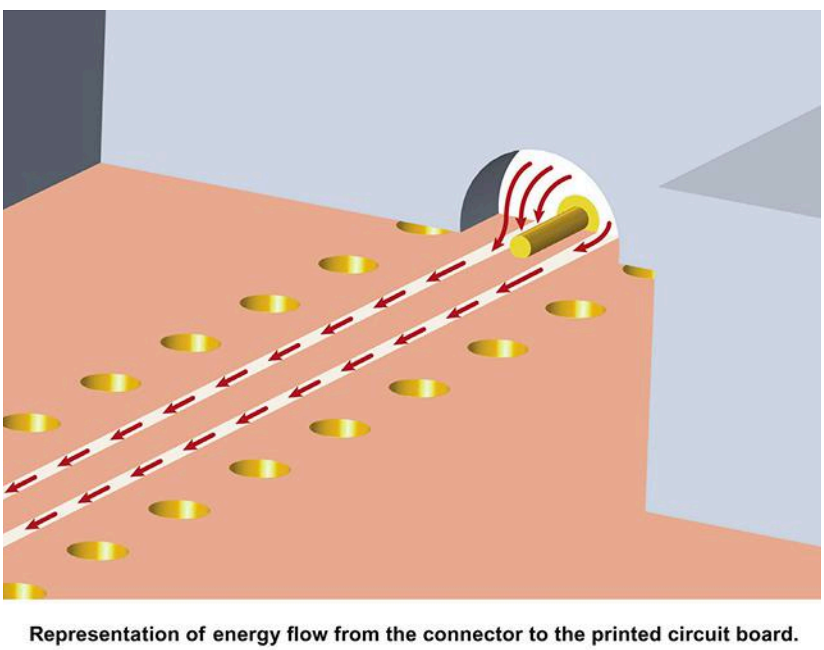

4. This figure illustrates the flow of energy from a connector to the printed circuit board (PCB).

OPTIMIZING THE CONNECTOR-TO-PCB TRANSITION

Energy flow from the coax to the PCB is represented in *Figure 4*. This simplified representation shows only the energy in the air portion of the transmission line. A significant amount of the energy is in the substrate and transitions from the dielectric of the connector to the substrate between the top and bottom conductors.

To fully capture the complexity of this transition at higher frequencies, a 3D simulation tool is required. Once the model is created and the ports are set to measure the energy flow (S-parameters), an optimization of the launch design can be done.

SOURCES OF DISCONTINUITY

The Pin Sitting on the Signal Line

The pin of the connector adds capacitance to the section of the board where it's electrically connected (Fig. 4, again). This capacitance increases if the pin is soldered. Therefore, soldering is not recommended. The signal line of the PCB where the connector makes contact needs to be adjusted to reduce the effect of this extra capacitance (*Fig. 2, again)*.

The Ground of the Connector Making Contact with the PCB

For a GCPW, the top ground spacing can be matched to the ground contact points of the connector. For a microstrip line, there's no top ground. That means there is not much to optimize to improve performance. If a short GCPW section is added to the edge of a microstrip line, a structure is created that can be optimized to the connector.

The largest discontinuities occur at the section between the launch pin of the connector and the edge of the board.

To simulate this, the TEM mode field is excited at the coaxial type lumped port, port 1. The field then propagates through the port 1 edge-launch connector and excites a planar mode on the GCPW. The symmetric electric field in the coplanar-waveguide is confined from the center conductor outwards to the conductors on each side and underneath. The listener port, port 2, is also terminated by the same type of coaxial lumped port.

THE NEED FOR A TRAINED OPERATOR OF THE SOFTWARE

The person running the simulation will need to know the basics of RF transmission lines. With this knowledge, one can properly oversee the implementation and then the results of the simulation. The software is able to quickly and easily explore a range of design features as defined by the user and provide data for each specific combination of features.

However, it cannot, for example, tell the user that a feature not in the design needs to be added, or that a feature in the design must be removed. These decisions have to be made by the user. The design can then be modified for further analysis through simulation. In this way, the software tool can be used to identify an optimized design and explore sensitivities in the design.

SENSITIVITY ANALYSIS

The user will need to understand board-processing techniques and variances that are inherent in the board fabrication process. Understanding the strengths and weaknesses of holding tolerances in the fabrication process can guide users in the realm of sensitivity analysis. One should try to make the most difficult board-processing features the least sensitive in the design.

CONCLUSION

Projects will benefit from a well-designed board launch. Without efficient and well-behaved transition of energy into and out of a board, the performance of a board—or the components on a board—cannot be properly determined. In test, yield can increase when components do not fail due to degradation of test results that result from connector-to-board transition performance. In design verification, the accuracy of test results will improve as well.

High-performance board launches and transmission lines are achievable in projects in which their performance is critical. While not "transparent," it's close enough that the connector transition does not interfere with board measurements. mw

(Continued from page 70)

19. Qing-Xin Chu and Huan Wang, “A Compact Open-Loop Filter With Mixed Electric and Magnetic Coupling,” *IEEE Transactions on Microwave Theory & Techniques,* Vol. 56, No. 2, 2008, pp. 431-439.
20. Huan Wang and Qing-Xin Chu, “An EM-Coupled Triangular Open-Loop Filter With Transmission Zeros Very Close to Passband,” *IEEE Microwave and Wireless Components Letters,* Vol. 19, No. 2, 2009, pp. 71-73.
21. Jayatilaka, C. Himal, and David M. Klymyshyn, “Half wavelength open loop bandpass filters with transmission zeros,” 2007 IEEE Asia-Pacific Microwave Conference, (APMC 2007).
22. T. Lim, B.-W. Min, and Y. Lee, “Miniaturisation method for coupledline bandpass filters with identical and minimal number of reactive elements,” *IET Microwave Antennas & Propagation,* Vol. 8, 2014, pp. 1192–1197.
23. L. Athukorala and D. Budimir, “Compact Filter Configurations Using Concentric Microstrip Open-Loop Resonators,” *IEEE Microwave and Wireless Components Letters,* Vol. 22, No. 5, 2012, pp. 245-247.
24. A. Boutejdar, A. Elsherbini, S. Amari, and A. S. Omar, “A New Technique to Double the Rejectband of a Low-pass Filter by Employing Coupled C-Open-Loop Resonators as Defected Ground Structure (DGS),” 2007 IEEE Asia-Pacific Microwave Conference, pp. 1-4.
25. A. Abdel-Rahman, A. K. Verma, A. Boutejdar, and A. S. Omar, “Compact stub type microstrip bandpass filter using defected ground plane,” *IEEE Microwave and Wireless Components Letters,* Vol. 14, No. 4, 2004, pp. 136-138.
26. P. Vagner and M. Kasal, “Bandpass filter design using an open-loop defected ground structure resonator,” 2010 15th International Conference on Microwave Techniques (COMITE), pp. 77-80.
27. Bian Wu, Xin Lai, Jia Chen, Xue-Feng Li, and Chang-Hong Liang, “Dual-mode filter with asymmetric response using square loop resonator DGS,” 2010 International Conference on Microwave and Millimeter Wave Technology (ICMMT), pp. 1298-1300.
28. Ahmed Boutejdar, Adel Elsherbini, and A. S. Omar, “Method for widening the reject-band in low-pass/band-pass filters by employing coupled C-shaped defected ground structure,” *IET Microwaves, Antennas & Propagation,* Vol. 2, No. 8, 2008, pp. 759-765.
29. N. Engheta and R. W. Ziolkowski, *Electromagnetic Metamaterials: Physics and Engineering Explorations,* Wiley, Hoboken, NJ, 2006
30. C. Caloz and T. Itoh, *Electromagnetic Metamaterials Transmission Line Theory and Microwave Applications,* Wiley, Hoboken, NJ, 2006.
31. G. V. Eleftheriades and K. G. Balmain, *Negative Refractive Metamaterials,* Wiley, Hoboken, NJ 2005.
32. Mohammed A. Fouad and Mahmoud A. Abdalla, “Ultra Compact CPW Dual Band Filter Based on Π-Generalized Metamaterial NRI Transmission Line,” *Journal of Electromagnetic Waves and Applications,* Vol. 29, No. 8, 2015, pp. 1093-1103.
33. Mohammed. A. Fouad, and Mahmoud A Abdalla, “A New π-T Generalized Metamaterial NRI Transmission Line for a Compact CPW Triple BPF Applications,” *IET Microwave, Antennas & Propagation,* Vol. 8, No. 13, 2014, pp. 1097-1104.
34. Ki-Cheol Yoon, Hyun-Wook Lee, Jong-Chul Lee, and Seong-Cheol Kim, “A Dual-Band Narrow Band-Pass Filter With Half-Wavelength Open Stubs Using The CRLH Metamaterial,” *Microwave and Optical Technology Letters,* Vol. 55, No. 8, 2013, pp. 1887-1890.
35. Mahmoud Abdalla, A. Y. Hassan, and A. M. Galal Eldin, “A Compact High Selective Coupled Gap CRLH TL Based Bandpass Filter”, 2015 9th International Congress on Advanced Electromagnetic Material in Microwave and Optics, September 7-12, 2015, United Kingdom.
36. J. B. Pendry, A. J. Holden, D. J. Robbins, and W. J. Stewart, “Magnetism from conductors and enhanced nonlinear phenomena,” *IEEE Transactions on Microwave Theory & Techniques,* Vol. 47, 1999, pp. 2075-2084.
37. Q. Xiang, Q. Feng, and X. Huang, “Tunable Bandstop Filter Based on Split Ring Resonators Loaded Coplanar Waveguide,” *ACES Journal,* Vol. 28, No. 7, 2013.
38. A. K. Horestani, M. Duran-Sindreu, J. Naqui, C. Fumeaux, and F. Martin, “Coplanar Waveguides Loaded with S-Shaped Split-Ring Resonators: Modeling and Application to Compact Microwave Filters,” *IEEE Antennas and Wireless Propagation Letters,* Vol. 13, 2014, pp. 1349-1352.
39. Jian Li, Yongjun Huang, Guangjun Wen, Xiaolin Xue, and Jiaming Song, “Compact and high-selectivity microstrip bandpass filter using two-stage twist-modified asymmetric split-ring resonators,” *Electronics Letters,* Vol. 51, No. 8, 2015, pp. 635-637.
40. A. Velez, F. Aznar, J. Bonache, M. C. Velazquez-Ahumada, J. Martel, and F. Martin, “Open complementary split ring resonators (OCSRRs) and their application to wideband CPW band pass filters,” *IEEE Microwave and Wireless Components Letters,* 2009, pp. 197-199.
41. M. A. Abdalla, M. A. Fouad, H. A. Elregeily, and A. A. Mitkees, “Wideband negative permittivity metamaterial for size reduction of stopband filter in antenna applications,” *Progress in Electromagnetics Research C,* Vol. 25, 2012, pp. 55-66.
42. Q.-L. Zhang, W.-Y. Yin, S. He, and L.-S. Wu, “Evanescent-mode substrate integrated waveguide (SIW) filters implemented with complementary split ring resonators,” *Progress in Electromagnetics Research,* Vol. 111, 2011, pp. 419-432.
43. J. Garcia-Garcia et al., “Miniaturized Microstrip and CPW Filters Using Coupled Metamaterial Resonators,” *IEEE Transactions on Microwave Theory and Techniques,* Vol. 54, No. 6, 2006, pp 2628-2635.
44. H. Nornikman, B. H. Ahmad, M. Z. A. Abdul Aziz, M. F. B. A. Malek, H. Imran, and A. R. Othman, “Study and simulation of an edge coupled split ring resonator *(Ec-Srr) on truncated pyramidal microwave absorber,” Progress in Electromagnetics Research,* Vol. 127, 2012, pp. 319-334.
45. L. Zhou, S. B. Liu, X. K. Kong, and Y. N. Guo, “Novel cross-coupled filter design using improved split-ring resonators based on stepped impedance resonator,” *Microwave and Optical Technology Letters,* Vol. 53, No. 9, 2011, pp. 1976-1980.
46. S.-H. Jang, and J.-C. Lee, “Design of novel cross-coupling elliptic function filters with the miniaturized edge-coupled split ring resonators,” *Microwave and Optical Technology Letters,* Vol. 45, June 2005, pp. 495-499.

JACK BROWNE | Technical Contributor

Sharing the Internet with Billions of Things

Wireless protocols such as Wi-Fi and Bluetooth work with smartphones around the world as controllers for electronic devices that sense and share data via the internet.

In many ways, the internet has become a form of "hard drive" for the masses. It's a place to store and find a seemingly unlimited amount of information as needed. The internet can be accessed from almost anywhere, with wired or wireless communications devices such as cellular telephones and WLAN laptop computers. But it's not just people connecting to each other via the Internet: Billions of things, as in Internet of Things (IoT) devices, also hook up with the internet—a number that's expected to grow dramatically in the next few years.

Recent market forecasts by organizations such as Gartner *(www.gartner.com)* estimate more than 20 billion worldwide IoT devices by 2020. While these IoT devices will occupy some of that seemingly unlimited memory storage capacity available from the many computers comprising the internet, they will also support numerous functions in homes, factories, even outdoors.

Many IoT devices are designed to make environments "smarter," including motor vehicles, homes, offices, and cities. While some may argue that the only "smart" cities will be those without IoT devices, the rise in applications of IoT technology is apparently unavoidable and will no doubt become relatively mundane with time. For example, users can check the temperature of the rooms in their homes while still at work by gaining remote access to the internet via cellphone.

Growing interest in IoT devices is evidence of how the wireless/cellular telephone has evolved into a "control center" for many users. The wireless/cellular telephone is not only an information center, it serves as a remote control for IoT devices.

The basic concept of a "smart home" is a residence in which electronic devices such as light switches, thermostats, radios, and televisions are connected to the internet and can be controlled by voice commands as a user walks through, or remotely by having a wireless/cellular telephone or "smartphone" function as a wireless remote control. The IoT devices are also sensors that can gather and exchange data, thus enabling, say, room temperatures to be adjusted according to occupancy to save on heating bills, or perform other dynamic actions for efficiency and economy.

1. Some IoT devices are as simple as this WeMo switchable ac outlet, which enables remote control of home electronic appliances using an existing Wi-Fi network and a free downloadable application to run on a smartphone. *(Courtesy of Belkin)*

Although many well-known professional organizations such as AT&T Business *(www.business.att.com)* and IBM *(www.ibm.com)* with its IBM Watson IoT service can organize a "smart business" with appropriate IoT devices, the majority of IoT users learn as they go with the technology. This typically involves a close-range wireless communications technology, such as Bluetooth or Wi-Fi, to connect IoT devices to a local wireless network for access by a user's cellphone. The phone would be equipped with appropriate application software to control the IoT devices.

The worldwide use of the interconnected computer servers that form the internet has grown into a massive global network known simply as "the cloud." In turn, IoT devices connected to any network with internet capability can be accessed by any communications device with similar access to the internet.

THE QUICKENING EVOLUTION

The use of things connected to the internet for different reasons isn't all that new—it's been taking place for several decades. And the number of commercially available IoT devices has grown quite large for applications within a home or office, around a home, for medical or health purposes, even for vehicular purposes as part of a smart car. In addition, as mentioned, for all IoT applications are typically controlled via the "brains" of the smart home or office, meaning a cellphone or tablet/laptop computer.

The number of commercial IoT products is currently in the thousands. Some are as mundane as night switches or ac outlets that can be turned on and off from a cellphone using Bluetooth or Wi-Fi *(Fig. 1)*. Some are functions that have been available as IoT devices for many years, such as remote-controlled thermostats that control a home or office building's temperature. Similarly, air conditioners can be remote-controlled via IoT outlets during warmer months. This allows, for example, a facilities manager to monitor and adjust the temperatures of a building and its different offices from a central, networked location.

Beyond the fundamental wireless control of heating, cooling, lighting, and power, there's been a rapid rise in the use of IoT devices for security purposes *(Fig. 2)*. In some applications, the security is as straightforward as a "smart lock" for a home's front door.

2. IoT door-lock products can be programmed to work with voice commands to replace the use of keys. *(Courtesy of August Home)*

3. IoT-based object-location technology has been applied to a tracking device, thin enough to remain in a wallet, which can be found using a cellphone when lost. *(Courtesy of Tile)*

4. Arlo Pro IoT security cameras feature advanced capabilities, such as motion and sound detection, which can be accessed through the internet. *(Courtesy of Netgear)*

Suppliers such as August Home actually offer third-generation IoT door-lock products that essentially turn a cellular telephone into a set of door keys. The latest smart locks from August Home can work with Echo and Alexa voice commands from Amazon to allow residential access to family and selected guests. They can also perform automatic functions, such as opening a locked door as the "key-bearer" (holder of the cellphone) approaches the front door as well as locking the door as the cellphone holder leaves the house.

Some of the more popular IoT devices are those used to locate lost personal effects, like keys or wallets. Tile, which is known for its key-finding use of IoT and Bluetooth technology, helps users who prefer to open their doors the old-fashioned way, but may have misplaced their keys. The company's object-location technology is in use throughout the world in hundreds of countries, and has recently been applied to a tracking device that's thin enough to remain within a wallet and help to find it with a smartphone *(Fig. 3)*.

KEEPING WATCH

In addition to locking the doors of a residence, many IoT devices can maintain remote surveillance over a home using IoT-enabled surveillance cameras. Most of these IoT cameras are simple to install and use, and can even record video to the cloud over multiple days.

5. "The Foundation" is a basic IoT-based security kit that allows a user to install a security system in a small house or apartment. *(Courtesy of SimpliSafe)*

For example, the Arlo Pro IoT security cameras from Netgear include motion and sound detection *(Fig. 4)*. The latest versions of the cameras (Arlo Pro 2) boast high-definition 1080p video resolution and support for Amazon Alexa voice commands. The Arlo Pro cameras allow users to connect a USB memory device to the camera base station for capture of video over time. The same base station contains a 100-dB siren that can be activated from anywhere by means of IoT network access.

The iCamera Keep Pro from iSmartAlarm is an IoT security camera that's activated by motion and sound detection. It can perform time-lapse and event-triggered video, and includes a motion-tracking feature that's able to follow a subject around a room. The camera has 1080p high-definition video resolution, and can store video data on a built-in SD card slot or to the cloud. The device features a 140-deg. field of view and night vision, and can improve its chances of keeping a subject on camera by means of motorized panning and tilting.

Some IoT security systems, such as those from SimpliSafe, are available as kits with different components for providing the amount of security coverage depending on the size of the house. The firm's security kit, known as "The Foundation," includes four essential components *(Fig. 5)*: a base station, a data-entry keypad, an entry sensor for a doorway, and a motion sensor that can be placed at a key location around a home.

The kit's components work together to provide remote monitoring and protection via the Internet. If one of the sensors detects an unwanted presence, an online message is sent via Internet and a 95-dB siren is sounded in the home by the basestation. The kit and larger ones offered by the company are available with and without monitoring services.

INDUSTRIAL IOT

For industrial IoT (IIoT) applications, devices such as the ZEM-61 wireless three-phase electricity monitor *(Fig. 6)* from EpiSensor *(www.episensor.com)* provide a simple means of remotely monitoring the energy use in a commercial or industrial facility, such as a warehouse. It's essentially a miniature test system with a 2.4-GHz ZigBee wireless radio housed within a compact waterproof enclosure measuring just 192 × 128 × 40 mm.

6. The ZEM-61 is an IIoT three-phase electricity monitor that can remotely monitor the energy use in a warehouse or factory. *(Courtesy of EpiSensor)*

Through IoT connections, the EpiSensor can report on a variety of energy-related parameters, including voltage, current, kilovolt-amps (kVA), and kilowatt-hours (kWh). It offers a wide voltage measurement range of 75 to 265 V, and an extended current measurement range of 0.1 to 3 kA with accuracy of ±1% or better. The IIoT unit features over-the-air software upgrade capability and can relay data from other wireless nodes within a facility.

In any operating environment, it's easy to see the convenience of IoT-enabled equipment and the attendant quick growth of IoT devices. Rather than try to control each IoT device with a separate software application on a smartphone, it can sometimes make more sense to use what are known as hub gateways. They allow for the connection of, and communication between, many different types of IoT devices. These may be devices that normally communicate on ZigBee, Bluetooth, and Wi-Fi, and would require those separate wireless links. With a hub gateway, devices with different wireless protocols can be controlled through that single gateway; for example, using voice control and programmed voice commands to control different IoT devices.

As the number of IoT devices escalates, so too does the concern over cybersecurity. There's always the threat of computer hackers gaining access to a home or business through a vulnerability in a network made possible by an IoT weak link.

Manufacturers of IoT-based products typically institute end-to-end security testing a part of every new product's development cycle, to better understand the capabilities of different IoT products in withstanding attacks from hackers. For example, a smart camera that's designed as part of the security system for a home can also function as a two-way monitoring device by a hacker gaining access from the outside. Organizations such as Securelist *(www.securelist.com)* have performed extensive experiments on different IoT devices and network setups to identify weak links and access points where hackers could gain access to an IoT-populated network. mw

RF SWITCHES

DC - 40 GHz

Type	Failsafe	Latching	Normally Open	Terminations	SMA	2.92mm	Type-N	7/16, 4.3-10	SC	High Power (CW)	Low PIM (dBc)	Cycle Life
SPDT	✓	✓	✓	50Ω, 2W	✓	✓	✓	✓	✓	2kW	-170	5M
Transfer	✓	✓			✓	✓	✓	✓	✓	2kW	-170	5M
SPMT*	✓	✓	✓	50Ω, 2W	✓	✓	✓	✓	✓	2kW	-170	5M

***SP3T to SP12T designs**

Visit www.e360microwave.com for data sheets and more information.

e360microwave offers relays and switches for ultra reliable test applications. Based on a 30-year heritage of innovative RF and microwave products and designs, our broad selection of relays and switches features excellent RF performance, reliability and repeatability. We can deliver 10,000s switches per month, quickly and at very competitive prices. All options are available and high-power and low PIM designs are a specialty.

Santa Clara, CA 95054 408-650-8360 (o), 408-650-8365 (f)
techsupport@e360microwave.com
sales@e360microwave.com

JACK BROWNE | Technical Contributor

Distributed Amplifier MMICs Boost Signals Over Wide Bands to 40 GHz

These three GaAs MMIC distributed amplifiers provide generous gain with low noise figures over wide, dc-coupled bandwidths to serve optical and RF/microwave applications.

Bandwidth is everything for some applications, including many communications systems, and boosting signal levels over broad bandwidths requires a special kind of amplifier. Typically, a distributed amplifier is used for such applications. As its name might suggest, gain is distributed among a number of transistors or active stages within the amplifier, such as field-effect transistors (FETs) in GaAs distributed amplifiers, to achieve level signal gain over wide bandwidths.

Commercially available amplifiers that deliver widely distributed gain with excellent gain flatness are the model CMD240 die, the CMD240P4 packaged amplifier (a CMD240 die mounted in a QFN package), the CMD242, and the CMD244 GaAs MMIC distributed amplifiers from Custom MMIC. These impedance-matched, 50-Ω dc-coupled amplifiers in their die and packaged forms are capable of bandwidths as wide as dc to 40 GHz in a single device (the model CMD242). They offer attractive combinations of low noise figures and flat-to-positive-sloping gain with frequency that remains stable with temperature.

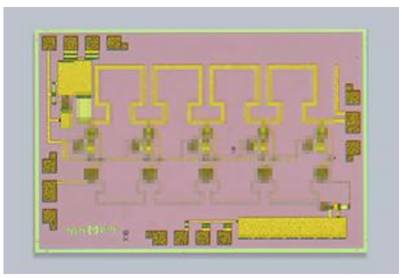

1. Model CMD240 is a GaAs MMIC distributed amplifier die with low noise figure and level gain from dc to 22 GHz.

2. The CMD240P is a QFN-packaged version of the CMD240 GaAs MMIC distributed amplifier for applications from dc to 22 GHz.

Such amplifiers are invaluable for wideband communications receiver front ends. Their low noise figure doesn't compromise receiver front-end sensitivity and they maintain sufficient gain to drive desired signals above the noise. In many cases, a single distributed amplifier may have sufficient bandwidth to serve multiple receive-frequency bands and receiver front ends if switched, helping to reduce the parts count on a portable radio design.

For example, model CMD240 is a GaAs MMIC distributed amplifier die that delivers typically more than 15 dB gain while holding noise figure to typically 2.2 dB or less from dc to 22 GHz *(Fig. 1)*. It provides +19 dBm typical output 1-dB compression point (output P1dB) and +28 dBm output third-order intercept point (IP3) across that wide frequency range when operating from +5 V dc drain voltage, −0.6 V dc gate voltage, and 80 mA typical current draw. Input return loss is typically 15 dB across the full dc to 22 GHz, while output return loss is typically 13 dB for the same range. The CMD240 has maximum rating of +20 dBm for input power.

As expected, there's slight degradation in the noise-figure performance at the band edges, but with maximum noise figure of only about 3 dB at 20 GHz. The 22-GHz distributed amplifier is also available in QFN packaged form, as model CMD240P4 *(Fig. 2)*.

A QUICK LOOK AT BROADBAND DISTRIBUTED GAAS MMIC AMPLIFIERS					
Model	CMD240[a]	CMD240P4[a]	CMD242[b]	CMD244	
Frequency range	DC-22 GHz	DC-22 GHz	DC-40 GHz	DC-10 GHz	10-24 GHz
Gain	15 dB	15 dB	11 dB	17.5 dB	18.5 dB
Noise figure	2.2 dB	2.2 dB	4.4 dB	3.0 dB	4.0 dB
Output P1dB	+19 dBm	+19 dBm	+18 dBm	+25 dBm	+23 dBm
Output IP3	+28 dBm	+26 dBm	+27 dBm	+33 dBm	+31 dBm
Input RL	18 dB	19 dB	18 dB	18 dB	15 dB
Output RL	15 dB	18 dB	18 dB	25 dB	15 dB
Supply current	80 mA	80 mA	100 mA	185 mA	185 mA
[a]Tested at 10 GHz and +5 V dc drain voltage. [b]Tested at 20 GHz and +8 V dc drain voltage.					

SPANNING DC TO 40 GHZ

When even more bandwidth is needed, model CMD242 is a GaAs MMIC distributed amplifier die with enormous range of dc to 40 GHz. It provides more than 10.5 dB typical gain and typically less than 4.4 dB noise figure from dc to 40 GHz *(see table)*. The broadband CMD242 achieves output P1 dB of +17.5 dBm from dc to 20 GHz and typically +19.0 dBm from 20 to 40 GHz. The amplifier's output IP3 is typically +28 dBm from dc to 20 GHz and typically +26 dBm from 20 to 40 GHz.

It's designed for maximum input power of +23 dBm. The wideband distributed amplifier is also rated for maximum power dissipation of 1.05 W and maximum thermal conductivity of 62.1°C/W. The CMD242 GaAs MMIC die is available with a second voltage gate ($V_{gg}2$) for optional gain control *(Fig. 3)*.

When more gain is needed, model CMD244 is a distributed driver amplifier die for applications from dc to 24 GHz *(Fig. 4)*. It features a positive gain slope with frequency, with typical gain of 17.5 dB from dc to 10 GHz, rising to 18.5 dB from 10 to 24 GHz. The noise figure does rise somewhat with frequency, as expected, with typical noise figure of 3 dB from dc to 10 GHz, rising to typically 4 dB from 10 to 24 GHz. Input return loss is typically 18 dB from dc to 10 GHz and 15 dB from 10 to 24 GHz, while output return loss is typically 25 dB from dc to 10 GHz and 15 dB from 10 to 24 GHz. The output P1dB is normally +25 dBm from dc to 10 GHz and typically +23 dBm from 10 to 24 GHz. The output IP3 is typically +33 dBm from dc to 10 GHz and +31 dBm from 10 to 24 GHz.

The CMD244 is rated for +15 dBm maximum input power. It's also rated for maximum power dissipation of 2.4 W and maximum thermal conductivity of 26.82°C/W. As with the CMD242, the CMD244 die comes with a second gate-voltage connection for optional gain control.

The GaAs MMIC distributed amplifier die are passivated for protection from moisture, and all of the distributed amplifiers are impedance-matched for broadband use in 50-Ω applications. They are characterized for operating temperatures from −55 to +85°C. Datasheets for the GaAs MMIC packaged amplifier and die are complete with assembly and application guidelines, including warnings about the potential damage to GaAs devices from electrostatic discharge (ESD). Datasheets for all of the distributed amplifiers can be downloaded from *www.custommmic.com/distributed-amplifiers/*. mw

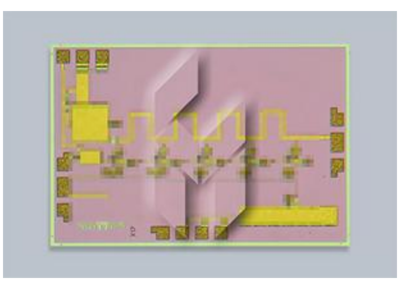

3. The CMD242 is a GaAs distributed amplifier die with typical gain of better than 10.5 dB across an impressive frequency range of dc to 40 GHz.

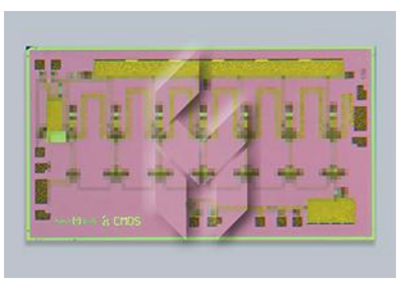

4. Model CMD244 is a GaAs MMIC distributed driver amplifier die with high gain from dc to 24 GHz.

CUSTOM MMIC, 300 Apollo Dr., Chelmsford, MA 01824; (978) 467-4290, www.custommmic.com.

JACK BROWNE | Technical Contributor

Amplifiers Boost Test Signals to 26.5 GHz

When higher-level test signals are needed, these GaN-based amplifiers provide the power, with healthy output levels over broad bandwidths from 700 MHz to 26.5 GHz.

If I only had a few more watts of power! That exclamation has no doubt haunted more than a few high-frequency engineers in RF/microwave laboratories for some time, as it's typically followed by a search for an amplifier capable of boosting low signals to levels suitable for analysis.

In many cases, such an amplifier may be part of the MPA Series of test-and-measurement instrument amplifiers from Maury Microwave *(www.maurymw.com)*. The test amplifier line covers some of the more popular high-frequency bands from 700 MHz to 26.5 GHz with high gain and as much 50 W saturated output power. The amplifiers can drive signals of interest to levels suitable for testing with measurement equipment such as a spectrum analyzer, scalar network analyzer (SNA), or a vector network analyzer (VNA).

The durable instrumentation amplifiers leverage the capabilities of gallium-nitride (GaN) power-amplifier (PA) modules to cover wide swaths of the total frequency range of 0.7 to 26.5 GHz, including 0.7 to 6 GHz; 2 to 6 GHz; 2 to 18 GHz; 6 to 18 GHz *(see figure)*; 8 to 12 GHz; and 18 to 26.5 GHz. Available output power typically decreases with increasing frequency. As much as 50 W saturated test signal power is available through 6 GHz, with up to 30 W test signal output power from 2 through 18 GHz, and as much as 5 W test-signal power from 18.0 through 26.5 GHz.

The amplifiers include built-in protection circuitry that monitors key functions, such as fan status, temperature, and amplifier module current draw. An amplifier will power down to prevent damage when faults are triggered to prevent damage.

The frequency breakdowns of the instrument amplifiers enable specifiers to focus on one or more frequency bands of interest. This helps to achieve test-signal power levels at microwave frequencies capable of applying real input-power stress to a device under test (DUT) at microwave frequencies.

For example, model MPA-0G7-6G-50 is able to produce at least 50 W saturated output power from 0.7 to 6.0 GHz. It can handle input signal levels as high as +3 dBm without overload, and delivers at least 49-dB small-signal gain with ±4 dB gain flatness. It also has a manual 20-dB gain adjustment range for varying the amount of gain provided to a DUT.

The MPA line of instrumentation amplifiers consists of rugged rack-mount units based on GaN power transistors, all of which are capable of 50 W saturated output power at microwave frequencies, such as this 6- to 18-GHz unit.

The MPA-0G7-6G-50, like the other members of the MPA instrument amplifier line, is constructed for high reliability, in a durable, rack-mount enclosure with generous heat fins and forced-air cooling to prevent heat buildup around the GaN active devices. It's designed to function with worst-case input VSWR of 2.50:1, while holding second-harmonic levels to typically −15 dBc and spurious levels to typically −65 dBc across the frequency range. It withstands load VSWRs as high as 3.0:1 while running at its rated saturated output-power level.

For those not needing as much test power, the MPA-0G7-6G-16 instrument amplifier provides at least 16 W saturated output power over the same 0.7- to 6.0-GHz frequency range. It has somewhat less (44-dB) small-signal gain and the same 20-dB gain-control range.

At the upper part of the frequency coverage, model MPA-18G-26G5-5 achieves at least 5 W saturated output power from 18.0 to 26.5 GHz. The instrument amplifier features typical 37-dB small signal gain, with typical gain flatness of ±4 dB and a 15-dB gain control range.

When less output power is needed over this upper-microwave-frequency range, the model MPA-18G-26G5-1 instrument amplifier provides 1 W output power with 30-dB small-signal gain and 15-dB gain control range. Given the high test frequencies of the second harmonics, those levels are not specified for these two 26.5-GHz amplifier models, but they're both rated for almost-negligible spurious levels of −65 dBc. mw

TO READ the article in its entirety, go to *www.mwrf.com.*

CHRIS DeMARTINO | Technical Editor

Solve 5G Test Challenges from End to End

Two companies have joined forces to create a solution that makes end-to-end, over-the-air 5G testing a reality.

This past April, the fifth annual Brooklyn 5G Summit convened at the New York University (NYU) Tandon School of Engineering in Brooklyn, N.Y. The focus was on the latest developments in the realm of 5G communications, which was brought into view through various talks and panel discussions. In addition, the exhibition featured several companies that demonstrated impressive technology.

One demonstration was hosted by National Instruments (NI; *www.ni.com*) in conjunction with W2BI (*www.w2bi.com*). Together, the two companies displayed an end-to-end 28-GHz test system that can emulate both the 5G network and the user equipment (UE). The test system integrates radio software layers with NI's mmWave transceiver system to enable end-to-end, over-the-air (OTA) 5G testing. One of the two PXI chassis represents a base station (gNodeB), while the other represents a UE (*see figure*).

James Kimery, director of marketing for RF, communications, and software-defined radio (SDR) initiatives at NI, was present to talk about the demonstration. "The physical layer on both sides (network and UE) was provided by NI and written in LabVIEW. What W2BI has done is integrate upper layers of the protocol stack. What that does is simulate the interaction between a UE and a base station at a very high level. This is almost exactly what 5G will be.

"The physical layer is a very close approximation of what the 5G New Radio (NR) physical layer will be. The upper layer is the closed-loop control of that communication. In this system, we have a phased-array antenna and a horn antenna. It is demonstrating some of the concepts of being able to switch the beams of both the transmitter and receiver to be able to get some characteristics of the beams themselves. And because the system can run the protocol stack, the physical layer can be controlled at a very high level."

Kimery also pointed out that the test system offers closed-loop control capability. "This system offers closed-loop control, meaning it's actually doing what a real base station or UE would do. The software itself is embedded in the FPGA physical layer platform and it runs real-time."

Another significant aspect of the overall test solution is the phased-array module, which Kimery explained in more detail. "This technology was developed by Ball Aerospace in conjunction with Anokiwave. This is one of the only systems I've seen that has a phased-array antenna inside a test simulator."

The headline of this year's Brooklyn 5G Summit was "Ready for Takeoff." The latest developments in the 5G world—such as what was described here—showed why 5G may soon indeed be ready for takeoff. mw

This 28-GHz test system offers end-to-end capability, emulating both the network and the UE.

JIYOUN MUNN | RF Technical Product Manager, COMSOL
www.comsol.com

Fast Numerical Analysis of Scattering and Radar Cross Section

To demonstrate the effectiveness of 2D axisymmetric modeling, the author presents a radar-cross-section (RCS) analysis that utilizes this modeling technique.

The ability to avoid enemy radar requires that modern fighter aircrafts, ships, and missiles have a very small radar cross section (RCS). Researchers and engineers are working on making these stealth objects rely on computational electromagnetics (EM) to optimize the RCS and scattering effects of an arbitrary object using radars. An object exposed to EM waves scatters the incident energy in all directions. The energy that returns to the source of the EM wave, known as backscattering, is the "echo" of the object. The intensity of the radar echo is what we refer to as RCS.

Best practices use a sphere to calibrate radar systems because a sphere will return an echo signal back to the target that sent it. The RCS wavelength consists of three parts: the Rayleigh, Mie, and optical region. The Mie and optical regions are of particular interest, because the analytical solution of the RCS is well-known.

BACK TO RCS BASICS

A classic benchmark example of Mie scattering of a sphere is a great place to start when examining this problem. In the following example, a plane wave illuminates a metallic sphere in free space, and its RCS is computed. The geometry consists of two concentric spherical shells *(Fig. 1)*. The innermost shell, adjacent to the sphere, represents the free-space domain, and the second shell represents a perfectly matched layer (PML) region.

The PML is used to provide an approximate reflection-free termination of the free-space domain. If analyzed with a fine frequency resolution, this can turn into a time-consuming task. Fortunately, when an object is axially symmetric—such as a sphere, which scatters isotropically—the entire 3D object does not have to be analyzed. The cross-sectional blueprint can be sufficient to analyze the EM wave propagation and resonant behavior of the object under certain circumstances.

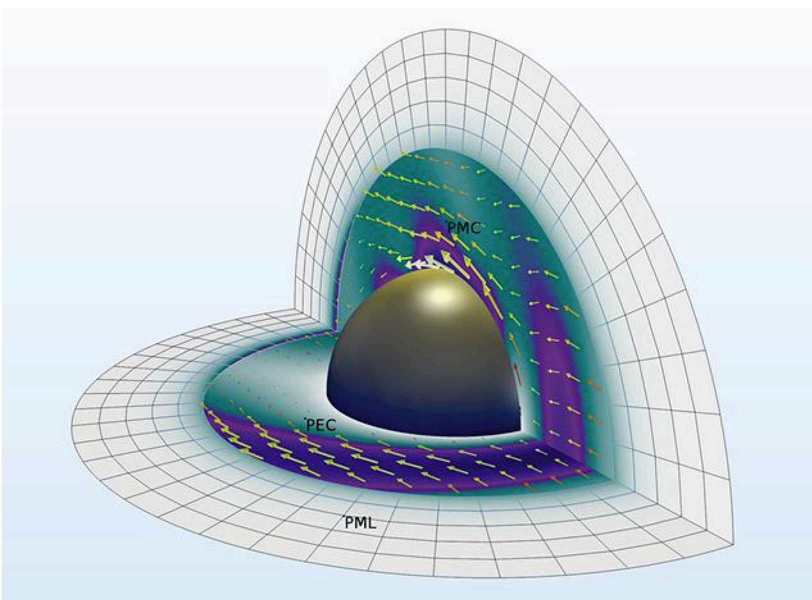

1. The norm of total electric field and the time-averaged power flow are visualized with the geometry of a perfect electric conductor (PEC) sphere in free space modeled in COMSOL Multiphysics.

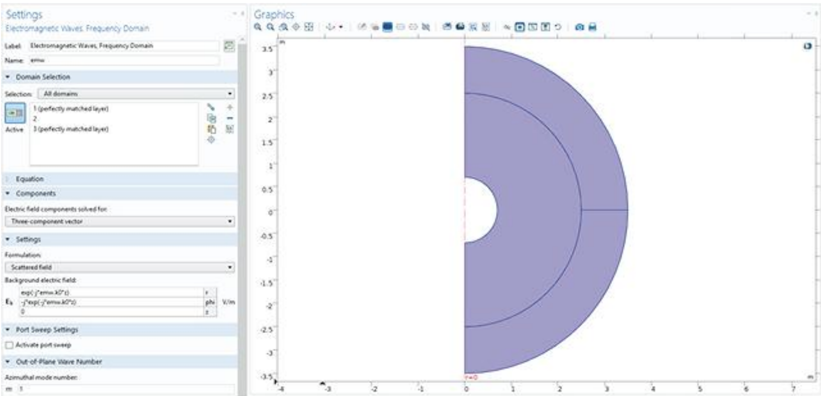

2. This figure shows background field settings of the scattered field formulation and 2D axisymmetric geometry that includes perfectly matched layer domains.

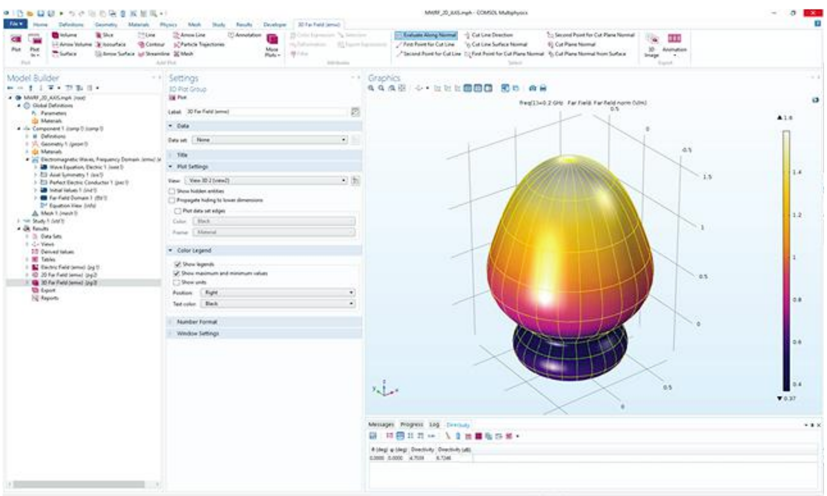

3. 3D far-field is visualized from a 2D axisymmetric simulation in COMSOL Multiphysics.

SIZE MATTERS

The RCS characteristics are largely influenced by the electrical size and nature of the target subjected to the radar beam. As the target—the sphere in our case—decreases in size, moving from the optical region to Rayleigh region via the Mie area, asymptotic methods are not accurate enough to capture all of the physical phenomena. To achieve accurate results, we must analyze the problem by solving full-wave equations. Under these circumstances, the computational costs are quite high. To ensure efficiency is prioritized, we take advantage of the 2D axisymmetric approach *(Fig. 2)*.

The variation of the scattered field is minimal for electrically small targets. Alternatively, electrically large targets can result in different RCS characteristics. Let's assume that our sphere is metallic, meaning it will have a high conductivity. For this model, the sphere's metallic surface is modeled as a perfect electric conductor (PEC).

All of the domain material is defined as a vacuum. The outermost domains are set to the spherical type of PMLs that absorb all outgoing waves. All of the simulation domains are excited by a circularly polarized background field, except for the PML area. The results of this reduced geometry representation are enough to describe the response of the original 3D geometry to the EM waves *(Fig. 3)*.

UNDER THE HOOD OF 2D AXISYMMETRIC MODELING

The far-field calculation boundary is specified to compute the scattered field from the sphere illuminated by the background field. We set the azimuthal mode for this 2D axisymmetric model to one. The mesh operation is performed based on the wavelength of the maximum frequency (200 MHz) used in the simulation via the physics-controlled mesh functionality.

Through the physics-controlled mesh, the maximum mesh element size is set to 0.2 wavelengths (five elements per wavelength) to ensure sufficient resolution of the wave. The PMLs are swept along the absorbing direction. With the low degrees of freedom represented in the model, the simulation takes just a few seconds to compute.

The results plot provides the norm of the total electric field distribution around the sphere, which describes the sum of the background and scattered field and the far-field approximation of the scattered field. In addition, the polar plot gives the modeling specialist insight into the far-field pattern on a specific plane, while the 3D far-field radiation pattern offers a clearer intuition of the scattered field *(Fig. 3, again)*. These plots are the results of the circularly polarized background field illumination on a conducting sphere.

Efficient modeling techniques are critical to modern-day design and simulation engineers in the RF and microwave industry, regardless of the numerical analysis method used. The goal of simulation is to describe real-world devices and objects as close as possible through mathematical formulation.

3D ANALYSIS OF THE 2D AXISYMMETRIC SIMULATION

In the real world, the scattered field response of a 3D metallic sphere is studied using a linearly polarized plane wave. The linear polarization can be formed by adding both a right-handed and left-handed circular polarization.

The 2D axisymmetric model is solved at m = 1 with the background field of left-handed circular polarization. The solution for the negative azimuthal mode with the right-handed circular polarization is easily extracted from the already-solved left-handed circular polarization case based on the symmetrical properties of the model. The coordinate transformation from cylindrical to Cartesian coordinate is involved when visualizing the 2D results in the 3D space. By conducting the 2D analysis on one side and mirroring the solution to the other side, we can translate that information into a 3D solution at a fraction of the computational cost.

The 1D plot of the RCS comparison shows a reasonable agreement between 3D and 2D axisymmetric models *(Fig. 4)*. The small discrepancy is observed from the forward- and backward-scattering responses, especially around the rotating axis.

Figure 5 shows the visualization of the 2D axisymmetric results in 3D. The rotating arrows represent the circularly polarized background field illuminating the sphere. The deformed slice plot is the norm of the r-component of the background field. The surface plot of the sphere is the norm of the total electric field. The other arrow plot describes the superposition of two circular polarizations that are equivalent to a linearly polarized background field in 3D.

CONCLUDING REMARKS

Efficient modeling techniques are critical to modern-day design and simulation engineers in the RF and microwave industry, regardless of the numerical analysis method used. The goal of simulation is to describe real-world devices and objects as close as possible through mathematical formulation. The preferred method to reduce computational time is to remove unimportant parts of an object that have negligible effects on the simulation results.

When simulating and analyzing axisymmetric objects such as spheres, as well as conical or dish antennas, the 2D axisymmetric modeling approach offers orders of magnitude faster computation compared to a full 3D model. The scattering of a linearly polarized background field, as well as the far-field radiation pattern of antennas excited by the TE_{11} circular waveguide mode in 3D, can be extracted from the fast 2D axisymmetric simulations.

Addressing a simple shape, such as a sphere, may appear to be a quick and easy analysis until we realize the impact of the electrical size of the model in terms of wavelength. To maintain integrity in modeling an electrically large real-world component, simplifying the simulation process without losing accuracy is possible by taking advantage of 2D axisymmetric studies. mw

JIYOUN MUNN is currently the Technical Product Manager of the RF Module at COMSOL. Munn is a senior member of the IEEE Antennas and Propagation Society, Microwave Theory and Techniques Society, and Electromagnetic Compatibility Society. He received his MSEE from the University of Michigan, Ann Arbor. He has published several papers and holds patents for antenna-interrogating systems.

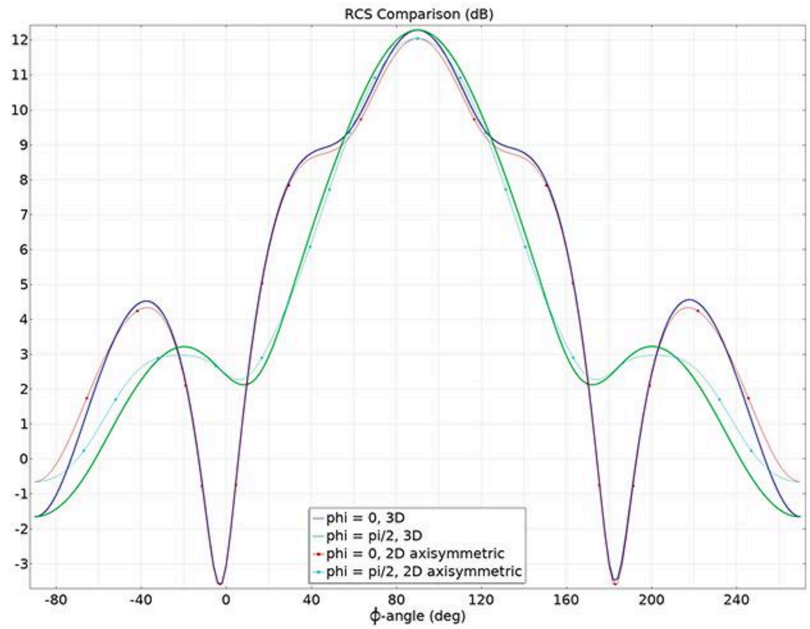

4. RCS is compared between a full 3D model and a 2D axisymmetric model.

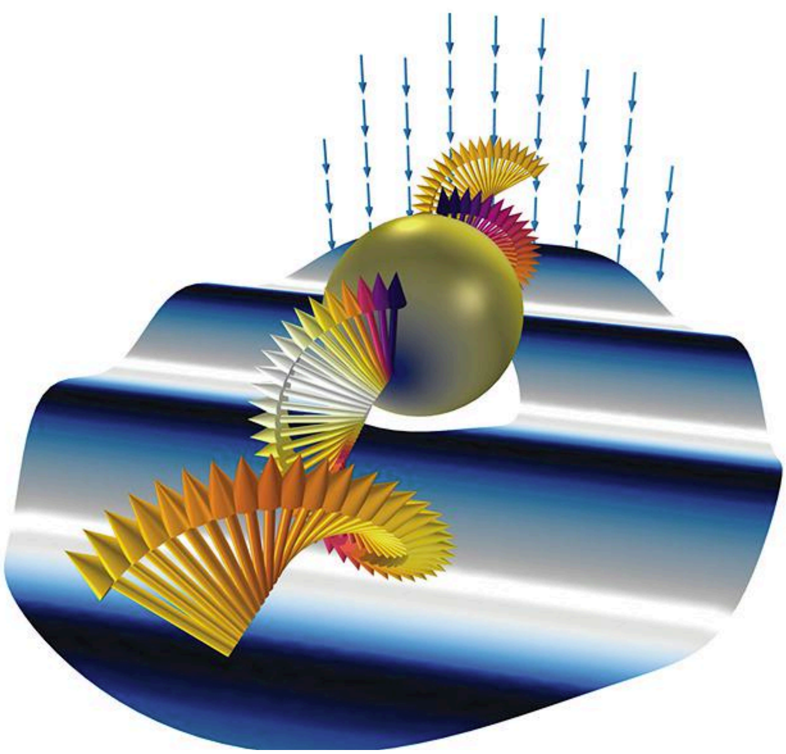

5. Here's a 3D representation of a 2D axisymmetric model.

CHRIS DeMARTINO | Technical Engineering Editor

Tackle the Intricacies of 5G

The accelerated standardization of 5G requires new tools and workflows to design and verify the highly integrated and adaptive signal processing, RF, and antenna devices associated with 5G New Radio (NR).

Without question, 5G wireless communications continues to dominate the headlines, as a host of companies are involved with the standard in some capacity. Last December, the non-standalone (NSA) 5G New Radio (NR) specification was released by the 3GPP. And very soon, the 5G standalone (SA) version will be completed.

"The 3GPP standards are specified in periodic releases," explained Ken Karnofsky, senior strategist for signal processing applications at MathWorks *(www.mathworks.com)*. "Release 15 marks the start of the 5G standard. Release 15 has been further divided into two phases: 5G NSA (December 2017) and 5G SA (June 2018).

"The 5G NSA specification introduces 5G NR radio access technologies that will work with the existing LTE network infrastructure," Karnofsky added. "This will enable faster commercialization of 5G NR technologies. 5G SA will introduce a new network architecture that will work alongside the LTE network."

In terms of what this all means to MathWorks, Karnofsky noted, "Because the NSA standardization has been accelerated, MathWorks is seeing a rapid shift from research to design of 5G radio access technologies across the supply chain. Meeting the accelerated timelines calls for new tools and workflows to design and verify the highly integrated and adaptive signal processing, RF, and antenna devices in 5G NR."

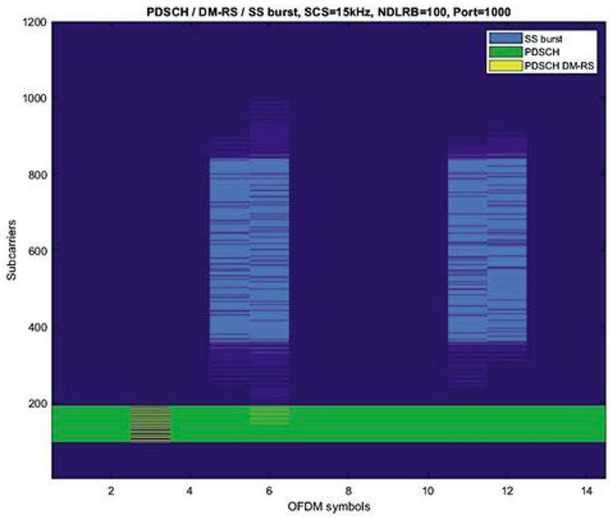

Shown is the resource grid for 5G downlink shared channel (PDSCH). The 5G NR physical layer supports flexible subcarrier spacing for wider channel widths and higher transmission rates. *(Courtesy of MathWorks)*

MORE THOUGHTS FROM KEN KARNOFSKY

TO MEET EMERGING 5G mobile broadband requirements, RF and digital engineers must address system performance changes and partition designs between RF/analog and digital components.

As advanced radios integrate RF and digital technologies to a degree never seen before, RF and digital engineers need to understand how the RF front end affects system performance. Moreover, they must know how to partition designs between RF/analog and digital components to meet the performance and efficiency requirements of emerging 5G technologies.

Emerging approaches are also adding fuel to the fire. Take, for example, technologies being developed for 5G, such as massive MIMO, mmWave, and the latest modulation schemes that require innovative combinations of new baseband technologies and RF architectures. Or consider IoT devices that require power-efficient RF modules to add wireless connectivity. These technologies only deepen the need for highly integrated design environments and flexible connectivity to prototyping and test hardware.

Advances in technology are presenting certain challenges for design environments and prototyping and test hardware. These challenges have spurred advances in modeling and simulation software including improved integration of RF, antenna, and digital modeling and simulation; faster simulation of complex RF architectures to facilitate rapid design exploration; and connectivity to a range of SDR and RF test hardware to accelerate and lower the cost of prototyping and design verification.

New design architectures and algorithms will affect every aspect of 5G systems, from antennas to RF electronics to baseband algorithms. The performance of these subsystems is so tightly coupled that they must be designed and evaluated together.

THE 5G VISION

With the activity surrounding the 5G NSA and SA specifications, the vision for 5G is vast in scope. "The 5G vision aims to provide much faster mobile broadband service (>10 Gbps) for applications such as immersive video and virtual reality," said Karnofsky. "It also aims to provide ultra-reliable and low-latency (<1 ms) communication for safety-critical applications, such as connected autonomous vehicles, as well as massive machine-type connectivity for Internet of Things (IoT) applications."

Karnofsky added, "Release 15 addresses only the first use case—enhanced mobile broadband service—so the product development activity is concentrated in the mobile device and infrastructure supply chain. 3GPP is organizing working groups to study and define the requirements for the low-latency and machine-type use cases. Before those technologies mature, we will see cellular communications introduced into cars and IoT devices based on current LTE standards such as cellular vehicle-to-everything (C-V2X) and NB-IoT."

MATHWORKS' 5G LIBRARY

MathWorks recently introduced its 5G Library, which is a free, downloadable add-on for LTE System Toolbox. The 5G Library enables engineers to explore the behavior and performance of 5G radio access technologies as defined by the Release 15 3GPP NR standard V15.0 *(see figure)*.

Included in the 5G Library are 5G channel models (TR 38.901) and physical layer algorithms defined in the initial 5G standard. It supports 5G Cyclic-Prefix OFDM (CP-OFDM) waveforms with filtering and windowing techniques for spectral shaping. The 5G NR frame numerology with flexible subcarrier spacing—as well as new channel coding schemes, such as LPDC and polar codes—are supported in the 5G Library. Another feature is the 5G link-level simulation reference design, which enables designers to measure 5G link throughputs.

"The 5G physical layer will depart from 4G LTE in a number of ways that improve spectral efficiency and data rates," Karnofsky explained. "One distinctive feature is a significant jump in the number of active antennas and antenna arrays, as well as the related issues of beamforming, millimeter-wave RF signal processing, and power amplifier (PA) linearization.

"With the 5G Library and related tools for baseband, RF, and antenna design," he added, "MATLAB provides a flexible framework development of proprietary physical layer algorithms, accelerating link-level simulations and automating verification of massive multiple-input, multiple-output (MIMO) antenna and RF designs." mw

CHRIS DeMARTINO | Technical Engineering Editor

These Tools Can Help You Defeat RF Interference

While wireless communication has become a part of everyday life, RF interference remains a headache. This article examines how interference can be detected using today's test-and-measurement equipment.

The explosion of wireless technology means that RF signals are literally everywhere. And that mass congestion of RF exacerbates the problem of RF interference. And with more and more wireless devices permeating our lives, the possibility clearly exists for interference to affect the performance and reliability of the wireless technology across the board.

Tracking down where interference is coming from requires the right mix of tools and techniques. In this article, we'll explain the premise of "interference hunting" by first discussing the different types of interference, and then get into the tools that can be used to detect it, supported by actual experiment results.

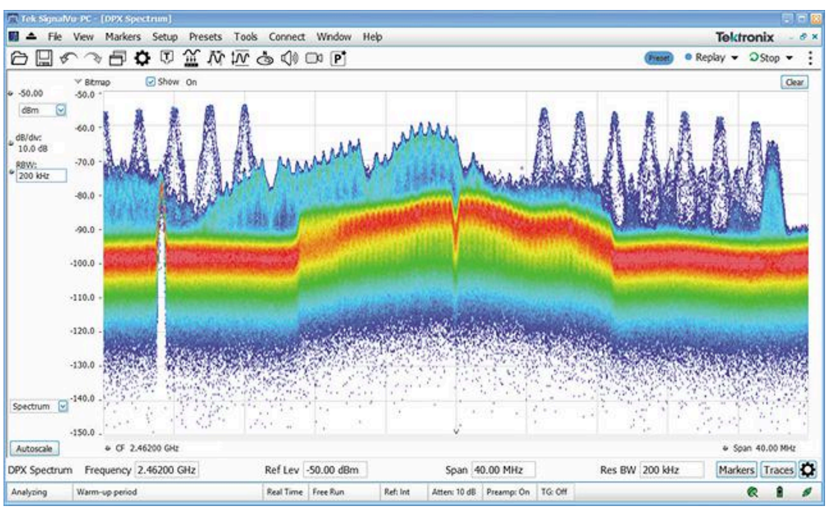

1. A DPX display is based on a color-coded scale that represents how often signals are present. The display shown reveals both WLAN and Bluetooth signals.

CATEGORIZING INTERFERENCE

RF interference is an issue that can lead to problems like dropped calls. There are three main types of interference.[1] The first is co-channel interference, which occurs when multiple transmitters are transmitting signals on the same channel. Today, essentially all frequencies are being shared. The second is adjacent channel interference, which is caused by signals that interfere with communication in adjacent frequency channels.

The third type is impulse noise, which can result from imperfect shielding that allows energy to leak and interfere with RF devices. In addition, noise can result from partial device failures, as well as other sources like industrial machinery.

DETECTING INTERFERENCE WITH REAL-TIME SPECTRUM ANALYZERS

Detecting interference typically involves using a spectrum analyzer. Today, suppliers offer both swept-tuned and real-time spectrum analyzers (RTSAs). While a traditional swept-tuned spectrum analyzer can be used for interference detection, it does have certain limitations when compared with an RTSA.

Swept-tuned spectrum analyzers can display measurement data by continuously sweeping across a given frequency range from the lowest to the highest frequency. This functionality allows measurement data to be displayed for each measurement step in the specified frequency range. Thus, a user can observe a spectrum display as the analyzer continuously sweeps across a range of frequencies.

However, the sweeping functionality of a swept-tuned spectrum analyzer also affects its capability to measure interfering signals. Capturing an interference signal with a swept-tuned spectrum analyzer requires that signal be present (i.e., in an "on" state) when the analyzer performs its measurement at the frequency of the interfering signal. But since a swept-tuned spectrum analyzer sweeps across a range of frequencies, the possibility exists that the interference signal is not present (i.e., in an "off" state) when the analyzer performs its measurement at the interfering signal's frequency.

Hence, an interfering signal that is present at some instances in time when the analyzer is sweeping also may not be present at the exact point in time when the analyzer performs a measurement at that interfering signal's frequency. In this case, the interference signal would essentially be undetected. This scenario is obviously more likely when trying to detect short-duration signals.

RTSAs differ from traditional swept-tuned spectrum analyzers, as they do not actually sweep across a frequency range. Rather they can continuously capture spectrum information for any span as high as the RTSA's maximum real-time span. This capability enables RTSAs to capture short-duration signals, making them an essential tool for RF interference detection.

DIGITAL PHOSPHOR TECHNOLOGY

Digital Phosphor technology (DPX) is a feature that Tektronix *(www.tek.com)* offers within its RTSAs *(Fig. 1)*.[2] Like a traditional spectrum-analyzer display, a DPX display shows amplitude versus frequency measurement data. However, a DPX display utilizes a color-graded feature, with the different colors indicating the occurrence of a signal as data is being collected. In Tektronix's SignalVu-PC software, which is used alongside the company's RTSAs, the default DPX bitmap color option is *Temperature*. Therefore, signals that are present more often are represented by warmer colors, while cooler colors represent signals that occur less frequently.

Viewing a DPX display allows users to observe multiple signals at the same frequency. This capability makes it possible to see low-amplitude signals in the presence of higher-amplitude signals at the same frequency. In other words, signals buried underneath other signals can be revealed by a DPX display.

It is important to note that a DPX display is not limited by the RTSA's real-time bandwidth. When setting the span wider than the real-time bandwidth, the DPX spectrum display is created by stepping through multiple real-time frequency segments.

RF INTERFERENCE TESTING

Now that we've discussed RTSAs and DPX displays, let's briefly get into how RF interference can be measured in the field. To demonstrate interference testing, a measurement was conducted using the Tektronix RSA306B RTSA along with Alaris Antennas' *(http://www.alarisantennas.com/)* DF-A0047-01 handheld wideband antenna *(Fig. 2)*. The antenna covers a frequency range of 9 kHz to 8500 MHz.

This measurement was performed outdoors in Forest Hills, N.Y., located in the New York City borough of

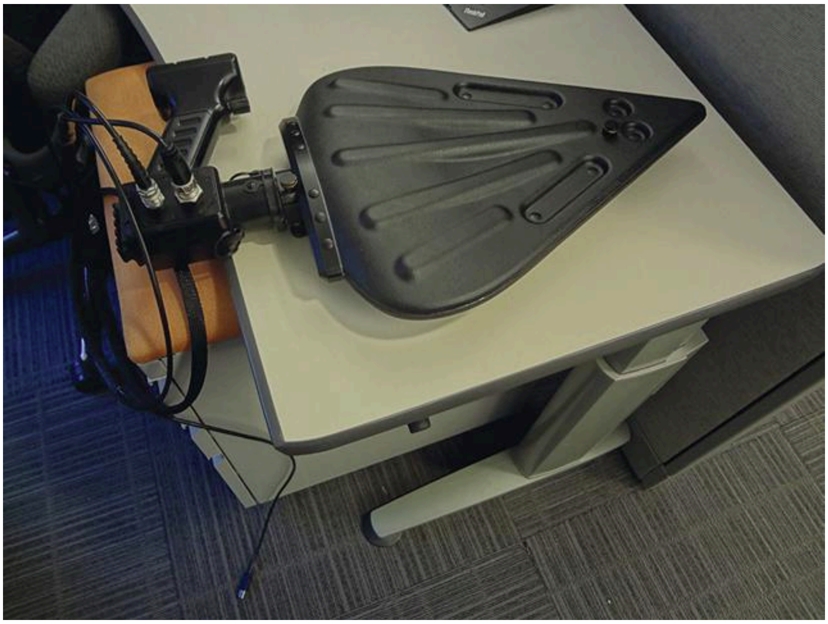

2. An antenna from Alaris Antennas was used with the Tektronix RSA306B RTSA for an interference-testing experiment.

Queens. The center frequency of the RTSA was set to 1935 MHz, while the span was set to 40 MHz. The antenna was pointed in the air to measure RF signals. The DPX display shows a higher concentration of RF energy around 1935 MHz *(Fig. 3)*. We won't break down into more-detailed analysis results here; still, the example illustrates how this type of testing can enable a user to track down an interfering signal upon detection. In other words, if interference is detected, these tools allow one to simply attempt to walk or drive to the location of the origin of the interfering signal.

This demonstration is obviously just a starting point; similar equipment could be used to conduct much more extensive interference detection tests. Tektronix also offers other features, such as mapping and the *Spectrogram* display feature, which are beyond the scope of this article.

In conclusion, it's imperative now more than ever that RF interference must be addressed. And as the Internet of Things (IoT) continues to churn out more wireless products, detecting RF interference will grow in importance. Companies such as Tektronix, among others, offer the tools to help make interference hunting efforts a success. mw

3. This DPX display was the result of an outdoor measurement.

REFERENCES
1. Tektronix, Interference Hunting, Application note
2. Tektronix, DPX Acquisition Technology for Spectrum Analyzers Fundamentals, Primer

Overlapped SB-AIS Signals

(Continued from page 87)

Step 2: Construct the matrix X as $[X_1\ X_2\ X_3\ ]^T$ and initialize the demixing matrix W as:

$$\begin{bmatrix} w_{11} & w_{12} & w_{13} \\ w_{21} & w_{22} & w_{23} \\ w_{31} & w_{32} & w_{33} \end{bmatrix}$$

Step 3: Centering of vector **X** as in Eq. 19:

$$\mathbf{X} = X - E\{X\} \quad (19)$$

Step 4: The whitening step, where the centered vector **X** is converted by linear transformation to a new vector with elements uncorrelated to each other. The transformed vector **Z** is expressed by Eq. 20:

$$\mathbf{Z} = D^{-0.5}E^{T}X \quad (20)$$

Step 5: Compute the weighting-update step for all the components of weight vector W_1, W_2, and W_3 by iterating Eq. 16 for i = 1 to 3.

Step 6: Perform symmetric orthonormalization to decorrelate the entire weighting vector W_1X, W_2X, and W_3X.

Step 7: Check for the stopping criterion, $\{1 - \min[abs(WWT)]\} > \varepsilon$. If satisfied, proceed to step 5.

Step 8: Compute the recovered modulated signal from vector **W** by using Eq. 13.

Step 9: Add the mean back to the recovered signal as in Eq. 21:

$$S + A^{-1}m \quad (21)$$

where m is the mean obtained in the centering step and A^{-1} is the demixing matrix.

Step 10: The recovered modulated signal has the same signal information

not to miss events! Register Today!

Physicians Panel Session:

Utilization of RF/Microwaves in Medicine, Thursday, 14 June 2018; Room 204B

Over the past three decades, collaboration between physicians and engineers has increased dramatically, to the benefit of our society. Biomedical engineering departments, the majority of which found in engineering schools and some within medical schools, offer seemingly unlimited opportunities and continue to attract a large number of students. To benefit from the merits of interdisciplinary cooperation and facilitate the transfer of technology to the market, existing large corporations, start-up medical companies, and research funding agencies now demand strong collaboration between engineers and physicians. With this in mind, IMS 2018 has made the subject of RF/microwaves in Medicine a major theme of the conference. The physicians on this panel will discuss the use of RF/microwaves in their respective fields. Topics ranging from microwave hyperthermia therapy for reoccurrences of breast cancer, advances in RF renal denervation, to back pain management using RF, will be highlighted!

Panelists:

1. Andrew Ng, Thomas Jefferson University Hospital, Philadelphia, PA
2. Daniel Frisch, Thomas Jefferson University Hospital, Philadelphia, PA
3. Donald Mitchell, Thomas Jefferson University Hospital, Philadelphia, PA
4. Ernest Rosato, Thomas Jefferson University Hospital, Philadelphia, PA
5. Eugene Viscusi, Thomas Jefferson University Hospital, Philadelphia, PA
6. Francis Kralick, Neurological Surgery, Shore Medical Center, Brigantine, NJ
7. Hamid RS Hosseinzadeh, School of Osteopathic Medicine, Stratford, NJ
8. Mark Hurwitz, Thomas Jefferson University Hospital, Philadelphia, PA
9. Nicholas Ruggiero, Thomas Jefferson University Hospital, Philadelphia, PA
10. William Jow, Medifocus Inc., Columbia, MD

Exhibition Dates and Hours

Tuesday, 12 June 2018	09:30 to 17:00
Wednesday, 13 June 2018	09:30 to 17:00
Exhibit-Only Time:	13:30 to 15:10
Industry Hosted Reception:	17:00 to 18:00
Thursday, 14 June	09:30 to 15:00

MicroApps

The Microwave Application seminars (MicroApps) offered Tuesday, 12 June through Thursday, 14 June, 2018, provide a unique forum for the exchange of ideas and practical knowledge related to the design, development, production, and test of products and services. MicroApps seminars are presented by technical experts from IMS2018 exhibitors with a focus on providing practical information, design, and test techniques that practicing engineers and technicians can apply to solve the current issues in their projects and products.

Industry Workshops

The Industry Workshops are 2-hour industry-led presentations featuring hands-on, practical solutions often including live demonstrations and attendee participation. These Workshops are open to all registered Microwave Week attendees at a nominal charge.

PENNSYLVANIA CONVENTION CENTER • PHILADELPHIA, PENNSYLVANIA, USA

Exhibition Dates: 12–14 June 2018 • Symposium Dates: 10–15 June 2018

Follow us on:

#IMS2018

IEEE

MTT-S

as the original ship transmitted signal and can be demodulated through GMSK demodulator to recover the data.

CHECKING RESULTS

The SB-AIS system architecture was simulated in a MATLAB- SIMULINK computer software environment. Even with a minimum difference of 0.0001 for the ratios of the three signals, all three ship data packets were recovered by using the algorithm. The simulation conditions, assuming one typical scenario as an example, are specified in *Table 2*. The mixing matrix can be a random matrix and a maximum Doppler frequency of ±4 kHz, so each ship carrier frequency can vary by as much as 480 ± 4 kHz.

In the simulation, source signals are three modulated GMSK signals with three different data sequences in Message 1 format as recommended by ITU-R. The modulated signals of the ships are multiplied by mixing matrix A *(Table 2, again)* to obtain the mixed signal. The sample length of mixed signal X and recovered ship signals Y are both 12401 in the simulation.

The novel approach successfully resolves AIS message collisions by means of signal processing. The technique of maximizing the cost function through iterative processing of time-series data to retrieve the AIS messages is exploited as a reliable solution.

The proposed innovative architecture incorporated with the blind source separation technique in a MATLAB/Simulink environment exhibits the capability to track a wide range of carrier frequency shift and has an excellent resistance to the path loss variations. The advanced receiver architecture can be implemented as a suitable scheme for an SB-AIS with high detection probability of ships in the coverage area. mw

ACKNOWLEDGMENTS: THE AUTHORS would like to thank Professor Brij Mohan, Member Secretary, Naval Research Board, New Delhi, and Commander Dr. Vijay Singh, Naval Research Board, New Delhi and Naval Research Board (NRB) for the encouragement to take up the work. The authors would also like to offer thanks for the support given by Dr. K. N. B. Murthy, Vice-Chancellor, PES University, Bengaluru, India. Furthermore, the technical support provided by Dr. J. Manikandan, Professor, Department of ECE, PES University, Bengaluru, India, is highly appreciated.

TABLE 2: SIMULATION CONDITIONS FOR SB-AIS ARCHITECTURE

Simulation parameter	Parameter value
Data packet 1, data packet 2, data packet 3	Message format 1 (ITU-R)
GMSK modulation carrier frequency	480,000 Hz
Doppler-shifted frequency	Ship 1: 481,000 Hz Ship 2: 484,000 Hz Ship 3: 482,000 Hz
Mixing matrix A based on path losses and antennae placement	$\begin{bmatrix} 0.92 & 0.95 & 0.86 \\ 0.73 & 0.7489 & 0.7652 \\ 0.78 & 0.86 & 0.88 \end{bmatrix}$

REFERENCES

1. Paolo Burzigotti, Alberto Ginesi, and Giulio Colavolpe, “Advanced receiver design for satellite-based automatic identification system signal detection,” *International Journal of Satellite Communications and Networking*, Vol. 30, 2012, pp. 52-63.
2. Ole Fredrik Haakonsen Dahl, “Space Based AIS Receiver for Maritime Traffic Monitoring Using Interference Cancellation,” *NTNU Innovation and Creativity*, June 2006.
3. Changchuan Lin, “AIS System and the Applications at the Harbour Traffic Management,” 4th International Conference on Wireless Communications Networking and Mobile Computing, 2008.
4. ITU-R, “Technical characteristics for an automatic identification system using TDMA in the VHF maritime mobile band,” Recommendations ITU-R M.1371-4 (04/2010).
5. Qing Hu, Yi Jiang, Jingo Zhang, Xiaowen Sun, and Shufang Zhang, “Development of Automatic Identification System Autonomous Positioning System,” *Sensors*, Vol. 15, 2015, pp. 28574-28591.
6. G. K. Hoye, T. Eriksen, B. J. Meland, and B. T. Narheim, “Space-Based AIS for Global Maritime Traffic Monitoring,” *Acta Astranautica*, Vol. 62, Nos. 2-3, 2008, pp. 240-245.
7. Torkild Eriksen, Gudrun Hoye, Bjorn Narheim, and Bente Jenslokken Meland, “Maritime traffic monitoring using a space-basedAIS receiver,” *Elsevier Science Direct, Acta Astronautica,* Vol. 58, No. 10, May 2006, pp. 537–549.
8. Andis Dembovskis, “AIS Message extraction from Overlapped AIS signals for SAT-AISapplications,” doctoral dissertation, Universität of Bremen, Bremen, Germany, March 2015.
9. Shou-zhong Zhu, Xiao-ling Wang, Wen-li Jiang, and Xi-xiang Zhang, “Combined iterative cross-correlation demodulation scheme for mixing space borne automatic identification system signals,” *Journal of Central South University,* 2013.
10. Shou-zhong Zhu, Zheng Liu, and Wen-li Jiang, “Counteraction of Constant Modulus Demodulation Scheme for Mixing Space Borne AIS Signals,” *Applied Mechanisms and Materials,* 2013.
11. Behzad Razavi, *RF Microelectronics,* 2nd ed., University of California, Prentice Hall PTR, 2012.
12. Justin Gaither, “Digital Phase Locked Loop (DPLL) Reference Design,” Xilinx XAPP854 (V1,0), October 10, 2006.
13. Zhu Shou Zing, Liu Zheng, Jiang Wen Li, and Guo Kun, “The Key Technology of Blind Source Separation of Satellite-Based AIS,” International Workshop on Informatics and Electronics Engineering (IWIEE), 2012.
14. Adel Belouchrani, Member, IEEE, Karim Abed-Meraim, Jean-Francois Cardoso, Member, IEEE, and Eric Moulines, Member, IEEE, “A Blind Source Separation Technique Using Second-Order Statistics,” *IEEE Transactions on Signal Processing,* Vol. 45, No. 2, February 1997.
15. Aapo Hyvarinen, “Fast and Robust Fixed-Point Algorithms for Independent component Analysis,” Helsinki University of Technology, Laboratory of Computer and Information Science, *IEEE Transactions on Neural Networks,* Vol. 10, No. 3, 1999, pp. 626-634.
16. Yajun Ma and Shexiang Ma , “An Improved Fast ICA Algorithm for Signal Separation of Satellite–Based AIS,” International Conference on Information and Communications Technologies (ICT 2014), 2014 .
17. Aapo Hyvtirinen, Juha Karhunen, and Erkki Oja, *Independent Component Analysis,* Wiley, New York,2001.
18. *http://pes.edu/cori/projects/space-based-automatic-identification-system/*

Broadband Amp Has Flat Gain from 50 kHz to 40 GHz

MODEL ZVA-403GX+ is an extremely broadband amplifier with outstanding gain flatness from 50 kHz to 40 GHz. Typical gain is 12 dB to 7.5 GHz, 11 dB to 30 GHz, and 10.5 dB to 40 GHz, with typical gain flatness of ±1.5 dB across the almost-40-GHz bandwidth. The wideband 50-Ω amplifier also achieves excellent noise figure, with typical performance of 6 dB from 50 kHz to 2 GHz, 4.5 dB from 2 to 7.5 GHz, and 4.0 dB from 7.5 to 26.5 GHz. The output third-order intercept point (output IP3) is typically +22 dBm from 50 kHz to 30 GHz and +21 dBm from 30 to 40 GHz. The RoHS-compliant amplifier is supplied in a package measuring just 0.84 × 0.96 × 0.36 in. with 2.92-mm coaxial connectors. It's a single-amplifier solution for many applications, including 5G wireless networks, wired and satellite communications systems, test equipment, and fiber-optic communications. It runs from a single +5-V dc supply and draws 100 mA typical current. Operating temperatures range from –10 to +85°C

MINI-CIRCUITS, P. O. Box 350166, Brooklyn, NY 11235-003; (718) 934-4500, *www.mini-circuits.com*

Eight-Way Divider Spans 0.5 to 2.0 GHz

EIGHT-WAY POWER-DIVIDER model APD-8-500M2G-SFF-30W is designed for broadband use from 0.5 to 2.0 GHz. It provides at least 20-dB isolation between ports with insertion loss of 1.5 dB or less. The VSWR is less than 1.40:1 at the input port and less than 1.25:1 at the output ports. Amplitude balance between channels is better than ±0.4 dB, while phase balance is better than ±0.4 deg. between channels. The right-way power divider measures 4.06 × 4.25 × 0.39 in. and is supplied with female SMA connectors. It's designed for operating temperatures from –55 to +85°C.

PLANAR MONOLITHICS INDUSTRIES INC., 7311-F Grove Road, Frederick, MD 21710; (301) 662-5019, FAX: (3010) 662-1731, *www.pmi-rf.com*

Adapters Add Phase Tuning to Coaxial Cables

SMA PHASE ADJUSTERS are adapters that can be added to RF/microwave coaxial cables to make critical phase adjustments at frequencies from dc to 18 GHz. The 3993 series of phase adjusters provide a 10 deg./GHz phase adjustment range with maximum VSWR of 1.30:1. Model 3993-1 is SMA male to SMA female adapter, model 3993-2 is SMA male to RG-402 0.141-in.-diameter semirigid cable, and model 3993-3 is SMA male to RG-405 0.085-in.-diameter semirigid cable.

COAXIAL COMPONENTS CORP., 1501 S. Decker Ave., Unit 201, Stuart, FL 34994; (866) COAXICOM, *www.coaxicom.com*

GaN Amplifier Powers 6 to 12 GHz

MODEL SSPA 6.0-12.0-100 iis a solid-state power amplifier (PA) based on GaN technology that's capable of at least 100 W output power from 6 to 12 GHz. The typical small-signal gain is 53 to 55 dB. The PA achieves a composite power-added efficiency of 14 to 16% with the maximum CW output power. Maximum input VSWR is 1.50:1, while maximum output VSWR is 2.0:1. The amplifier can be blanked on and off in less than 10 μs. It includes reverse-polarity protection, output-short and open-circuit protection, and over/undervoltage protection. Operating temperatures range from –40 to +85°C.

AETHERCOMM INC., 3205 Lionshead Ave., Carlsbad, CA 92010; (760) 208-6002, *www.aethercomm.com*

Chip Antennas Fit Tight 3G/4G PCBs

THE INTEGRA AND INVERSA chip antennas are designed for use in 3G and 4G wireless applications requiring tight PCB spacing. The antennas are just 3.3 mm high and can work effectively even with a small ground plane. For PCBs smaller than 75 mm in length, the antennas feature an additional active tuning circuit to overcome reductions in bandwidth from the limited ground plane. The antennas can work singly or in pairs for MIMO and diversity systems. The antennas are made in left and right versions for placement in left or right corners of a PCB. The Integra antennas cover 791 to 960 MHz, 1710 to 2170 MHz, 2300 to 2400 MHz, and 2500 to 2600 MHz for European markets, while the Inversa antennas cover 698 to 798 MHz, 824 to 960 MHz, 1710 to 2170 MHz, 2300 to 2400 MHz, and 2500 to 2690 MHz for global wireless markets.

ANTENOVA LTD., Second Floor, Titan Court, 3 Bishop Square, Hatfield, Herts AL10 9NA UK; +44 (0) 1223 810600, *www.antenova-m2m.com*

SDPT SMT Switch Spans 100 MHz to 30 GHz

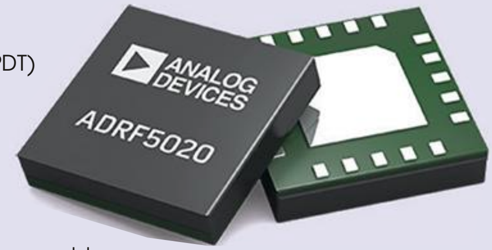

THE BROADBAND MODEL ADRF5020 silicon single-pole, double-throw (SPDT) RF/microwave switch covers a wide frequency range from 100 MHz to 30 GHz with 2 dB or less insertion loss to 30 GHz, and 60 dB or more isolation between ports to 30 GHz. The tiny surface-mount-technology (SMT) switch handles power levels to +24 dBm in both its through and terminated signal paths, and has Class 1 electrostatic discharge (ESD) sensitivity according to the 1-kV human body model (HBM). The switch is capable of +28 dBm typical output power at 1-dB compression, with a typical third-order intercept (IP3) point of +52 dBm. Its switching speed is 15 ns to reach within 0.1 dB of a final RF output level for a switched port. The nonreflective 50-Ω component is supplied in a 20-terminal, 3- × 3-mm land-grid-array (LGA) package.

ANALOG DEVICES INC., P. O. Box 9106, 1 Technology Way, Norwood, MA 02062; (781) 329-4700, (800) 262-5643, *www.analog.com*

Speedy Pulse Generator Passes 70-ps Rise Times

MODEL 765 IS a fast-rise-time pulse generator capable of rise times (20 to 80%) of better than 70 ps at +5 V dc and 50 Ω. It has two or four adjustable channels, with maximum repetition rate of 500 MHz per channel. The output voltage is fully adjustable with control via a 7-in. touchscreen display. The instrument is capable of producing advanced pulse sequences, such as double or quad pulse trains, with independent timing parameters. Pulse widths can be set from 300 ps to 1 second with 10-ps resolution. The instrument is able to be set to continuous, single, burst, gated, and external trigger modes for flexible testing.

BERKELEY NUCLEONICS CORP., 2955 Kerner Blvd., San Rafael, CA 94901; (877) 938-1621, *www.berkeleynucleonics.com*

GaAs MMIC Switches Control DC to 18 GHz

A PAIR OF GAAS MMIC nonreflective switches help rout signals at high speeds from dc to 18 GHz. Model CMD235C4 is a single-pole, five-throw (SP5T) switch with typical insertion loss of 2.5 dB and port-to-port isolation of 40 dB at 10 GHz. Model CMD236C4 is a single-pole, six-throw (SP6T) switch with typical insertion loss of 2.5 dB across the frequency range and port-to-port isolation of 42 dB at 10 GHz. Both switches have typical input 1-dB compression point (P1dB) of +21 dBm and switching speed of about 60 ns. They are housed in RoHS-compliant 4- × 4-mm surface-mount packages.

CUSTOM MMIC, 300 Apollo Dr., Chelmsford, MA 01824; (978) 467-4290, *www.custommmic.com*

Probes and Positioner Check Circuits to 20 GHz

A LINE OF FOUR ground-signal-ground (GSG) and ground-signal (GS) test probes is supported by a precision RF PCB probe positioner. The probes are available for testing to 20 GHz with return loss of better than 10 dB. They feature gold-plated contacts and compliant coaxial GSG or GS pogo pins. The probes, which come with pitch of 800 or 1500 μm plus a 3.5-mm female coaxial interface, can be cable mounted. They can be used by hand, with or without a probe positioner. The probe positioner includes a magnetic mounting plate with on-off positioner switch. It provides multiple-axis positioning control for precise placement of the probes.

PASTERNACK ENTERPRISES INC., P. O. Box 16759, Irvine, CA 92623; (866) 727-8376, (949) 261-1920, *www.pasternack.com*

Coaxial Attenuators Pad Signals to 50 GHz

RFMW LTD. has announced design and sales support for XMA Corp.'s 8582-6150-xx series of 2.4-mm, 50-GHz coaxial attenuators. The attenuators are available in standard attenuation values of 3, 6, 10, 20, and 30 dB, and handle power levels to +30 dBm (1 W). The VSWR for all attenuation models/values is 1.35:1 from dc to 26.5 GHz, 1.60:1 from 26.5 to 40.0 GHz, and 1.75:1 from 40 to 50 GHz. The attenuators are designed for operating temperatures from –55 to +100°C.

XMA CORP. STOCKING DISTRIBUTOR, RFMW LTD., 188 Martinvale La., San Jose, CA 95119; (408) 414-1450, *www.rfmw.com*

Product SPOTLIGHT

MMIC Gain Equalizers Tackle DC to 6 GHz

Mini-Circuits' EQY-Series Microwave Gain Equalizers are absorptive gain equalizers available with negative gain slopes of 1, 2, 3, 4, 5, 6, 8, and 10 dB for leveling the amplitude response of circuits from DC to 6 GHz. For example, a gain equalizer with 1-dB slope exhibits typical insertion loss of 1.57 dB at 10 MHz, dropping consistently to 0.39 dB at 6 GHz for leveling of broadband gain. Similarly, the input/output VSWR is typically 1.07:1 at 10 MHz, rising to typically 1.27:1 at 6 GHz. The tiny equalizers are fabricated with a highly repeatable, GaAs Integrated Passive Device (IPD) MMIC semiconductor process and supplied in miniature 8-lead MCLP™ surface-mount packages measuring just 2 × 2 mm. The RoHS-compliant gain equalizers handle power levels to +31 or +32 dBm.

Coaxial Termination Extends DC to 65 GHz

Mini-Circuits' model ANNE-50E+ wideband coaxial termination absorbs power levels to 1 W (+30 dBm) from DC to 65 GHz. The RoHS-compliant, 50-Ω termination has typical return loss of 26 dB to 18 GHz, 22 dB to 40 GHz, and 20 dB to 65 GHz for low reflections while absorbing high-frequency energy. It measures only 0.69 in. long with 0.36 in. diameter and is equipped with 1.85-mm connectors which mate with 2.4-mm and V connectors. The wideband termination has an operating temperature range of -55 to +100°C and is well suited for applications in test and measurement, military and aerospace systems, and broadband communications systems, including 5G systems.

Directional Coupler Handles 20 W to 40 GHz

Mini-Circuits' Circuits' model ZDC20-20403-K+ is a coaxial directional coupler that handles as much as 20 W power from 18 to 40 GHz. It maintains 20-dB coupling with worst-case full band coupling flatness of ±1.3 dB and typical full band coupling flatness of ±0.8 dB. The coaxial coupler has typical directivity of 14 dB from 18.0 to 23.5 GHz, 12 dB from 23.5 to 30.0 GHz, 11 dB from 30.0 to 35.0 GHz, and 9 dB from 35.0 to 40.0 GHz. Mainline insertion loss is typically 0.7 dB to 26.5 GHz and 0.9 dB to 40.0 GHz. Return loss is typically 19 dB, from 18 to 40 GHz. The directional coupler measures 1.25 × 0.65 × 0.45 in. (31.75 × 16.51 × 11.43 mm with female 2.92-mm connectors can pass as much as 3 A current from input to output. It has an operating temperature range of -55 to +100°C.

DOSCIS 3.1 Diplexer Screens 5 to 1220 MHz

Mini-Circuits' model DPLB-8510A04+ is a low-cost, 75-Ω surface-mount diplexer with a total frequency range of 5 to 1220 MHz. It has a lowpass band of 5 to 85 MHz and a highpass band of 102 to 1220 MHz, making it well suited for DOCSIS 3.1 cable-television and multiband-radio applications. Passband insertion loss for both bands is typically 1 dB or less. The diplexer provides stopband isolation of typically 48 dB between lowpass and highpass bands, with crossover isolation of typically 9 dB between the two bands. The RoHS-compliant diplexer measures 1.181 × 1.181 × 0.280 in. (30.00 × 30.00 × 7.11 mm) and handles power levels to 1 W (+30 dBm). It is designed for operating temperatures from -40 to +85°C.

Absorptive SPDT Switch Promises 10 Million Cycles from DC to 26.5 GHz

Mini-Circuits' model MSP2TA-26-12+ single-pole, double-throw (SPDT) switch is a reliable fail-safe absorptive switch that operates in break-before-make configuration with low loss and high isolation from DC to 26.5 GHz. The switch, which is guaranteed for 10 million switching cycles and handles as much as 20 W signal power, is designed for +12 V DC control. It features typical switching speed of 20 ms with low insertion loss of typically 0.25 dB to 12 GHz and 0.54 dB to 26.5 GHz. Isolation between ports is typically 80 dB through 12 GHz and 65 dB from DC to 26.5 GHz. The rugged SPDT switch is ideal for use in test systems. It has an operating temperature range of -15 to +45°C.

Flexible Cables Make Stable Measurements from DC to 50 GHz

Mini-Circuits' T50 Series Flex-Test™ coaxial test cables provide low insertion loss with excellent phase and amplitude stability with flexure for test-and-measurement applications from DC to 50 GHz. The cables employ a triple-shielded configuration with unique molded boot for excellent shielding effectiveness (SE). They are terminated with stainless-steel 2.4-mm female connector at one end and stainless-steel 2.4-mm male connector at the other end, and available in 2- and 3-ft. lengths. The typical insertion loss (for a 2-ft. length) is 1.4 dB from DC to 18 GHz, 1.8 dB from 18.0 to 26.5 GHz, 2.2 dB from 26.5 to 40.0 GHz, and 2.7 dB from 40.0 to 50.0 GHz. The return loss for the same cable length is typically 24 dB from DC to 18 GHz, 20 dB from 18.0 to 40.0 GHz, and 19 dB from 40.0 to 50.0 GHz. The RoHS-compliant cables handle as much as 144 W at 2 GHz, 38 W at 26.5 GHz, and 25 W at 50 GHz.

This index is provided as an additional service by the publisher, who assumes no responsibility for errors or omissions.

Subscription Assistance and Information:
(ISSN 0745-2993)
Microwaves & RF is published monthly. Microwaves & RF is sent free to individuals actively engaged in high-frequency electronics engineering. In addition, paid subscriptions are available. Subscription rates for U.S. are $95 for 1 year ($120 in Canada, $150 for International). Published by Informa Media Inc., 9800 Metcalf Ave., Overland Park, KS 66212-2216. Periodicals Postage Paid at Kansas City, MO and additional mailing offices. POSTMASTER: Send change of address to Microwaves & RF PO Box 2100, Skokie, IL 60076-7800. For paid subscription information, please contact Microwaves & RF at PO Box 2100, Skokie IL 60076-7800. Canada Post Publications Mail agreement No. 40612608. Canada return address: IMEX Global Solutions PO Box 25542, London ON N6C 6B2.

Back issues of MicroWaves and Microwaves & RF are available on microfilm and can be purchased from National Archive Publishing Company (NAPC). For more information, call NAPC at 734-302-6500 or 800-420-NAPC (6272) x 6578. Copying: Permission is granted to users registered with the Copyright Clearance Center, Inc. (CCC) to photocopy any article, with the exception of those for which separate copyright ownership is indicated on the first page of the article, provided that a base fee of $1.25 per copy of the article plus 60 cents per page is paid directly to the CCC, 222 Rosewood Dr., Danvers, MA 01923. (Code 0745–2993/02 $1.25 +.60) Copying done for other than personal or internal reference use without the expressed permission of Informa Media Inc., is prohibited. Requests for special permission or bulk orders should be addressed in writing to the publisher.

Only MACOM Can Enable 5G Antennas Without Compromise

Accelerating the sub-6GHz network transition to 5G requires breakthroughs that enable higher data throughput, superior service quality and increased subscriber coverage. To meet these stringent requirements, while delivering a reliable solution at commercially viable cost structures, demands true innovation. To date, critical challenges remain:

- **Cost structures are not yet viable for mainstream deployments**
- **Supply chains for key technologies are not robust across the industry**
- **Quality of service goals are constrained by the performance of traditional RF technologies**
- **Form factor and associated thermal constraints inhibit the move to advanced beam forming architectures**

5G visionaries need to balance these demands carefully, avoiding compromises in mission-critical performance attributes, cost and supply chain security. Today, only MACOM is equipped to strike that perfect balance, enabling the next generation of 5G wireless deployment.

MACOM's 5G Technology Advantage

Our broad array of 5G offerings spans a range from discrete components to fully integrated front-end modules. But the real value of our unrivaled RF to light portfolio is in its unique and fully integrated core technology differentiators. These include:

GaN

Patented GaN-on-Silicon Technology

By implementing GaN-on-Si technology in mainstream CMOS factories, we're dramatically scaling capacity, cost structure and supply chain flexibility—and doing so without sacrificing critical performance parameters such as power density, gain and efficiency.

Our power transistors, MMICs and PAs are tailored for mainstream 5G basestation deployment. So your antenna and radio designs can set new standards for data rate, range and energy efficiency.

Product Highlight

MAGM-103436-040A0P

- Fully matched 2-stage GaN-on-Si MMIC
- Ideal for 64 TRx M-MIMO applications
- Targeted frequency range 3.4 – 3.8 GHz
- Better efficiency than LDMOS- >40% at 5 W average power
- Proprietary wideband circuit topology meets stringent 5G TDD Linearity
- Cost reducing QFN package

	LDMOS	MACOM GaN-on-Silicon	Benefits
Power Efficiency	–	>10% Improvement	*Lower Operating Costs, Simpler Cooling*
Power Density	1–1.5 W/mm	4–6 W/mm	*Smaller Footprint and Lower Costs*
Easy Matching	Difficult	Easy	*Time-to-Market and Smaller Footprint*
Cost and Capacity	Silicon	Silicon	*Competitive Cost and Capacity*
Linearity	DPD friendly	DPD friendly	*Competitive Bill of Materials*

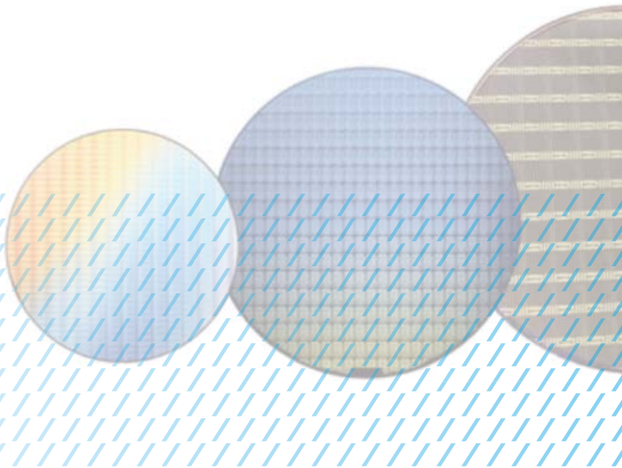

Switch

Proprietary Switch Technology

MACOM's leadership position in microwave switches has been established for decades. Our switch technologies assure a high level of antenna performance by enabling lower insertion loss in front-end transmit/receive topologies.

Delivered as integrated FEM solutions or individual components, lower insertion loss fuels extended range and expanded subscriber coverage.

Functional Schematic

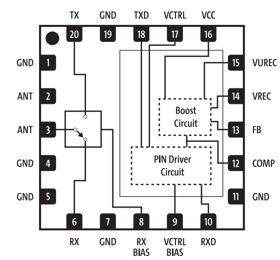

PRODUCT HIGHLIGHT

MAMF-011070

125 W High Power Switch

- > Integrated DC Boost & Bias Controller
- > Lowest insertion loss Tx = 0.3 dB | Rx = 0.4 dB at 2.7 GHz
- > High input power 125 W at 85°C
- > High isolation Rx = 43 dB at 2.7 GHz
- > 5 V single voltage supply
- > Broadband coverage 0.7 – 6.0 GHz

ANT to TX Insertion Loss (PCB loss de-embedded)

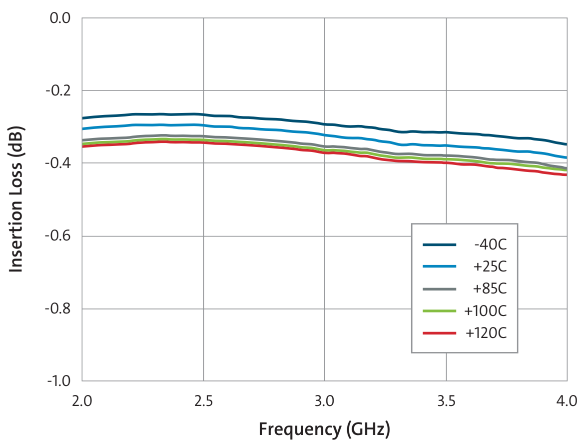

Beamforming

Coherent Beamforming Technology

Leveraging MACOM's pioneering work in phased array antenna techniques, coherent beamforming allows each element of a radio to operate in concert. This creates highly agile, narrowly-focused beams that directly link subscribers to the basestation with amplified reach and range.

Noise, interference and reflections are eliminated as operators detect and track users as they move in and out of the antenna's coverage area.

MACOM Sub-6 GHz Coherently Combined 5G Antenna

Join the Next 5Generation
Visit MACOM's IMS booth #1125 to see how we're shaping the future of 5G connectivity. You'll also see our latest RF-related advancements that prove *RF Matters Here,* including:

- GaN-on-Si Technology for Basestations and RF Energy Applications
- The World's First GaN-on-Si Based RF Energy Toolkit
- MACOM's RF Cross Reference Showcase

MACOM™
Partners from RF to Light

www.macom.com